Title
Investigations into malaria infection at the maternal-fetal interface and the characterization of placental polysialic acid

Author
Hromatka, Bethann S.

Publication Date
2011

Peer reviewed|Thesis/dissertation

Investigations into malaria infection at the maternal-fetal interface and the characterization of placental polysialic acid

by

Bethann S. Hromatka

DISSERTATION

Submitted in partial satisfaction of the requirements for the degree of

DOCTOR OF PHILOSOPHY

in

Biomedical Sciences

in the

GRADUATE DIVISION

of the

UNIVERSITY OF CALIFORNIA, SAN FRANCISCO

To the pregnant women around the world who suffer from malaria

ACKNOWLEDGEMENTS

This dissertation is dedicated to underprivileged individuals who suffer from diseases that their counterparts in developed countries are spared. I have always been passionate about infectious diseases and when I started graduate school I set out to study those of parasitic origin. Because I sought out an inspiring mentor who let me run wild with my ideas, I ended up working on placental malaria, a disease that primarily affects pregnant women in sub-Saharan Africa and Asia. Thus, this work is dedicated to these women, who under different circumstances could lead healthy lives. I would also like to thank the pregnant women in Kinshasa, Democratic Republic of the Congo and San Francisco who generously donated their placentas.

None of the following would be remotely possible without the unwavering support of my thesis mentor, Dr. Susan Fisher. She is an extremely creative, determined, and brilliant scientist, and it has been a privilege to be under her mentorship. I continually find it quite remarkable that she gave me carte blanche to develop my thesis and allowed me to start our placental malaria work *de novo*. I am impressed that she could engage the placental malaria field, which was new to her, and continually support me in my endeavors. Although she guided me, she never attempted to steer my hypotheses or conclusions, which in my experience, is quite rare for someone of her tenure. I will be forever indebted to her for encouraging me to find my own way and develop my ideas.

I am also indebted to Dr. Phil Rosenthal, my committee chair, who offered endless advice and spent many hours editing our malaria manuscript. Dr. Steve Rosen also guided my development as a novice glycobiologist and showed extreme enthusiasm for my work. I would like to thank Dr. Mike McCune and Dr. Jim McKerrow for thoughtful conversations and mentoring. I am indebted to the BMS program. Lisa Magargal and Monique Piazza held my hand through school-related challenges (*e.g.*,

journal clubs, thesis committee meetings, filing this dissertation) as well as personal dilemmas. I have to give a shout out to my former boss and mentor, Dr. Alexander Johnson, who encouraged me to apply to PhD programs and continually advised me over the years.

Many members of the Fisher lab helped me develop my projects. Dr. Penelope Drake was both a collaborator and stand-in PI for my work on placental polysialic acid. Thank you for the wonderful insight, the numerous meetings, your constant encouragement, and the fun times in Berlin. Drs. Alicia Barcena, Yan Zhou, and Aka Prakobphol offered advice, experimental expertise, reagents, and/or editing. Dr. Michael McMaster edited our malaria manuscript and offered numerous laughs—thank you for your humor. Drs. Jennifer Adibi and Richard Niles provided critical biostatistical help and thoughtful conversations. I am indebted to Dr. Mirhan Kapidzic (Miko), Haley Stolp, Gabriel Goldfien, and Jake Scott for placenta collection and cell preparation. Thank you to the other students in the lab—Elizabeth Co and Nathan Hunkapiller—for fun times and help along the way.

My work on placental malaria would not have been possible without the collaboration with Dr. Antoinette Tshefu's group at the University of Kinshasa in the Democratic Republic of the Congo. I am indebted to Dr. Sadiki Ngeleza for placenta collection and fixation. Thank you for making the trip to San Francisco and showing such enthusiasm for our project. I learned upon your arrival that it was your first time out of sub-Saharan Africa. Your impressions of my city and university were enlightening and I learned a tremendous amount from you.

I would also like to acknowledge some very close friends. First, I would like to thank my dear friend Dr. Marine Champsaur, who was always there for me through the thick and thin. Thank you for all of the intellectual conversations over salads and coffee. Thank you also for being more than just a science buddy—you helped me grow and are

always an inspiration to me. I'd also like to acknowledge other scientist friends. Dr. Leo Sugrue—your insight and love for science and medicine is ever inspiring. Dr. Brian Margolin and Matthew Forve—ever since our days at the University of Oregon, both of you always believed in me. Thank you to my non-scientist friends: Emily Blaskovich, Kelly Lyon, Julia Horvath, Antje Froehler, Charisma Wrigley, Miguel Aguilera, Eric Darius, and Dr. Jeff Graf (although we all know you are a physicist at heart). I am thankful for the fun times that made my longish tenure as a graduate student bearable.

My parents, Susan and Joe, deserve a very large treasure trove of thanks. They always supported me and encouraged me to pursue my passions. I would like to thank my brothers, Matthew, Timothy and Andrew for keeping it real and reminding me to never lose sight of my roots. I'm indebted to my in-laws in the Bay Area: Tom, Mary, Anne, Liz, Brad, Evan, and Grace. This clan has adopted me and is a constant source of encouragement. All of my family shows interest in my work and offers endless support in the form of delicious meals, outdoor adventures, and fun conversations.

Finally, I would like to thank the newest addition to my family—my husband Tom. I met you at the end of my first year of graduate school and your support for my endeavors has been unwavering. You are a constant joy to come home to and I always know that you "have my back". Thank you for your love, your patience, and your humor.

This work was supported by NIH 1R21AI079329-01A1 and a fellowship from the National Science Foundation.

Contribution of co-authors to the presented work

Chapter 2 of this dissertation is based on a manuscript that has been submitted for publication. The following co-authors contributed samples, performed data analysis: Sadiki Ngeleza[2], Jennifer J. Adibi[1], Richard K. Niles[1], and Antoinette K. Tshefu[2]. Susan J. Fisher[1] supervised this work.

Chapter 3 is based on unpublished data. The following individuals contributed samples, helped collect data, or performed data analysis: Sadiki Ngeleza[2], Jennifer J. Adibi[1], Stephanie Valderramos[1], and Antoinette K. Tshefu[2]. Susan J. Fisher[1] supervised this work.

Chapter 4 is based on a manuscript that is in preparation. The following co-authors contributed samples, cell preparations, or helpful advice: Mirhan Kapidzic[1], Haley Stolp[1], Gabriel A. Goldfien[1], Ie-Ming Shih[2], and Susan J. Fisher[1]. Penelope M. Drake[1] supervised this work.

[1] Departments of Obstetrics and Gynecology, Anatomy, the Center for Reproductive Sciences, and The Eli and Edythe Broad Center of Regeneration Medicine and Stem Cell Research, University of California, San Francisco, San Francisco, California.

[2] Kinshasa School of Public Health, Kinshasa, Democratic Republic of the Congo.

[3] Department of Pathology, Johns Hopkins University School of Medicine, Baltimore, MD, USA.

Investigations into malaria infection at the maternal-fetal interface and the characterization of placental polysialic acid

Bethann S. Hromatka

ABSTRACT

The human placenta is an organ that is derived from the fertilized embryo. It develops in advance of the embryo/fetus and through its specialized trophoblast populations, forms an "anchor" between mother and offspring. It carries out numerous important functions, including maintaining the pregnant state by secreting hormones and other molecules, and promoting tolerance of the genetically foreign (*i.e.,* hemiallogeneic) embryo/fetus. The human placenta is bathed in maternal blood, which allows for nutrient uptake, waste elimination, and gas exchange. Finally, the placenta must defend the embryo/fetus from blood-borne pathogens. In this dissertation, I discuss placental malaria, which is characterized by the accumulation of parasitized erythrocytes at the maternal surface of the placenta. Although placental and congenital infection does not often occur (*i.e.*, parasites are not usually found inside the placenta or embryo/fetus), infant low birth weight and pre-term labor are associated outcomes.

Since examination of the placenta usually helps to explain an abnormal neonatal outcome, the characterization of *Plasmodium falciparum*-infected placental biopsies formed the basis of my studies. I carried out an in-depth histological analysis of samples obtained from pregnant women in Kinshasa, Democratic Republic of the Congo. These placentas, which were severely infected, displayed loss (necrosis) of syncytiotrophoblasts, the cells that cover the chorionic villi and form the primary barrier between maternal and fetal circulations. In parallel, I immunolocalized putative receptors for *P. falciparum* and my results suggested that histological changes (including

syncytiotrophoblast loss) influenced their availability, such that many were only exposed in the infected state. Together, these results suggested that a reexamination of the mechanisms involved in initial adhesion was warranted and prompted me to carry out a binding screen to identify novel glycan receptors. *P. falciparum*-infected erythrocytes bound Lewis blood group antigens that were spatially and temporally positioned to initiate infection. Finally, I explored the possibility that parasitized erythrocytes might adhere to the uterine arterioles, which channel maternal blood to the intervillous space. Overall, my studies revealed that *P. falciparum* sequestration involves a complex series of interactions with both fetal and maternal cells, and is influenced by histological changes that expose receptors. As an offshoot, I also examined the role of Hofbauer cells, the fetal macrophage, in relationship to hemozoin, the byproduct of heme digestion by *Plasmodium* parasites.

As my work on placental malaria familiarized me with glycobiology, I undertook a second project investigating the role of polysialic acid during placental development. Previous studies in the nervous and immune systems demonstrated that this cell-surface glycan has an enormous hydrated volume and globally modulates cell-cell interactions. In this dissertation, I showed that it is expressed by human placental trophoblasts and regulated as a function of gestational age—abundant early in pregnancy and barely detectable at term. It promoted cellular migration and invasion. Intriguingly, my results suggested that placental polysialic acid is associated with desmosomes, cell adhesion complexes. Together, these studies demonstrated that polysialic acid influences development of the human placenta.

Table of Contents

LIST OF FIGURES AND TABLES

.

CHAPTER 1. AN INTRODUCTION TO PLACENTAL DEVELOPMENT AND PREGNANCY COMPLICATIONS RELEVANT TO THIS STUDY

1.1. THE FUNCTION AND DEVELOPMENT OF THE HUMAN PLACENTA

1.1.1. Overview

During pregnancy, the human placenta initiates and maintains a physical connection to the mother, setting up an exchange system that supports growth and development of the fetus (106, 155). Specifically, the placenta anchors the fetus to the uterus, secretes hormones and other molecules required for pregnancy maintenance, and promotes tolerance of the genetically foreign (*i.e.,* hemiallogeneic) embryo/fetus, while shielding it from many pathogens. The human placenta is bathed in maternal blood; at term, the placental blood space contains ~150 milliliters of maternal blood, and this volume is replaced approximately three to four times per minute (106).

1.1.2. Salient aspects of human placental development

The placenta is a short-lived organ, developing rapidly during the first half of the 40-week gestation period and completing its role after delivery when it is expelled as the “afterbirth”. As observed during the genesis of all organs, the placenta displays marked cellular changes during development (as reviewed by 155). Prior to implantation, the trophectoderm covering of the embryo differentiates at the blastocyst stage. During the next two weeks of development, the basic building blocks of the placenta, termed chorionic villi, form three-layered structures consisting of epithelial-type trophoblast cells on the outside, mesenchyme underneath, and vasculature within the mesenchyme that transports blood to and from the embryo/fetus (106). During the first half of pregnancy, specialized placental cytotrophoblasts (CTBs) invade the uterus in order to divert maternal blood to the developing embryo/fetus; robust blood flow is established by the

end of the first trimester. By mid-pregnancy, the mature architecture of the maternal-fetal interface, the region where fetal- and maternal-origin cells commingle, is established and placental development is largely complete. For the remainder of gestation, the placenta continues to produce hormones, nourishes and protects the fetus from infectious agents, and prevents rejection by the maternal immune system. Interestingly, complications that become apparent relatively late in pregnancy may actually reflect cellular and molecular errors that occurred much earlier in placental development (as reviewed by 135).

1.1.3. Formation of the mature placenta

In the first trimester of human pregnancy, the placental chorionic villi house CTB progenitors (pCTBs) that become depleted during the course of gestation. These cells differentiate adopting one of two fates (for review see 155). In one pathway, pCTBs located at the bases of anchoring villous columns (Fig 1.1 D) acquire an invasive, tumor-like phenotype. Consequently, they invade the uterine wall, breach maternal blood vessels and colonize the vasculature, a biased process that preferentially involves the arterial circulation. During invasion, the invasive CTBs (iCTBs) undergo an epithelial-to-endothelial transformation that entails a dramatic switch in their repertoire of adhesion molecules and growth factors (see review above and 153, 221). Due to its crucial role in regulating blood flow and immune functions, correct formation of the basal plate (Figure 1.1 D), the region where cytotrophoblasts and uterine cells commingle, is absolutely critical for normal pregnancy. In the other differentiation pathway, pCTBs located in floating chorionic villi (Figure 1.1 C) fuse, forming a layer of syncytiotrophoblasts (*i.e.*, syncytium), a multinucleate transport epithelium that is in direct contact with maternal blood. The syncytium is the primary site for the passage of nutrients, oxygen and waste material between the maternal and fetal circulations (106).

1.2. PREGNANCY COMPLICATIONS RELEVANT TO THIS STUDY

1.2.1 Overview

Complications of pregnancy can be classed into different categories. They can involve the mother's health, the baby's health, or both. Pre-existing conditions may lead to some complications, while others arise during pregnancy. The complications I discuss in this thesis largely involve the placenta. However, it is possible that genetic contributions—either maternal or embryonic/fetal—also influence these diseases. First, I introduce placental malaria, as this has been the primary focus of my dissertation and will be discussed in Chapters 2 and 3. This pregnancy complication is an infectious disease caused primarily by *Plasmodium falciparum*. While other species also cause infection during pregnancy (*e.g., P. vivax*), they were not the focus of my work. Women in malaria-endemic regions are routinely infected with *P. falciparum*, but they acquire a very severe form of disease during pregnancy. It is widely believed that molecules expressed by the placenta elicit a strain of malaria that the mother's immune system does not recognize. Accordingly, she lacks immunity to the antigenic repertoire that is displayed by the pregnancy-specific forms of *P. falciparum*. Importantly, women gain immunity in subsequent pregnancies such that multigravidae are largely immune to placental malaria. At the end of this chapter, I introduce gestational trophoblastic disease, which represents a unique group of both benign and malignant complications. Gestational trophoblastic disease is directly relevant to my work on placental polysialic acid (polySia), which is presented in Chapter 4.

1.2.2. Definition, Clinical Outcomes, and Prevalence

Definition

Placental malaria is defined as the sequestration of *P. falciparum*-infected red blood cells (iRBCs) at the maternal surface of the placenta. Here, the parasites accumulate at much higher densities than in the peripheral circulation. As to a mechanism of retention, iRBCs are thought to adhere to the STB layer that covers the chorionic villi and faces maternal blood (for review see 163). They also sequester in the intervillous space, where maternal blood flows, although the mechanisms of retention in this location are poorly understood. Interestingly, parasites are not thought to cross into the placenta and fetuses are not reportedly infected during the prenatal period. Beyond this definition, characterizing placental malaria in its entirety is difficult because it is not clearly understood why the accumulation of iRBCs at the maternal-fetal interface results in the observed clinical outcomes.

Clinical outcomes

Consequences for the fetus include spontaneous abortion, stillbirth and perinatal mortality, intrauterine growth restriction (IUGR), premature delivery, low birth weight, and anemia (for reviews see 24, 48). However, in sub-Saharan Africa where infection with *P. falciparum* is the most prevalent, low birth weight appears to be the most consistent outcome (85). Consequences for the mother include hypertension, anemia, pulmonary edema, renal failure, and death (see reviews cited above and 125). Although not well understood, it is likely that the clinical outcomes that are associated with placental malaria result from secondary and indirect effects including: the accumulation of maternal inflammatory cells in the intervillous space, the release of pro-inflammatory cytokines, hypoxia, reduced blood flow, reduced angiogenesis, and ultimately poor placental growth and function (as reviewed by 163). Therefore, poor fetal outcome is likely the result of altered placental function (*e.g.*, exchange of substances such as

oxygen, nutrients, and waste) and/or developmental defects that arise during the earliest stages of pregnancy when the formative stages of placental development occur.

Prevalence

As long as Woman has walked the earth, malaria appears to have stalked her (55). Worldwide, approximately 50 million pregnancies per year are exposed to this disease, with the highest burden of infection in malaria-endemic regions of sub-Saharan Africa (as reviewed by 48). In regions with year-round, stable transmission, approximately 25% of all women present with infected placentas at parturition. Approximately 6-13% are infected in areas with mild, seasonal malaria. Primigravidae (first time mothers) are at higher risk and the severity of disease significantly decreases with succeeding pregnancies, an observation that has prompted hope for a pregnancy-specific vaccine (see review cited above). This phenomenon also suggests that pregnancy-induced immunosuppression cannot account for the severity of placental malaria. Instead, there is good evidence that protective antibodies, which recognize antigenically and functionally distinct infected-red blood cell (iRBC) subpopulations, develop through multiple pregnancies (69). As I discuss in a later section, these antibodies have been shown to functionally block iRBC binding to putative placental receptors (161). A recent investigation of primigravidae in Tanzania provided an excellent summary of the prevalence of this disease (126). In this study, placentas from 26% of the participants (n=35/132) contained iRBCs. Interestingly, only ~ 70% of the women with placental involvement (n=24/35) also tested positive for iRBCs in their peripheral blood circulation. This finding suggested that nearly one third of the women had an infection that was confined to the placenta and thus hidden from the peripheral circulation. In addition, approximately half of the placentas that did not harbor iRBCs (n=46/97) exhibited evidence of prior infection as determined by the deposition of

hemozoin, a byproduct of hemoglobin digestion by *P. falciparum*. Together, this study and others (for review see 48) showed that > 50% of placentas from women living in malaria-endemic regions are infected at some point during gestation. Interestingly, some studies have suggested that the peak of parasite burden occurs early in gestation, between 9 and 16 weeks (23). As discussed earlier, this is a critical time in the explosive process of placental development.

1.2.2. Pathogenesis, Severe Malaria, and iRBC Sequestration

Pathogenesis

Malaria is a febrile infection, classically characterized by periodic chills, rigors, and high fevers, which occur at regular intervals of 48 hrs (180). For pregnant and non-pregnant human hosts, the infection begins when malaria sporozoites in the salivary glands of infected mosquitoes are injected into the human bloodstream during a blood meal. Within minutes of injection, the sporozoites home to the liver and invade hepatocytes by binding to heparan sulfate proteoglycans (HSPGs) (76). The parasites mature into liver-stage schizonts, which within a few days burst, releasing thousands of uninucleate merozoites. This new form goes on to infect circulating erythrocytes by binding to sialic acid residues on glycophorin A (for review see 102). Within the RBC, the merozoites undergo an intraerythrocytic 48-hour (hr) life cycle that is tightly synchronized amongst all of the parasites in the body. At any given time, the entire parasite population is at the same stage. Although not well understood, this synchronization results from the dynamic iRBC–human host relationship, and does not occur amongst cells cultured *in vitro* (104). During intraerythrocytic growth, parasites completely remodel the RBC, creating a hospitable environment that enables completion of their life cycle. At the end of the 48-hr cycle, which manifests as fever in the host, multinucleate schizonts burst out of the RBC, releasing approximately 32 motile merozoites that within minutes invade

new cells. Erythrocyte rupture releases cellular debris and toxins that also elicit fever in the host.

What is severe malaria and what is the host response to infection?

Four *Plasmodium* species infect humans and cause malaria, but only the most deadly one, *P. falciparum*, sequesters in the placenta and microvasculature of the brain, heart, and lungs (121). Cytoadherence to host cells in these organs underlies the sequestration, which is thought to be a mechanism that evolved for avoiding splenic clearance. iRBCs also adhere to circulating cells, for example to uninfected RBCs through a process called rosetting (168). The receptors for rosette formation include the blood group antigens A and B, CD36, heparan sulfate (HS)/HS-like GAGs, and complement receptor-1 (for reviews see 34, 216). iRBCs also adhere to platelets via CD36 (see reviews above). In severe *P. falciparum* malaria, iRBCs clumps may accumulate in small capillaries and postcapillary venules, which reduces blood flow and leads to tissue damage. Obstruction of the microcirculation of the brain (cerebral malaria) or trophoblast surface of the placenta (placental malaria) leads to organ failure and possibly death. While parasite burden is a clear determinant in malaria pathogenesis, interactions of iRBCs with the host immune system ultimately lead to the most severe pathologies. For example, in both the microvasculature and the maternal blood spaces of the placenta, iRBC adherence to host cells leads to the production of inflammatory cytokines, for example TNF-α, IFN-γ, and IL-1, and the recruitment of immune cells (for reviews see 34, 163, 174). It has been suggested that the uncontrolled host response also promotes severe malarial anemia.

How is P. falciparum sequestration achieved?

iRBCs have been visualized by electron microscopy to adhere to host cells through interactions between parasite-encoded proteins and host receptors (176). The cytoadhesion of iRBCs to endothelial, placental, and other cells is thought to be largely mediated by the *P. falciparum* erythrocyte membrane protein 1 (PfEMP1) family (for review see 102). PfEMP1 proteins are very large (6–13 kb), and have a two-exon structure with the first exon encoding an extremely diverse extracellular binding region, and the second exon encoding a more conserved cytoplasmic tail (see review cited above). Most of the binding activity is attributed to the 2-7 Duffy binding-like (DBL) domains and a cysteine-rich interdomain region (CIDR). Although PfEMP1 proteins are parasite-encoded, they are expressed on the iRBC cell surface, a location that facilitates interactions with host molecules, but also renders the cells vulnerable to recognition by the human immune system. To evade the host protective antibody response, the PfEMP1 family undergoes clonal antigenic variation whereby the ~ 60 *var* genes that encode PfEMP1 proteins are activated or silenced at the level of transcription (91). One *var* gene, called *var2csa*, is commonly expressed by parasites isolated from pregnant women, and is expressed in a mutually exclusive manner throughout the intraerythrocytic life cycle (173). As I discuss in the next section, VAR2CSA is thought to be the primary PfEMP1 protein that mediates binding to chondroitin sulfate A (chondroitin-4-sulfate, CS-A) and the only CS-A-binding protein that displays a placental antigenic phenotype (54, 199).

The mechanisms underlying *var* gene mutual exclusion (*i.e.*, only one *var* gene is expressed at a time) have not been fully elucidated, but it is generally accepted that *var* gene transcription is regulated through epigenetic chromatin remodeling and locus repositioning (56, 63, 65). Translation of a single *var* transcript occurs in the second half of the life cycle (*i.e.*, the late trophozoite and schizont stages) and results in the expression of a single PfEMP1 variant on the surface of the iRBC at approximately

10,000 copies per cell (91). Most natural infections are composed of a diverse mixture of iRBCs expressing different *var* genes and binding to distinct host receptors. It has been estimated that 18% of parasites will switch the expression of one *var* gene for that of another in a single life cycle (80). Adding to their diversity, *var* genes are frequently recombined, and it is estimated that thousands of *var* variants exist in the field (64). There is some evidence that proteins other than PfEMP1 may also mediate cytoadhesion. For example it has been reported that ring-stage parasites, which do not yet express PfEMP1 on the iRBC surface, can cytoadhere (146).

What are the molecular determinants of iRBC adhesion to the placenta?

iRBCs accumulate in the intervillous space and numerous *in vitro* and *in vivo* studies point to the involvement of CS-A (for review see 163). CS-A was originally identified as a placental receptor by monitoring binding of iRBCs to placental cryosections under static conditions (67) and in shear stress (18). In addition, numerous groups adhered iRBCs to CS-A-coated glass slides or Petri dishes (see review cited above). The parasites used for these studies included field placental isolates (*i.e.*, parasites captured from placental blood) as well as lines that were panned *in vitro* on CS-A and/or mammalian cell lines (*e.g.*, CHO cells). Additional *in vivo* evidence comes from antibody studies. Numerous groups showed that multigravid women possess antibodies that in some cases block iRBC adhesion to CS-A *in vitro* (161). Some of the antibodies react with VAR2CSA.

Interestingly, while many placental isolates cytoadhere to CS-A *in vitro*, others do not. This has prompted some researchers to suggest that CS-A is not the only receptor and that as yet unidentified molecules also mediate cytoadhesion (as reviewed by 163). While a few reports have implicated intercellular adhesion molecule-1 (ICAM-1) (191) and hyaluronic acid (hyaluronan, HA) (11) as receptors, the findings are controversial.

Although it is clear that ICAM-1 mediates iRBC cytoadhesion in post-capillary venules of the microvasculature (17), whether it plays a role during pregnancy is not clear. Two previous studies (172, 191) and my results (see Chapter 2) showed that STBs express this receptor. Maternal monocyte infiltrates in infected placentas also express ICAM-1 (172, 191). However, placental parasites do not appear to bind to ICAM-1 *in vitro* (12). The reverse scenario was originally for HA. Placental isolates adhered to HA *in vitro* (11), but STBs did not express this glycan (133). A more recent publication attributed the observed *in vitro* results to CS-A contamination of the HA preparations (74). Finally, there is evidence that some placental iRBC isolates bind CD36 *in vitro* (12); although this receptor is a marker of monocytes/macrophages, it is not expressed by placental cells that contact maternal blood (see Chapter 2 for my confirmation of this information). Interestingly, it has also been suggested that iRBCs sequester in the placenta via immunoglobulin (Ig) molecules (39, 62, 152) and that VAR2CSA contains IgG- and IgM-binding domains (152). Nonimmune IgG may bridge iRBCs and STBs, likely via neonatal Fc receptors, which are abundantly expressed on STBs and facilitate the transfer of maternal IgG across the placenta (15).

There are substantially more reports detailing the receptors involved in cytoadhesion between iRBCs and endothelial cells in the microvasculature. In fact, CS-A, in particular CS-A chains on thrombomodulin, was first identified as an endothelial receptor (162). There is strong evidence that CD36, a scavenger receptor, and ICAM-1 are endothelial receptors for iRBCs (as reviewed by 175). Finally, P-selectin, E-selectin, VCAM-1, PECAM-1, and NCAM-1 may also mediate cytoadhesion (see review above and 147). Thus, it is hypothesized that iRBC sequestration in the microvasculature is mediated by multiple host receptors that act in a cooperative fashion.

Are PfEMP1 interactions with host molecules glycan-dependent?

The carbohydrate requirement is exemplified by PfEMP1 interactions with CS-A, a chain of alternating sugars [4-SO_4-*N*-acetylgalactosamine (GalNAc) and glucuronic acid (GlcA)] that is attached to a protein core. PfEMP1 may also interact with HA, a chain of alternating sugars [*N*-acetylglucosamine (GlcNAc) and glucuronic acid (GlcA)]; HA is a protein-free glycan that is secreted into the extracellular compartment (136, 210). The putative receptors CD36, ICAM-1, VCAM-1, PECAM-1, and NCAM-1 are all heavily glycosylated glycoproteins that can theoretically interact with ligands in glycan-dependent or -independent manners. ICAM-1 interactions with its multiple ligands are both glycan-dependent, for example with the C-type lectin DC-SIGN (57), and glycan-independent, for example with the leukocyte integrins LFA-1 and Mac-1 (31, 97, 182). Although the purported ICAM-1 binding region for PfEMP1 (N-terminal domain D-1) lacks *N*-linked glycans (97), it has not been experimentally shown whether PfEMP1 binding to ICAM-1 is glycan-dependent or -independent. Similarly, it is not known if PfEMP1 interacts with CD36, VCAM-1, or PECAM-1 via carbohydrate motifs; however, it was reported that iRBCs can cytoadhere to desialylated NCAM-1 (147). Interestingly, distinct PfEMP1 domains are implicated in binding to CD36 (7, 8), ICAM-1 (189), and CS-A (156).

1.3 GESTATIONAL TROPHOBLASTIC DISEASE

1.3.1 Definition, clinical outcomes, and prevalence

Gestational trophoblastic disease represents a unique group of benign and malignant diseases. The abnormal cells originate from placental trophoblasts. Currently, the World Health Organization characterizes gestational trophoblastic disease based on histologic characteristics and groups the following as forms: hydatidiform moles (complete or partial), invasive moles, choriocarcinomas, placental site trophoblastic

tumors, epithelioid trophoblastic tumors, exaggerated placental site tumors, and placental site nodules (for reviews see 181, 205). In many cases, the manifestations are interrelated. Most gestational trophoblastic diseases arise after pregnancy, although they all originate from the placenta. Choriocarcinoma, the most serious form of gestational trophoblastic disease, most often follows a molar pregnancy. This disease can be controlled by removal of the lesion (*e.g.,* hydatidiform mole), or chemotherapy in the case of malignant forms. Many manifestations of gestational trophoblastic disease respond well to chemotherapy (111) and all are very rare.

1.3.2 Etiology

The pathogenesis of gestational trophoblastic disease, except in the case of hydatidiform moles, is largely unknown because few molecular studies have been performed. This is primarily due to the relative rarity of this disease and the lack of relevant experimental models. For some women, multiple molar pregnancies occur, a finding that may point to a genetic contribution (211). Histologic examination of gestational trophoblastic disease lesions has revealed that they are primarily composed of cells that arise from trophoblasts, and in most cases, they contain intermediate trophoblasts (*i.e.,* immature, largely undifferentiated trophoblasts) (reviewed by 181). These cells resemble the population of first- and second-trimester cytotrophoblasts that invade the uterus and remodel maternal blood vessels. In some cases, they contain mixed populations of trophoblasts, for example choriocarcinomas usually contain cytotrophoblasts, intermediate trophoblasts and syncytiotrophoblasts (see review above).

It has been suggested that the mechanisms underlying trophoblast invasion are similar to those involved in tumor cell invasion (33, 214). For example, like cancer cells, cytotrophoblasts express matrix metalloproteinases (MMPs), which promote cell

invasion *in vitro* (reviewed by 35). However, unlike malignant tumors, cytotrophoblast invasion is tightly regulated during normal pregnancy—confined spatially to the decidua and inner third of the myometrium and limited temporally to the first and second trimesters (60). There is evidence that both the cytotrophoblasts and the local uterine microenvironment regulate invasion (30, 60). For example, impaired invasion has been attributed to intrinsic cytotrophoblast behaviors such as failure to adopt a vascular phenotype (222). On the uterine side of the equation, maternal macrophages have been shown to induce cytotrophoblast apoptosis *in vitro* (157, 217). Thus, exaggerated or insufficient invasion likely results from a variety of factors. Not surprisingly, the trophoblasts found in gestational trophoblastic disease lesions appear to be highly proliferative, invasive, and migratory both *in vivo* and *in vitro* (reviewed by 181). Finally, there is some evidence that the molecules that modulate cytotrophoblast differentiation and invasion are dysregulated in gestational trophoblastic disease (reviewed by 109). In Chapter 4, I present my work on placental polysialic acid and demonstrate that this unusual glycan promotes cytotrophoblast migration and invasion *in vitro*, and is upregulated in biopsies of gestational trophoblastic disease lesions.

1.4 FIGURES

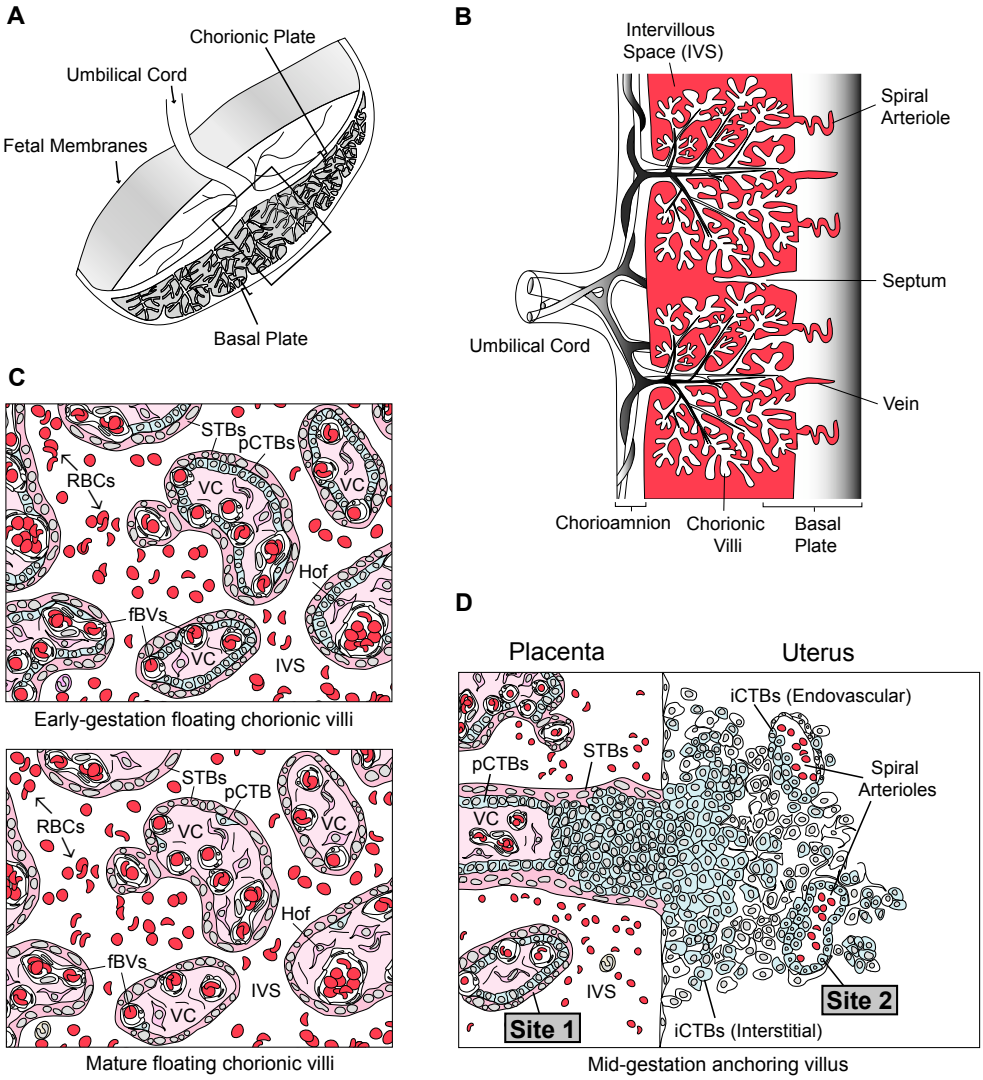

Figure 1.1 The human maternal-fetal interface.

(A) The human placenta at delivery. The placental surface that was adjacent to the uterine wall is termed the basal plate (bracket). The boxed area is diagrammed in panel B. (B) The placenta contains tree-like chorionic villi. Uterine spiral arterioles deliver maternal blood to the intervillous space (IVS), thus perfusing the placenta. Uterine protrusions into the intervillous space are termed septa. (C) Cross-section of floating chorionic villi. During early gestation (top panel) progenitors (pCTBs, grey) form a polarized epithelium that is attached to the basement membrane surrounding the stromal villous core (VC). pCTBs detach from this membrane and fuse to form syncytiotrophoblasts (STBs, pink). At term (bottom panel), the pCTB layer is largely depleted. The VC contains the intrinsic placental vascular (fetal blood vessels; fBVs), mesenchymal cells and macrophage-like Hofbauer cells (Hof). The intervillous space contains maternal blood, primarily red blood cells (RBCs). (D) Cross-section of an anchoring chorionic villus. In the basal plate region, invasive CTBs (iCTBs, grey) form a bridge between the placenta and the uterus. Interstitial iCTBs comingle with uterine cells. Endovascular iCTBs invade and subsequently line uterine spiral arterioles. Based on the physical relationship between maternal and embryonic/fetal cells, malaria infection is most likely to occur via STBs on the surface of floating and anchoring villi (site 1) and endovascular iCTBs (site 2). In both locations, placental cells are in direct contact with maternal blood. (Fig 1A, D were adopted from 212).

CHAPTER 2. PATHOMOLECULAR ANALYSES OF CD36, ICAM-1, CS-A AND LEWIS ANTIGENS SUGGEST A STEP-WISE PROCESS ESTABLISHES PLACENTAL MALARIA

2.1 ABSTRACT AND INTRODUCTION

2.1.1 Abstract

During pregnancy, *Plasmodium falciparum*-infected red blood cells (iRBCs) cytoadhere to the placenta. Infection is likely initiated at two sites where placental trophoblasts contact maternal blood: Site 1) via invasive cytotrophoblasts (iCTBs), which line uterine vessels that divert blood to the placenta, and Site 2) through syncytiotrophoblasts (STBs), transport epithelial cells that form the surface of chorionic villi and line the intervillous space. Here, we investigated molecular mechanisms of iRBC sequestration in relationship to the microanatomy of the maternal-fetal interface. Histological analyses revealed STB denudation in placental malaria, which brought the stromal cores of chorionic villi in direct contact with maternal blood in the intervillous space. The frequency of this lesion, which associated with hemozoin deposition (p=0.01) and leukocyte infiltration (p=0.001), decreased with increasing parity and birthweight. Immunolocalization of known iRBC receptors (CD36, ICAM-1/CD54 and chondroitin sulfate A [CS-A]) in placentas from women with uncomplicated pregnancies showed that STBs did not stain, while the underlying villous stroma was immunopositive. iCTBs expressed ICAM-1. In malaria infection, STB denudation exposed CD36 and CS-A in the villous core to maternal blood. STBs expressed ICAM-1; receptors were also detected on maternal leukocytes and uterine cells. Finally, we investigated iRBC adherence to novel receptors by screening an array of 377 glycans for structures that supported *P. falciparum* adhesion. iRBCs bound Lewis (Le) antigens that immunolocalized to STBs.

Our results suggested that *P. falciparum* interactions with STB cell surface Le antigens initiate placental malaria. Subsequent pathological alterations, which expose CD36, ICAM-1 and CS-A, propagate the infection.

2.1.2 Author Summary

In Africa and Asia, placental malaria is primarily caused by *P. falciparum,* which cytoadheres to fetal/embryonic trophoblast cells that are in direct contact with maternal blood. Like many pregnancy complications, placental malaria is associated with pathologies that change the anatomy of the chorionic villi, the functional subunits of the human placenta. Here, we hypothesized that malaria-associated histopathologies, which altered the repertoire of placental cells that were in contact with parasitized blood, influenced iRBC cytoadhesion. Specifically, *P. falciparum* infection led to a loss of the syncytiotrophoblast (STB) cell layer that covers the tree-like chorionic villi, which in turn, exposed underlying stromal receptors to maternal blood. These results suggested that the known receptors, including CS-A, the best studied of the molecules that are expressed by the placenta, are involved in advanced stages of infection. This implied that placental malaria is initiated by as yet unidentified receptors. To address this theory, we screened a carbohydrate library for structures that mediated iRBC adhesion. We identified Lewis family members, human blood group antigens that vary at the population level, as potential placental receptors. Together, our results provide new insights into the pathomolecular development of placental malaria.

2.1.3 Introduction

Approximately 50 million women around the globe are at risk for malaria during

pregnancy each year. Within sub-Saharan Africa, 25-30 million women become pregnant annually and are susceptible to infection with *Plasmodium falciparum*, which causes the most severe forms of human malaria (48, 164). Infection during pregnancy is most common in primigravid and secundigravid women, and is associated with infant low birthweight (LBW), intrauterine growth restriction (IUGR), and pre-term labor (163, 164). Annually, in Africa, an estimated 100,000 infant deaths are due to malaria-related LBW. Placental malaria is also associated with maternal complications including anemia (25) and a preeclampsia-like syndrome (21); approximately 10,000 maternal deaths result from malaria-related anemia. In sub-Saharan Africa, roughly one in four women show signs of placental infection at the time of delivery (48); however, incidences vary widely depending on geographic location and method of diagnosis. Although a few cases of congenital infection have been described, transplacental transfer of parasites from maternal to fetal blood does not often occur (15). Rates of malaria peak during the second trimester of pregnancy; cases decline towards term (22).

The hallmark of placental malaria is the sequestration of iRBCs in the maternal blood spaces of the placenta (*i.e.*, the intervillous space). The anatomy of this region and the relevant cell types are shown in Figure 1.1. The mature placenta is an entirely embryonic/fetal disk-shaped structure (Figure 1.1 A) composed of tree-like chorionic villi (boxed area enlarged in Figure 1.1 B), which are the basic structural units of this organ. The villi are perfused with maternal blood by the uterine spiral arterioles. In normal pregnancy, two types of embryonic/fetal cells are in direct contact with maternal blood: multinucleated STBs and mononuclear CTBs. This anatomical arrangement is established during development. CTB progenitors (pCTBs) form a polarized epithelium that is attached to the basement membrane surrounding the stromal cores of chorionic villi, which also contain the intrinsic placental vasculature and fetal macrophage-like Hofbauer cells. In early-gestation floating chorionic villi (Figure 1.1 C, top panel), pCTBs

detach from this basement membrane and fuse to form STBs, which line the intervillous space in an anatomical relationship analogous to the endothelial cells of blood vessels. STBs are transport epithelial cells that influx nutrients/gas and efflux waste. STBs also express fetal Fc receptors (103, 184), which enable the transfer of maternal IgG. Alternatively, pCTBs differentiate into invasive CTBs (iCTBs) (Figure 1C, top panel), forming columns of cells that subsequently anchor to and then penetrate the uterine wall (Figure 1.1 D). During interstitial invasion, iCTBs commingle with uterine decidual, myometrial, and immune cells. During endovascular invasion, masses of iCTBs breach the uterine spiral arterioles and replace the resident maternal endothelial cells. Endovascular iCTBs express an unusual repertoire of cell adhesion molecules, including those typical of endothelial cells, VE-cadherin, PECAM-1 and VCAM-1, as well as NCAM-1 (221).

Parasite sequestration has been proposed to occur through iRBC interactions with STBs, intervillous fibrin deposits (26, 70), leukocyte infiltrates (191) and/or platelets (208). Of these mechanisms, iRBC cytoadhesion to STBs is the best described. This interaction is mediated, at least in part, through parasite-encoded variant surface antigens (*e.g.*, PfEMP1) (9). The PfEMP1 family member VAR2CSA is commonly displayed by mature-stage placental iRBC isolates (94, 171) and is a potential vaccine candidate (13, 27). iRBCs isolated from the human placenta preferentially bind in vitro to bovine chondroitin sulfate glycosaminoglycans (CS-GAGs) containing the CS-A motif (12, 66), and numerous groups have demonstrated that the CS-A motif and VAR2CSA function as a receptor-ligand pair (53, 170, 198). Importantly, pregnant women naturally develop protective VAR2CSA-specific antibodies during pregnancy; primigravid women have low levels and are most susceptible to placental malaria and poor birth outcomes, while higher titers are found in multigravidae and correlate with increased infant birthweights (161, 164). While CS-A appears to be the principal iRBC receptor in the

placenta, other molecules, in particular CD36 and ICAM-1, play more significant roles in *P. falciparum* adherence in the microvasculature and brain, respectively (83, 196). ICAM-1 expression has been demonstrated on STBs and maternal monocyte infiltrates in infected placentas (172, 191); some placental iRBC isolates bind CD36 in vitro (12). iRBC adherence to STBs may also be mediated through adsorption of IgG-bound iRBCs to syncytial Fc receptors (62, 151) and through iRBC adhesion to hyaluronic acid (HA) (11); however, a more recent report found that STBs do not express HA (133).

A number of histopathological changes have been observed in *P. falciparum*-infected placentas. Some of these lesions are specific to the intervillous space. Maternal leukocytes, primarily monocytes with some lymphocytes and neutrophils, are mobilized to this location (140, 141, 204, 215), and have been associated with poor pregnancy outcome including LBW (117, 140, 141, 165). The monocytes often contain hemozoin in their cytoplasm (165, 204). This pigmented material is the by-product of *P. falciparum* digestion of hemoglobin. Hemozoin, which can also be observed in intervillous fibrin clots or found free (71, 204), signifies that the placenta was infected by *P. falciparum* earlier in gestation (28). Although parasitization of fetal vessels has not been reported (15), there is substantial evidence that malaria infection also alters the anatomy of the chorionic villi (28, 29, 40, 71, 72, 204). One of the most notable features is the accumulation of large deposits of hemozoin deep within the villi, often in areas of intravillous fibrinoid necrosis (28, 29, 40, 204), which is increased in parasite-infected placentas (204). Punctate pigment can also be found inside STBs and stromal cells (40, 71, 72, 204, 215). Additional villous changes include increased syncytial knotting (215), thickening of the trophoblast basement membrane (28, 29, 72, 204, 215), loss of microvilli (215) and marked thinning and/or loss of the STB layer that covers the chorionic villi (*i.e.*, STB denudation) (40, 204). In most cases, the frequency of these

villous lesions has not been studied and in general, it is not known if they are associated with adverse pregnancy outcomes.

Here, we investigated the mechanisms involved in iRBC sequestration at the maternal-fetal interface. The CS-A motif is reportedly expressed by STBs or found free-floating in the intervillous space (1, 130, 131). However, studies employing a full panel of monoclonal antibodies to localize CS-GAGs and other cytoadhesion receptors (CD36 and ICAM-1) in human placental samples spanning the course of gestation are lacking. STBs and maternal leukocytes at the placental surface (Figure 1.1 D, site 1) are believed to promote sequestration. To our knowledge, it has not been determined if iCTB-remodeled uterine arterioles (Figure 1.1 D, site 2), which supply blood to the intervillous space, might also retain parasites. The expression of CD36, ICAM-1, and CS-A on these vessels has not been explored previously. Finally, most receptor expression studies were not performed in the context of the histopathological changes that accompany infection. To fill these gaps, we immunolocalized known receptors in healthy placentas collected throughout the course of pregnancy. We focused on the chorionic villi and the intervillous space (Figure 1.1 D, site 1), and on iCTBs that line uterine arterioles that channel maternal blood to the placenta (Figure 1.1 D, site 2). We also examined receptor expression in placentas infected with *P. falciparum*. Our results revealed that placental malaria is associated with histopathological changes that expose cytoadhesion receptors that are normally masked. Finally, we carried out an in vitro glycan binding screen and determined that the placenta-binding *P. falciparum* CS2 strain preferentially adhered to Lewis (Le) antigens. Interestingly, immunoblotting and immunostaining revealed that human placental STBs expressed many of these glycans, for example Le^x, sialyl Le^x (sLe^x), Le^y, and Le^b. Together, these results suggested that placental malaria is the result of a complex series of interactions between iRBCs and a number of placental and maternal cells.

2.2. RESULTS AND DISCUSSION

2.2.1 Frequency of STB denudation and associations with clinical parameters

STB loss is a prominent feature of placental malaria

Many pregnancy complications, including infectious processes, change the repertoire of fetal placental cells that are in contact with maternal blood in the intervillous space. Accordingly, we hypothesized that histopathological alterations could influence cytoadhesion. Initially, we carried out a morphological analysis of *P. falciparum*-infected placentas (Figure 2.1). Samples were collected from Kinshasa, Democratic Republic of the Congo (n=17 cases and 17 uninfected controls) and consisted of five full-depth biopsies, two from the center and three from the periphery of each placenta. Control term placentas had the expected cellular composition, *i.e.*, a villous core composed of stromal cells and fetal blood vessels completely surrounded by a covering of multinucleated STBs (Figure 2.1 A). The intervillous space contained primarily free-floating RBCs. At this magnification (400x), approximately one leukocyte per field was observed. At least three previous studies described STB loss in placental malaria (40, 72, 204), but there has not been a systematic attempt to determine whether these changes are focal or widespread. Analysis of multiple sites at various depths showed that infected placentas commonly displayed loss of the STB covering. Typically, areas of denudation (dotted lines, Figures 2.1 B & C and Figure 2.2), which brought villous cores into direct contact with the intervillous space, were continuous with aggregates of STB nuclei (STB Agg, Figures 2.1 B & C). In some cases, the exposed villous cores resembled normal stroma. In other instances, they were largely acellular and eosinophilic, consistent with intravillous fibrinoid (also called subsyncytial fibrinoid or

villous fibrinoid necrosis), which is composed of extracellular matrix molecules and fibrin (15). Intravillous fibrinoid, subsyncytial in location, is distinct from perivillous fibrinoid, which is fibrin deposition at the periphery of degenerating villi. Often, the exposed regions were reservoirs for iRBCs and maternal leukocytes. Hemozoin-containing cells, with the morphological appearance of monocytes, were commonly observed (Figure 2.1 D). In many cases, iRBCs appeared to cytoadhere to the exposed villous stroma (Figure 2.1 E). Within the lesioned villi, hemozoin deposits (Figure 2.1 F) were commonly observed in acellular regions that lacked nuclei. Together, these results showed that in placental malaria, dramatic morphological alterations bring maternal blood in direct contact with the villous core.

Next, we quantified the observed pathologies (Table 2.3). The mean percentage of villi displaying regions of STB denudation was 11% higher in *P. falciparum*-infected versus control samples (standard error (SE)=2.2%, $p<0.0001$; Figure 2.3 A). The observed range was 10.0% to 39.0% for *P. falciparum*-infected and 3.0% to 13.0% for uninfected placentas. The mean number of maternal leukocytes per field was 18% higher in malaria-infected versus control samples (SE=7.0%, $p=0.01$; Figure 2.3 B). For infected placentas, we scored for the frequency of hemozoin-containing villi and iRBCs (Table 2.2). The mean percentage of hemozoin-containing villi was 9.0% (range of 0%-27.0%) and the mean number of iRBCs per field was 100.7 (range 0.07- >1000). As expected, control placentas did not contain hemozoin or iRBCs. Finally, we used linear regression analysis to investigate if STB denudation correlated with parameters of infection and inflammation. In the malaria group, STB denudation was positively associated with hemozoin-containing villi (regression coefficient (β)=3% increase in denuded villi with each 5% increase in hemozoin-containing villi, SE=1%, $p=0.01$; Figure 3C) and the presence of maternal leukocytes (β = 2.1% increase in denuded villi for every 10 leukocytes, SE=0.5%; $p=0.001$; Figure 2.3 D). No relationship was observed

with iRBC frequency (p=0.88; Figure 2.3 E). These data demonstrated that STB denudation was a prominent feature of placentas categorized as having chronic infection as indicated by the presence of hemozoin. Together, these results are evidence that the syncytial barrier was severely compromised in the setting of malaria. Our findings suggested that scoring for STB denudation could be a valuable component of the pathological criteria that are used to categorize placental malaria.

Placental STB denudation, which was more common in placentas from primigravidae, was associated with lower birthweights

Next, we determined whether STB denudation was associated with parity or infant birthweight. Given our small sample size (n=34), we were statistically underpowered to detect significant ($p<0.05$) relationships, but in most cases, the trends were marginally significant ($p<0.10$). First, we analyzed maternal characteristics (Table 2.1). The median age (24.5 versus 28.2; p=0.05) was lower, while the proportion of primigravidae (53% versus 18%; p=0.07) and prevalence of LBW (35% versus 6%; p=0.09) was higher in women who provided infected, compared to uninfected placentas. Next, we performed regression analyses to test for associations in our histopathological and clinical data. There was an inverse association between STB denudation and parity in the combined cases and controls dataset (β=-2.0% decrease in denuded villi for every live birth, SE=0.82%, p=0.01; data not shown). The test for an interaction between parity and malaria status yielded a p-value of 0.06, indicating a marginally significant difference in trends between the two groups (Figure 2.3 F). We did not detect a significant association between STB denudation and infant birthweight in the combined cases and controls (p=0.19; data not shown), nor was there a significant difference in trends between the groups (test for interaction p=0.19). However, when we log transformed the variable for STB loss to improve model fit, we obtained a more significant interaction

term that was consistent with the visual interpretation of the data (p=0.08; Figure 2.3 G). Finally, we asked if STB denudation changed in relationship to gestational age at birth (Figure 2.3 H). There was no overall association (p=0.81) and no significant difference in trends between the cases and controls (p=0.38). Although maternal leukocyte infiltration has been associated with placentas from primigravidae and lower infant birthweights (117, 165), we did not detect a relationship between leukocytes and parity (p=0.49; data not shown) or birthweight (p=0.72; data not shown). Overall, these data suggested that STB denudation correlated with maternal characteristics that group with severe placental malaria.

2.2.2 Immunolocalization of CD36, ICAM-1 and CS-A in the human placenta

Placental CD36, ICAM-1 and CS-A expression in relationship to maternal blood flow during normal pregnancy

Next, we explored the spatial relationship between known iRBC receptors and maternal blood flow. First, we analyzed the expression patterns of the well-studied receptors, CD36 and ICAM-1, in healthy human placental biopsies (first trimester, second trimester, and term). We employed antibodies that are used for immunolocalization and function perturbation, *i.e.*, blocking iRBC binding to CD36 (99) or ICAM-1 (16). We investigated the presence of these receptors in cells that might mediate cytoadhesion: STBs that cover the floating chorionic villi (Figure 1.1 D, site 1) and endovascular iCTBs that line uterine blood vessels (Figure 1.1 D, site 2). In floating chorionic villi (Figure 2.4 A), regardless of gestational age, CD36 staining (top panels) was observed in fetal blood vessels and the villous stromal core (green), but not in STBs or underlying pCTBs. ICAM-1 immunoreactivity (bottom panels) was not detected in first-

trimester chorionic villi, but was identified in fetal blood vessels of second-trimester and term samples (green). STBs and pCTBs did not stain.

Next, we analyzed second-trimester basal plate biopsies that contained iCTB-remodeled uterine arterioles (Figure 2.4 B). iCTB invasion of uterine arterioles begins in the first trimester, peaks in the second trimester and regresses at term. Accordingly, our studies focused on mid-gestation. In all samples, anti-CD36 and anti-ICAM-1 monoclonal antibodies reacted with the uterine extracellular matrix (green). Although iCTBs in the basal plate failed to express CD36, ICAM-1 was detected on iCTBs that lined the uterine vessels (bottom panel, green). Similar staining patterns were observed at term (data not shown). Isotype control antibodies were used to monitor binding via Fc receptors and did not react with any of the samples (data not shown). Together, these results suggested that CD36 and ICAM-1 are not normally in contact with the intervillous space. However, endovascular iCTBs, which are in direct contact with maternal blood, expressed ICAM-1, a known receptor for iRBCs.

iRBCs isolated from term placentas bind in vitro to CS-GAGs bearing the CS-A motif (12, 66). CS-GAGs are unbranched polysaccharides of variable length consisting of repeating disaccharide units of D-glucuronic acid (GlcA) and *N*-acetyl-D-galactosamine (GalNAc). These proteoglycans are usually found in the extracellular matrix. CS disaccharides are named according to the position of sulfation: C-4 of GalNAc (*i.e.*, chondroitin-4-sulfate/CS-A), C-6 of GalNAc (*i.e.*, chondroitin-6-sulfate/CS-C), both substituents of GalNAc (*i.e.*, chondroitin-4,6-sulfate/CS-E) and C-6 of GalNAc plus C-2 of GlcA (*i.e.*, CS-D). Given that CS-A is usually present in a heterogeneous mixture of CS-GAGs, we immunolocalized a broad array of these structures in floating chorionic villi (first-trimester, second-trimester and term). First, we employed monoclonal antibodies that recognize epitopes containing CS-A: CS-56, LY111, and 473HD (Figure 2.5 A, upper half; antibody specificities are described in Figure 2.6) (47, 95, 186, 190). In

floating chorionic villi, these antibodies strongly reacted with fetal blood vessels and/or the stromal villous cores (green); however, STBs and underlying pCTBs did not stain. Anti-CS phage display antibodies (186) displayed a similar pattern of reactivity (data not shown). All antibodies failed to react with sections that were pre-treated with chondroitinase ABC to remove CS-A (Figure 2.8 B). Next, we immunolocalized unsaturated disaccharide isomers (ΔDi) created by chondroitinase ABC digestion of CS/dermatan sulfate (DS) proteoglycans (*i.e.*, stubs). For this purpose, we used three monoclonal antibodies: 2-B-6 (anti-proteoglycan ΔDi-4S), 3-B-3 (anti-proteoglycan ΔDi-6S), and 1-B-5 (anti-proteoglycan ΔDi-0S) (37, 145) (Figure 2.5 A, lower half; mAb specificities are described in Figure 2.6). In floating chorionic villi, these antibodies, including 2-B-6 that specifically recognizes epitopes derived from digestion of CS-A, reacted strongly with fetal blood vessels and/or the stromal villous core (green). Undigested (*i.e.*, minus chondroitinase ABC) samples did not stain. STBs and pCTBs were not immunoreactive. Together, these data showed that the stromal villous core expresses CS-A, the most well studied placental receptor, while STBs and underlying pCTBs do not.

Next, we analyzed second-trimester basal plate biopsies that contained iCTB-remodeled uterine arterioles (Figure 2.5 B). In all samples, the CS mAb panel reacted strongly with the uterine extracellular matrix (green), but failed to stain endovascular iCTBs that lined the uterine vessels. Isotype control antibodies were used to monitor binding via fetal Fc receptors and did not react with any of the samples (Figure 2.8 A). Together, these results suggested that CS-A, which is expressed amongst a heterogeneous mixture of CS-GAGs, is not in contact with maternal blood flow during normal pregnancy.

Placental CD36, ICAM-1 and CS-A expression in relationship to maternal blood flow during malaria infection

We hypothesized that the expression patterns of CD36, ICAM-1 and CS-A were altered in malaria-infected placentas. To address this question, we localized these molecules in biopsies collected from term deliveries in Kinshasa. Samples obtained from uninfected African women had the same staining patterns for the molecules of interest as shown for the healthy term placentas (data not shown). In infected samples, analysis of the chorionic villi (Figure 2.7 A) revealed that CD36 was expressed in the villous core. Strikingly, due to STB denudation, immunopositive stromal areas were often in direct contact with maternal blood in the intervillous space. Staining for ICAM-1 was primarily detected in association with fetal blood vessels and STBs. In the latter case, immunoreactivity, which varied among samples, was largely restricted to cells that contacted iRBCs, leukocytes, or STBs of villi that were partially denuded of syncytium. Two antibodies that reacted with CS-A (CS-56 and Ly111) showed staining throughout the villous core (within stroma or intravillous fibrinoid), which in some areas was continuous with the intervillous space. We attempted to stain these formalin-fixed, paraffin-embedded biopsies with the 2-B-6 stub mAb, but were unable to obtain a clear pattern of immunoreactivity due to non-specific reactivity with undigested negative control samples (*i.e.*, in the absence of chondroitinase ABC treatment). This phenomenon was not observed in the paraformaldehyde-fixed, frozen samples (see Figure 2.5). We also analyzed term basal plate biopsies that contained iCTB-remodeled uterine arterioles (Figure 2.7 B). As shown for control samples collected in San Francisco (see Figure 2.4), iCTBs that lined the arterioles expressed ICAM-1. In this same location, CD36 and CS-A immunoreactivity was not detected (data not shown). Isotype control antibodies, which were used to monitor binding via fetal Fc receptors, did not react with the samples (Figure 2.8 A). Together, these findings suggested that

malaria infection led to placental changes that resulted in the expression of known iRBC receptors on embryonic/fetal cells that are in direct contact with maternal blood.

Next, we examined the antigenic repertoire of maternal cells that come in contact with the placenta. First, we analyzed maternal leukocytes in the intervillous space. Cells with a morphological appearance of monocytes that were adherent to the placental surface or free floating in the intervillous space, stained for CD36 (upper panel) and ICAM-1 (lower panel). CD36 is normally expressed by monocytes (194) and ICAM-1 immunostaining has been detected in the setting of malaria (32). In many cases, maternal leukocytes appeared to bridge iRBC adherence to the placenta. Staining for the known receptors was also observed in association with the portion of the uterus that lines the intervillous space (Figure 2.7 D). In the context of malaria, CD36 immunoreactivity was often associated with acellular regions (top panel). In contrast, ICAM-1 expression was often cellular (bottom panel). Although CS-A was localized in the deeper uterine regions, maternal cells at the boundary with maternal blood failed to express this receptor (data not shown). Finally, placental septa, uterine protrusions into the intervillous space, also exhibited immunoreactivity (Figure 2.7 E). In these regions, staining for CD36 and ICAM-1 was similar to that detected in association with the uterine surface (data not shown). Two antibodies that reacted with CS-A (CS-56 and Ly111) showed widespread staining throughout the septal stroma, which in some cases was continuous with the intervillous space. These areas appear to be reservoirs for iRBCs, which were numerous in these regions. Finally, in all locations, fibrin deposits occasionally stained for CD36, which could be a product of maternal platelets (data not shown) (208). In all cases, isotype control antibodies failed to react (Figure 2.8 C). Together, these data demonstrated that maternal leukocytes at the placental surface and uterine cells that line the intervillous space express known receptors.

2.2.3 Glycan array binding screen for identification of new receptors

A glycan binding screen reveals a role for Lewis antigens in cytoadhesion

Our results suggested that CD36, ICAM-1 and CS-A primarily acted in the later stages of placental malaria, after STB denudation and leukocyte infiltration. However, during initial adhesion, iRBCs commonly cytoadhere to STBs and we hypothesized that novel receptors would mediate this interaction. Accordingly, we carried out a binding screen that utilized glycan arrays. Previously, this approach was used to identify ligands/receptors involved in pathogen adherence to host cells (223). We focused on carbohydrate structures because the placenta expresses an unusual repertoire of glycans and modulates glycosylation as a function of gestational age (148). In these experiments, we bound fluorescently-labeled iRBCs to printed slides displaying 377 natural and synthetic glycan motifs (87, 188). These arrays, which present numerous structural motifs that are recognized by glycan-binding proteins, do not include CS-GAGs that contain the CS-A motif. We used the *P. falciparum* CS2 line, which was generated by panning on Chinese hamster ovary (CHO) cells and purified CS-A (36). For this reason, it is often used to study iRBC adherence in vitro. The results from two independent experiments are summarized in an annotated heat map of potential binding partners (Figure 2.9 A) and the oligosaccharide structures are included in Figure 2.10. iRBCs adhered to saccharides that carried a subset of Lewis (Le) blood group structures—(s)Le^x, Le^y, Le^b—sialyl N-acetyllactosamine (LacNAc), sulfated derivatives of LacNAc and Le^x, and the blood group A antigen. Together, these results suggested that iRBCs can bind core motifs that are common in glycan structures (*e.g.*, LacNAc) and specialized termini including Le antigens and sulfate-containing carbohydrate substituents.

Next, we used an immunoblotting approach to determine whether STBs expressed the motifs that iRBCs bound on the arrays. These experiments utilized STB plasma membrane fractions that were prepared from placentas of different gestational ages and collected in San Francisco. Figure 2.9 B shows the high molecular weight regions of the blots where most of the specific immunoreactivity was detected. Preparations from six- and nine-week placentas had appreciable levels of Le^x expression that was apportioned among several glycoproteins (top, left). Antibody reactivity appeared to decline with advancing gestational age. sLe^x expression was limited to a subset of high molecular weight species that also appeared to be more abundant during early gestation (top, middle). The HECA-452 antibody, which recognizes sLe^x and 6-sulfo sLe^x (the sulfate is permissive, but not required for reactivity) (119), had a similar pattern of expression (top, right). In contrast, the MECA-79 antibody, that binds related glycans including 6-sulfo LacNAc, did not react with STB preparations (data not shown). Le^a expression was not detected (bottom, left). The expression of two additional Le antigens—Le^y and Le^b—is genetically determined, *i.e.*, some individuals make them while others do not (112). Le^y (bottom, middle) expression was observed in most samples collected during the first half of pregnancy, while Le^b (bottom, right) immunoreactivity was primarily confined to a 9-week preparation.

Finally, we immunostained tissue sections of first-trimester floating chorionic villi (collected locally) with antibodies that recognized the Le antigens that were detected by immunoblotting (Figure 2.9 C). No expression of Le^y or Le^b was observed (data not shown), which may be explained by genetic variation. Patchy Le^x (top panel) and sLe^x (middle panel) expression was detected in association with STBs. The HECA-452 antibody, which recognizes sLe^x and 6-sulfo sLe^x (119), also stained STBs (lower panel). In infected placentas at term, no (s)Le^x immunoreactivity was visualized (Figure 2.9 D). In contrast, Le^x (Figure 2.9 D, top panel) and sLe^x (bottom panel) were expressed by

cells with the morphological appearance of maternal monocytes to which iRBCs cytoadhered. HECA-452 immunoreactivity was not detected. Together, these results demonstrated that STBs expressed sulfated and unsulfated (s)Le^x glycan motifs, and suggested that these carbohydrate structures are positioned to initiate cytoadhesion in the absence of malaria-related pathologies. At later stages of infection, leukocyte-associated (s)Le^x motifs may also bind iRBCs.

2.2.4 Discussion of findings

At the onset of this study, we aimed to identify placental cells and molecules that were positioned to mediate iRBC cytoadhesion. We investigated iRBC-host interactions throughout the course of human pregnancy and in the context of malaria-associated histopathological changes. Initially we focused on STBs and iCTBs because these fetal/embryonic cells are normally in contact with maternal blood (Figure 1.1, sites 1 and 2, respectively). iRBC adherence to STBs is well established. However, a role for iCTBs, which line the maternal vessels that channel uterine blood to the placenta, has not been described. Although rarely discussed, available evidence suggests that placenta-associated maternal leukocytes, platelets, and fibrin deposits may also mediate adherence (26, 70, 191, 208). As to the receptors involved, a physiological role for CS-A is well documented. Less is known regarding the well-accepted microvasculature receptors (CD36 and ICAM-1). Finally, it is possible that the placenta, a transient organ that produces many unique proteins and carbohydrates, may have novel molecular mechanisms for interacting with iRBCs.

STB denudation, which is normally uncommon, was first described in *P. falciparum*-infected human placentas over thirty years ago (72, 204) and more recently documented by Crocker *et al.* (40). Here we show, for the first time, that this

histopathology is a prominent feature of infected placentas and our results suggested that this phenomenon influences cytoadhesion. STB loss was approximately two-fold higher in *P. falciparum*-infected placentas; in extreme cases, 39% of the villi exhibited this lesion (Figure 2.3 A). STB denudation appeared to be a feature of chronic infection, as it correlated with the presence of hemozoin and increased numbers of maternal leukocytes, but not with the occurrence of iRBCs as an isolated feature (Figure 2.3 C-E). Syncytial loss also associated with placentas from primigravidae (Figure 2.3 F), a group that is susceptible to the most severe forms of disease. Intriguingly, STB denudation exposed known receptors to maternal blood. Immunolocalization of CD36 and CS-A revealed that they were abundantly expressed in the villous stromal core, a location that is not normally in contact with the intervillous space. However, upon STB loss, CD36 and CS-A were in direct contact with iRBC-containing maternal blood. Our results also suggested that STB denudation negatively impacts pregnancy outcome. These cells comprise the placental transport epithelium and we hypothesized that a reduction in the syncytial surface area would correlate with reduced infant birthweights. In support of this theory, we observed an inverse relationship between STB denudation and birthweight (Figure 2.3 G). Interestingly, STB loss is also a feature of preeclampsia (219) and smoking during pregnancy (115); however, a direct association with outcomes has not been investigated. Although we do not know why STB denudation occurs in the setting of malaria, there is some evidence that inflammation may be the cause. For example, in vitro experiments demonstrated that monocyte adhesion to syncytium and concomitant production of tissue necrosis factor alpha (TNF-α) promoted STB loss (77). Since increased levels of TNF-α are associated with placental malaria (68), this mechanism may account for the loss of syncytial integrity that we observed in our samples.

Our results suggested that CS-A, the best-described placental receptor, is not positioned to initiate infection. iRBCs from the intervillous space bind this glycan in vitro

(12, 66). Ricke *et al*. (161) showed that antibodies from malaria-exposed pregnant women blocked this interaction and multigravidae had higher antibody titers that correlated with favorable outcomes. In this context, our results show that STB denudation brings placental CS-A in contact with iRBC-containing maternal blood. We employed three antibodies that recognize this disaccharide amongst a heterogeneous mixture of CS-GAGs, and used a fourth monoclonal antibody that binds stubs that are the products of CS-A digestion. In all samples (n=18), regardless of infection status or tissue processing technique (paraformaldehyde-fixed, frozen versus formalin-fixed, paraffin-embedded), the villous core expressed CS-A, while STBs, iCTBs and the intervillous space did not (Figures 2.5 & 2.7). Our conclusions vary from previously published reports (1, 114, 130, 131). The reasons may include methodological differences (immunolocalization versus biochemical fractionation or cell culture models). Achur *et al*. (1) HPLC-purified CS proteoglycans from human placentas. Agreeing with our data, the majority (74%) was in the fibrous (*i.e.,* stromal) cores. In contrast, they concluded that the remaining CS-GAGs were STB-associated (2%) or free-floating in the intervillous space (24%). We speculate that uterine or stromal contamination of these fractions could account for the latter findings. Using a cell culture model, Maubert *et al.* (114) reported that multinucleated cells derived from primary CTBs expressed CS-A. Most investigators agree that these cells, which express the iCTB marker, HLA-G, are analogous to trophoblast giant cells that reside within the uterine wall rather than STBs (4). In a few cases, immunolocalization of placental CS-A has been attempted (130, 131). However, the results from these studies are difficult to interpret because the authors used different tissue processing techniques (*e.g.*, microwaving prior to embedding) and, in some instances, polyclonal antibodies that, to our knowledge, recognize undefined epitopes. In our experience, unambiguous detection of placental antigens is complicated by blood clotting that results from suboptimal tissue handling,

STB expression of fetal Fc receptors (103, 184), and abundant endogenous peroxidase activity, which must be controlled for to prevent nonspecific reactivity.

Our results also suggested that there are numerous mechanisms for iRBC sequestration at the maternal-fetal interface. Endovascular iCTBs, which line uterine arterioles that channel maternal blood flow to the placenta, expressed ICAM-1 regardless of infection status (Figures 2.4 and 2.7). Therefore, these cells are positioned to mediate cytoadhesion via this or other iRBC receptors that they express: VCAM-1, PECAM, and NCAM-1 (38, 147, 221). In many instances, potential cytoadhesion mechanisms were only apparent when we analyzed infected samples. In agreement with Sugiyama *et al.* (191) and Sartelet *et al.* (172), we found that malaria is associated with patchy STB ICAM-1 expression (Figure 2.7), which is induced by interleukin-1 (IL-1) and TNF-α. We also showed, for the first time, that the uterine surface that lines the intervillous space expresses CD36 and ICAM-1, while the uterine septa express CS-A (Figure 2.7). In general, exposure of receptors to maternal blood in these locations only occurred in the setting of infection. Interestingly, our results indicated that maternal monocytes, which bind iRBCs (6), significantly contribute to the retention of parasites in the intervillous space. iRBCs appeared to interact with monocytes that expressed known receptors (ICAM-1 and CD36) (Figure 2.7) and glycans that iRBCs adhered to on the arrays [(s)Le^x] (Figure 2.9). In many cases, monocytes also bound STBs, bridging iRBCs and the syncytium. Finally, we speculate that CD36 (3, 116) and/or CS-A (137, 206), which are expressed on platelets, could promote iRBC cytoadhesion.

Together, our findings suggested that the known receptors are primarily positioned to mediate cytoadhesion in advanced and/or chronic infection, which correlates with STB denudation and leukocyte infiltration. This implies that, at the onset of infection, as yet unidentified molecules facilitate binding to the intact syncytium and/or iCTBs. During the first trimester, blood slowly percolates in the nascent intervillous

space and placental iCTBs begin to invade the uterine vasculature (15). By the beginning of the second trimester, remodeling of the uterine arterioles establishes robust blood flow to the placenta (Figure 1.1 C). Here, we demonstrated that Lewis antigens [(s)Le^x, Le^y and Le^b], which bound iRBCs, are positioned to promote placental cytoadhesion (Figure 2.9). Interestingly, STBs expressed (s)Le^x and related sulfated glycans in the first trimester and down regulated their expression with advancing gestational age. Le^y and Le^b were detected to varying degrees in some samples, but were absent in others. Le^y and Le^b expression in epithelial tissues is influenced by secretor status (112); only individuals with a functional *FUT2* allele (secretors) express these antigens. Thus, our findings raise the possibility of a genetic component to protection from placental malaria. It is intriguing to speculate that non-secretor embryos/placentas might be partially protected. The lack of a functional *FUT2* allele, attributable to a mutation in the *Sec1* gene, occurs in 20% of Europeans and North Americans. To our knowledge, the prevalence of *Sec1* mutations in Africans is unknown.

In summary, this work contributes to our understanding of iRBC sequestration by the placenta. The results showed that numerous placental and maternal cells are positioned to promote cytoadhesion. Most importantly, our results suggest, for the first time, that cytoadhesion is strongly influenced by STB denudation. Since this lesion correlates with lower infant birthweights, we propose that scoring for STB loss could be a valuable component of the pathological criteria that are used to categorize placental malaria. As to the molecules involved, our data clarified the localization pattern of CS-A, CD36 and ICAM-1. However, our results also suggested that the mechanisms that mediate initial iRBC adhesion to intact chorionic villi should be revisited. In this regard, a novel glycan binding screen identified new candidate receptors. In future studies, we will explore the physiological relevance of these Lewis carbohydrate antigens in the pathogenesis of placental malaria.

2.3 MATERIALS AND METHODS

Ethics Statement

This study was approved by the Kinshasa School of Public Health Ethics Committee and the University of California, San Francisco Committee on Human Research. Written informed consent was obtained from all participants.

Participant Recruitment

Biopsies of normal placentas were obtained from patients undergoing elective terminations of pregnancy (5-22 wks) or from women who had uncomplicated deliveries in San Francisco, California. Biopsies of *P. falciparum*-uninfected and -infected placentas were obtained from term deliveries at the Kingasani Maternity Hospital, Kinshasa, Democratic Republic of the Congo. Women were categorized based on a diagnosis of malaria at the time of delivery. Exclusion criteria included other pregnancy complications: hypertension, preeclampsia, chorioamnionitis or maternal anemia. Malaria-negative women received antenatal care at the Kingasani Maternity Hospital and intermittent preventative therapy (IPT) (two doses of sulfadoxine pyrimethamine for HIV-negative women and three doses for HIV-positive women). Malaria-positive women did not receive antenatal care at Kingasani Maternity Hospital and IPT status was unknown.

Tissue sampling and handling

Placentas collected in San Francisco were biopsied and frozen at -80°C as previously described (219). Biopsies collected in Kinshasa were obtained within 20 min of delivery and transferred to 10% neutral buffered formalin 10:1 (ml:gram wet weight). To account for heterogeneity across the maternal-fetal interface, five full-depth biopsies (basal plate

to fetal membranes; see Figure 1A) were collected from the center (n=2) and periphery (n=3). Biopsies were fixed for 24 hr, transferred to 70% ethanol, paraffin-embedded, and sectioned (5 μm).

Histology

34 cases and controls (n=17/group) were randomly selected based on the sample sizes of previous studies in which we analyzed the effects of preterm labor or preeclampsia on the basal plate region of the placenta (219). H&E-stained sections were examined by transmission light microscopy. Three randomly chosen fields per biopsy were scored at 400x for the number of: (1) iRBCs; (2) hemozoin-containing villi/total number of villi; (3) leukocytes in the IVS; and (4) denuded villi/total villi. Nucleated cells in the IVS were assumed to be maternal leukocytes. In general, there was good agreement among the scores for each of the 15 400x fields that were examined per placenta.

Statistical analyses

Maternal age, parity, birthweight and gestational age were compared between cases and controls. For continuous parameters, p-values were based on a t test comparing the means, assuming normal distribution and equal variance. For non-continuous values, p-values were based on the Fisher's exact test to estimate differences in proportions between the two groups. The descriptive statistics for the infection and histopathological features were calculated using summarized data for the 15 400x fields that were analyzed per placenta. For departures from normality in dependent variables, values were log transformed, which allowed them to pass the Kolmogorov-Smirnov test for normality. In order to assess equal variance, we plotted the residuals and did not see any departures from the equal variance assumption. Linear regression models were fit to estimate univariate associations. We estimated all associations using linear and log

values and compared the two to obtain the best model fit. Unless stated, we reported results on a linear scale. To evaluate statistical differences in the slopes for the cases versus the controls, we estimated the interaction effects. This was done by entering a multiplicative interaction term into the model (*e.g.*, malaria status x live births) along with the two individual variables (*e.g.*, malaria status or live births). P-values reported the statistical significance of the test of the null hypothesis: the slopes of the lines for the two groups are parallel. If the p-value was ≤ 0.10, we concluded that there was a difference in the trend between the two groups, *i.e.*, that the lines were not parallel. Analyses were carried out using the statistical software package SAS 9.2 (SAS).

Immunolocalization

For immunofluorescence detection, frozen biopsies were cryosectioned (5 µm), fixed in ice-cold methanol/acetone (2:1) for 5 min and nonspecific reactivity was inhibited by incubating the sections for 1 hr in blocking buffer: 1% BSA, 0.1% fish gelatin, 0.1% Triton-X-100, and 0.05% Tween-20. Tissue sections were incubated overnight at 4°C with the following primary monoclonal antibodies (singly or in combinations): anti-CD36 (185-1G2; 10 µg/ml; Thermo Scientific), anti-ICAM-1 (15.2; 20 µg/ml; Thermo Scientific), anti-CS-A (LY111; 20 µg/ml; Seikagaku), anti-CS-A (CS-56; 12 µg/ml; Sigma-Aldrich), anti-CS-A (473HD; 1:100; kind gift of Dr. Andreas Faissner), anti-4S (2-B-6; 7 µg/ml; Seikagaku), anti-6S (3-B-3; 7µg/ml; Seikagaku), anti-0S (1-B-5; 7µg/ml; Seikagaku), anti-Le^x (HI98; 5.0 µg/ml; BD Pharmingen), anti-sLe^x (CSLEX1; 5.0 µg/ml; BD Pharmingen), anti-human cutaneous lymphocyte antigen (HECA-452; 2.5 µg/ml; BD Pharmingen), anti-cytokeratin 7 (OV-TL 12/30; 5 µg/ml; Dako), and a rat anti-cytokeratin 7 (7D3; 1:100; (46)). To control for anti-GAG Ab specificity and to expose stubs, sections were pre-incubated with chondroitinase ABC (10 mU/µl in 0.1% BSA; Seikagaku) at

37°C for 2 hr. Binding of primary mAbs was detected with FITC- or TRITC-conjugated, species-specific, secondary antibodies (Jackson ImmunoResearch). As controls, irrelevant mouse IgG2a (BioLegend), mouse IgG1 (BioLegend), mouse IgM (eBioscience), rat IgM (BD Pharmingen) or PBS was substituted for the primary antibody. Sections were mounted with DAPI-containing Vectashield (Vector Laboratories) and imaged with a Leica CTR5000 upright microscope or a Leica TCS SP5 confocal microscope. The staining pattern of each antibody and sample type was evaluated in three independent experiments.

For histochemical detection, tissue sections were deparaffinized in xylene and rehydrated in a series of graded ethanol solutions. Antigens were retrieved by heating for 30 min at 95°C in 10 mM sodium citrate and 0.05% Tween 20 (pH 6.0). Endogenous peroxidase activity was blocked by incubation in 0.3% H_2O_2 (30 min at RT). Signals from native IgG bound to fetal Fc receptors were blocked by incubation with goat or donkey anti-human IgG (1.0 µg/ml; Jackson ImmunoResearch; 1 hr at RT). To block unoccupied Fc receptors, samples were incubated in 1.5% serum from the species in which the secondary Ab was produced. Tissues sections were incubated overnight at 4°C with the following primary monoclonal antibodies (mAbs) or polyclonal antibodies (pAbs): anti-ICAM-1 pAb (1:10; Cell Signaling), anti-CD36 pAb (1:25; Sigma-Aldrich), anti-Le^x mAb (HI98; 5.0 µg/ml; BD Pharmingen), anti-sLe^x mAb (CSLEX1; 5.0 µg/ml; BD Pharmingen), and the GAG-specific antibodies described earlier. Binding of primary antibodies was detected with species-specific, biotin-conjugated, secondary antibodies (Jackson ImmunoResearch) plus ABC-peroxidase (Vector Laboratories). The reaction was developed with the 3-amino-9-ethylcarbazole (AEC) substrate (Vector Laboratories) and sections were counterstained with hematoxylin. For controls, rabbit polyclonal IgG (BD Pharmingen), mouse IgM (BioLegend) or PBS was substituted for the primary

antibodies. The staining pattern of each antibody was evaluated in three to six independent experiments. To evaluate hemozoin deposition relative to antigen expression, the sections were viewed with polarized light, which illuminates this pigment (166).

Parasite culturing and labeling

P. falciparum line CS2 (MRA-96; MR4) was cultured in fresh human erythrocytes diluted to a 2% hematocrit with RPMI 1640 supplemented with 25 mM HEPES, 2 mg/ml sodium bicarbonate, 100 μM hypoxanthine, 50 μg/ml gentamycin, and 0.25% Albumax II (Invitrogen). The cultures were maintained in a humidified incubator at 5% CO_2, 5% O_2, and 37°C. PCR-based testing for mycoplasma contamination (Stratagene) was done on a regular basis. Cultures were synchronized according to standard methods (105). When they reached ~5% parasitemia and the majority were schizonts (~ 1 week post-thawing), the cells were centrifuged at 10,000 RPM for 5 min and washed twice with RPMI 1640. Then they were resuspended (1.0×10^{10}/ml) in RPMI 1640 containing 25 nM Mitotracker (Invitrogen) and 0.0025% DMSO and incubated for 15 min in the culture conditions described above. The labeled cells were centrifuged (10,000 RPM, 5 min), washed once with RPMI 1640, and resuspended (2×10^{10} cells/ml) in PBS containing 1% BSA.

Mapping candidate P. falciparum carbohydrate receptors using glycan arrays

iRBCs were screened for adherence to printed glycan microarrays (version 3.1) developed by the Consortium for Functional Glycomics (87, 188). The array contained 5,632 spots of 377 natural and synthetic glycans with amino linkers printed on chemically modified glass slides. Each glycan was printed in 12 spots at 10 μM (six spots) and 100 μM (six spots). As landmarks, one hundred sixty spots were printed with biotin and as controls, 936 spots were empty. The arrays were rehydrated by incubating

in 20 mM Tris-HCl, 150 mM NaCl, 2 mM $CaCl_2$, 2 mM $MgCl_2$ and 0.05% Tween 20 for 5 min at RT. 1 x 10^{10} Mitrotracker-labeled iRBCs/RBCs (~ 5% parasitemia) in 0.5 mls of PBS + 1% BSA were added to each array along with 2µl Cy5-Streptavidin (Zymed), which bound to biotin spots and formed grid coordinates. To facilitate interactions with carbohydrate receptors, which often require sheer stress (107). The slides were rotated (40 revolutions/min) on a 30 cm platform shaker for 30 min at RT. Then they were washed twice with 20 mM Tris-HCl, 150 mM NaCl, 2 mM $CaCl_2$, 2 mM $MgCl_2$), air-dried and imaged using a GenePix Autoloader 4200AL microarray scanner (Axon Instruments) set to 5 µm resolution. iRBC adherence was confirmed by microscopy. The entire experiment was performed twice.

The two-color TIFF images were analyzed with SpotReader (version 1.3.1.0; Niles Scientific). The software created a grid of circles superimposed on images of the signals, and computed the median intensity for all pixels inside each circle (foreground fluorescence) and in the region surrounding each circle (background fluorescence). Relative fluorescent units (rfu) were computed as the foreground minus background intensity. The data were exported to Excel and median values were computed for the 12 data points that were collected for each structure. Control spots were analyzed in parallel. The values were normalized by subtracting the mean signal across the entire array and dividing by the standard deviation of the control spot readings. Spots with rfu measurements ~ five-fold higher than the median of all glycan signals and ~ 50-fold higher than the controls were scored as positive. In general, there was good agreement among the six 100 µM spots for each of the 9 glycans that represented the top 3% of all hits (Figure S3). The primary data are available at the Consortium for Functional Glycomics website, http://functionalglycomics.org.

Immunoblotting

STB plasma membrane preparations were isolated as previously described (187) with minor modifications. Briefly, placental chorionic villi were manually dissected into 5-10 mm pieces, resuspended in ice-cold PBS containing a protease inhibitor cocktail (Pierce) and stirred for 1 hr. The samples were passed through a 70 µm filter and the membrane fraction was isolated by a series of centrifugation steps: 1000xg (10 min), 14,000xg (20 min) and 100,000xg (1 hr). Pellets were resuspended in PBS and dispersed by repeated aspiration with a 26-gauge needle. Protein concentrations were determined by using the Bradford assay (Bio-Rad). STB preparations (40 µg/lane) were separated on 3-8% NuPAGE Tris-Acetate gels in Tris-Acetate SDS buffer (Invitrogen) and transferred to nitrocellulose (Bio-Rad). Nonspecific reactivity was blocked by incubating the transfers for 1 hr in PBS containing 0.05% Tween 20 (PBST) and 5% nonfat dried milk (blocking buffer). Blots were incubated overnight at 4°C with the following monoclonal antibodies: anti-Le^x (HI98; 4.0 µg/ml; BD Pharmingen), anti-sLe^x (CSLEX1; 4.0 µg/ml; BD Pharmingen), anti-Le^y (F3; 1:250; Abcam), anti-Le^b (LWB01; 1.2 µg/ml; NeoMarkers), anti-Le^a (LWA01; 1.2 µg/ml; NeoMarkers), HECA-452 (2.0 µg/ml; BD Pharmingen), or MECA-79 (2.0 µg/ml; BD Pharmingen). After washing three times for 5 min in PBST, the transfers were incubated for 1 hr at RT with peroxidase-conjugated, species-specific, secondary Antibodies (1:2500; Jackson ImmunoResearch). Finally, they were washed three times for 5 min in PBST and antibody reactivity was detected with ECL Plus (GE Healthcare).

2.4 ADDENDUM: LECTIN CHARACTERIZATION OF STB PLASMA MEMBRANES

2.4.1 Introduction and rationale

Dr. Lara Mahal's group pioneered a recombinant lectin microarray that can be used to characterize cellular glycopatterns (143). These microarrays primarily contain plant-derived, carbohydrate-binding proteins (*i.e.*, lectins) that are immobilized onto a slide. Fluorescently labeled protein/carbohydrate samples are hybridized to the arrays—the pattern of binding depends on the makeup of the glycans in the preparation. A benefit to performing lectin microarray profiling (as opposed to analysis by mass spectrometry) is that *N*- and *O*-linked glycans do not need to be separated prior to analysis and bulky glycans (*e.g.*, polysialic acid) do not need to be removed. However, while lectins are highly specific for glycans, they often recognize more than one motif (see table 2.3 for lectin specificities). Therefore, lectin microarrays can reveal glycopatterns, but cannot necessarily provide information about specific glycan epitopes.

Here, I describe the purification and labeling of STB plasma membrane preparations, which in collaboration with Dr. Mahal's group, were profiled on lectin microarrays. The goal of these experiments was to understand the glycosylation patterns of the STB plasma membrane throughout the course of human pregnancy. We hoped that obvious changes would emerge and hypothesized that the STBs might regulate glycosylation as a function of gestational age. Since we were investigating iRBC binding to glycans and hypothesized that they bound carbohydrate motifs on the STB plasma membrane, we hoped that data generated from these experiments would prove useful insights into the mechanisms that mediate initial iRBC adhesion to the placenta.

2.4.2 Results and discussion of findings

STB plasma membranes were prepared from human placentas. Three first-trimester (T1-T3), second-trimester (T4-T6), and term (T7-T9) preparations were labeled with Cy3 and Cy5 mono-reactive dyes. It was noted that precipitates were present in

some of the samples, which may have resulted from extended storage at -80°C. Reference samples were generated by combining equal parts of the Cy3- or Cy5-labeled preparations (T1-T9). Then, each Cy3- and Cy5-labeled sample was hybridized to lectin microarrays along with the reference that was labeled with the opposite dye (*e.g.*, Cy5 or Cy3 reference). The slides were dried, scanned, and the data were analyzed according to previously published methods (144). An additional normalization step was performed to control for overall differences in relative fluorescent units (rfus) across the arrays. Specifically, the median for each of the four data channels (Cy3 sample, Cy3 Reference, Cy5 sample, and Cy5 Reference) was subtracted from each lectin rfu.

First, the data were visualized without clustering (Figure 2.13 A). Although we hypothesized that some glycans would be regulated as a function of gestational age, we only identified a few lectins with finding patterns that grouped according to trimester. For example, WFA, WGA, and GRFT had lower rfus with term (green) as compared to first- and second-trimester samples (red). Next, the data were visualized with clustering (Figure 2.13 B), which confirmed our initial findings. Overall, the samples did not cluster according to gestational age.

More commonly, we observed differences between the samples (as opposed to between the gestational ages), which may be attributed to distinct glycosylation patterns among individuals or to suboptimal handling of the dye-labeled preparations. It is possible that the dye stability was compromised, because the samples were stored for ~ one year prior to hybridization. For example, UEA-1, which binds α-linked fucose residues, and SSA, which recognizes Siaα2-6Gal/GalNAc, grouped together in the samples T3, T4, T6, T7, and T9 (Figure 2.13 B). Another grouping that included T3, T5, T8, and T9 had strong reactivity with DBA, which recognizes GalNAc, MAA, that binds

α2,3 sialic acid, and PTL-I, that reacts with a number of glycans including α-linked GalNAc, A-antigen, and Fucα1,2GalNAcα1,3Gal. A third grouping that included T1, T4, T6, T7, and T9 showed binding for VFA, LFA, and VVA. VFA recognizes Man>Glc>GlcNAc, LFA, binds sialic acid on O-linked glycans, and VVA reacts with Man. A fourth grouping that included samples T3, T5, T6, T8, and T9 had strong reactivity with DSA, which recognizes LacNAc (GlcNAcβ1-4Gal) and GlcNAcβ1-4GlcNAc oligomers. Together, these disparate patterns did not reveal an easily distinguishable glycosylation pattern for STB plasma membrane proteins.

2.4.3 Materials and methods

Isolation and labeling of STB plasma membranes

STB plasma membrane preparations were isolated as previously described (187) with minor modifications. Briefly, placental chorionic villi were manually dissected into 5-10 mm pieces, resuspended in ice-cold PBS containing a protease inhibitor cocktail (Pierce) and stirred for 1 hr. The samples were passed through a 70 μm filter and the membrane fraction was isolated by a series of centrifugation steps: 1000xg (10 min), 14,000xg (20 min) and 100,000xg (1 hr). Pellets were resuspended in PBS and dispersed by repeated aspiration with a 26-gauge needle. Protein concentrations were determined by using the Bradford assay (Bio-Rad). For labeling, one vial of Cy3 or Cy5 mono-reactive dye (GE Life Sciences) was resuspended in 12μl DMSO, and 4μl were used to label 320μg of protein at a concentration of 1mg/ml in 0.1M sodium carbonate buffer, pH 9.3. Samples were incubated for 30 min at room temperature (RT) and free dye was removed with Zeba desalt spin columns (Pierce). The A280, A552, and A650 were measured and the ratio of dye to protein was calculated.

Microarray hybridization and data analysis

The manufacture of lectin microarrays has been previously described (144). For single-color experiments, 10 µg of labeled cell sample in a final volume of 100 µl (in PBS) was added to each array. For two-color ratiometric analysis, 10 µg of each orthogonally labeled cell sample in a final total volume of 100 µl was used. The samples were hybridized to the slides by gentle rocking for 2 hr at RT. Then each microarray well was rinsed three times for three min with PBS containing 0.05% Tween 20 (PBST). Afterwards, the slides were immersed in PBS for 5 min, dried in a slide spinner and scanned using a GenePix 4100A fluorescent slide scanner (Molecular Devices). The data were extracted with GenePix Pro 5.1 software (Molecular Devices) and analyzed as previously described with an added normalization step. The median for each of the four data channels (Cy3 sample, Cy3 Reference, Cy5 sample, Cy5 Reference) was subtracted from each lectin rfu. Then, the Yang method (as described here 144) was used to calculate the dye-bias-corrected ratios. To create the hierarchical clustering map, Cluster 3.0 with Java TreeView (http://rana.lbl.gov/EisenSoftware.htm) was used.

2.5 CONCLUDING REMARKS

In this chapter, I described investigations into the sequestration of *P. falciparum* at the maternal-fetal interface. First, I expanded upon three previously published reports of STB denudation (40, 72, 204). This histopathology was significantly increased in infected placentas exposing villous core molecules, which should normally be masked, to maternal blood. Next, I immunolocalized receptors for *P. falciparum* in both uninfected and infected placentas. My results suggested that, in general, known receptors were only exposed to maternal blood in the setting of infection (either upon STB denudation or in association with leukocyte infiltrates).

I was particularly surprised to find that STBs do not express CS-A, since a large number of reports have suggested otherwise. Indeed, it appears that my results challenge a prevailing dogma that VAR2CSA-expressing iRBCs cytoadhere to CS-A, which according to two immunolocalization studies (131, 132), is expressed by STBs and by material in the intervillous space. Since maternal blood flows through the intervillous space at high sheer stress, it is particularly puzzling to understand how CS-A could localize to this location in healthy placentas. Intriguingly, Muthusamy *et al.* (131) demonstrated reactivity of anti-CS antibodies with healthy placentas only when they microwaved the tissues for "preservation of the fragile matrix-like materials in the intervillous space." I speculate that microwaving may change the biochemical make up of the tissue, perhaps inducing blood clotting or creating neo-antigens. In our experience, many antibodies react, presumably non-specifically, with clotted blood.

However, in my opinion, there is one possible explanation for these discrepancies. It has been reported (and I have visualized) what appear to be fibrin clots in *P. falciparum*-infected placentas. Fibrin is a fibrous protein, which together with platelets, form the basis of blood clots. Curiously, there are a handful of reports regarding CS-A expression by platelets (137, 206). One report showed that platelets release a peculiar chondroitin 4-sulfate proteoglycan upon aggregation (134). This CS proteoglycan only contained 5-6 chondroitin sulfate chains and consisted solely of 4-sulfated (CS-A) disaccharides, which suggested that it was a chondroitin 4-sulfate homopolymer. Thus, it seems plausible that CS-A-containing blood clots could accumulate in the intervillous spaces of infected placentas.

My immunostaining experiments with infected placentas did not directly address this possibility. Although I did not detect intervillous CS-A in infected samples with the antibodies that I employed (CS-56 and Ly111), it is unlikely that they would have reacted with chondroitin 4-sulfate homopolymers. Although I attempted to stain formalin-fixed,

paraffin-embedded infected samples with the 2-B-6 stub mAb (anti-proteoglycan ΔDi-4S), it reacted non-specifically with undigested negative control sections (*i.e.*, in the absence of chondroitinase ABC treatment) and was, therefore, unusable. As described earlier, this antibody did not react with paraformaldehyde-fixed/frozen, undigested, (negative control) samples and was, therefore, employed for the uninfected samples that were collected in San Francisco. Thus, while my results do demonstrate that chondroitin 4-sulfate homopolymers were not present in the intervillous spaces of uninfected samples, which were washed and not microwaved, they do not address whether these unusual CS-A chains are present in infected placentas. Since platelets and thrombosis have already been implicated in placental malaria, this would be a very interesting topic to explore further.

Although our glycan binding screen identified new candidate receptors that might mediate adhesion to the placenta, it also confirmed previous reports regarding cytoadhesion in the non-pregnant host. For example, *P. falciparum* binding to the blood group A antigen provides further evidence that this glycan mediates rosetting, a form of cytoadhesion in which a single iRBC binds multiple uninfected RBCs. Rosetting occurs more frequently *in vitro* with erythrocytes from individuals who express group A as compared to B or O, and enzymatic conversion of A to O abolishes rosetting (42). The results of the glycan array experiments also suggested other novel concepts. Specifically, we found additional evidence that iRBC sequestration resembles leukocyte recruitment. Ho *et al.* (89) demonstrated that iRBCs roll and tether on human blood vessels, which was blocked by anti-CD36 and anti-ICAM-1 antibodies. In addition to mimicking leukocyte behavior, our data suggested that iRBCs may bind the same carbohydrate epitopes that recruit leukocytes to high endothelial venules—sLe^x and sulfated sLe^x (120). It will be interesting to determine if function-perturbing antibodies that target these structures block iRBC adhesion to the microvasculature and/or the

placenta.

2.6 FIGURES AND TABLES

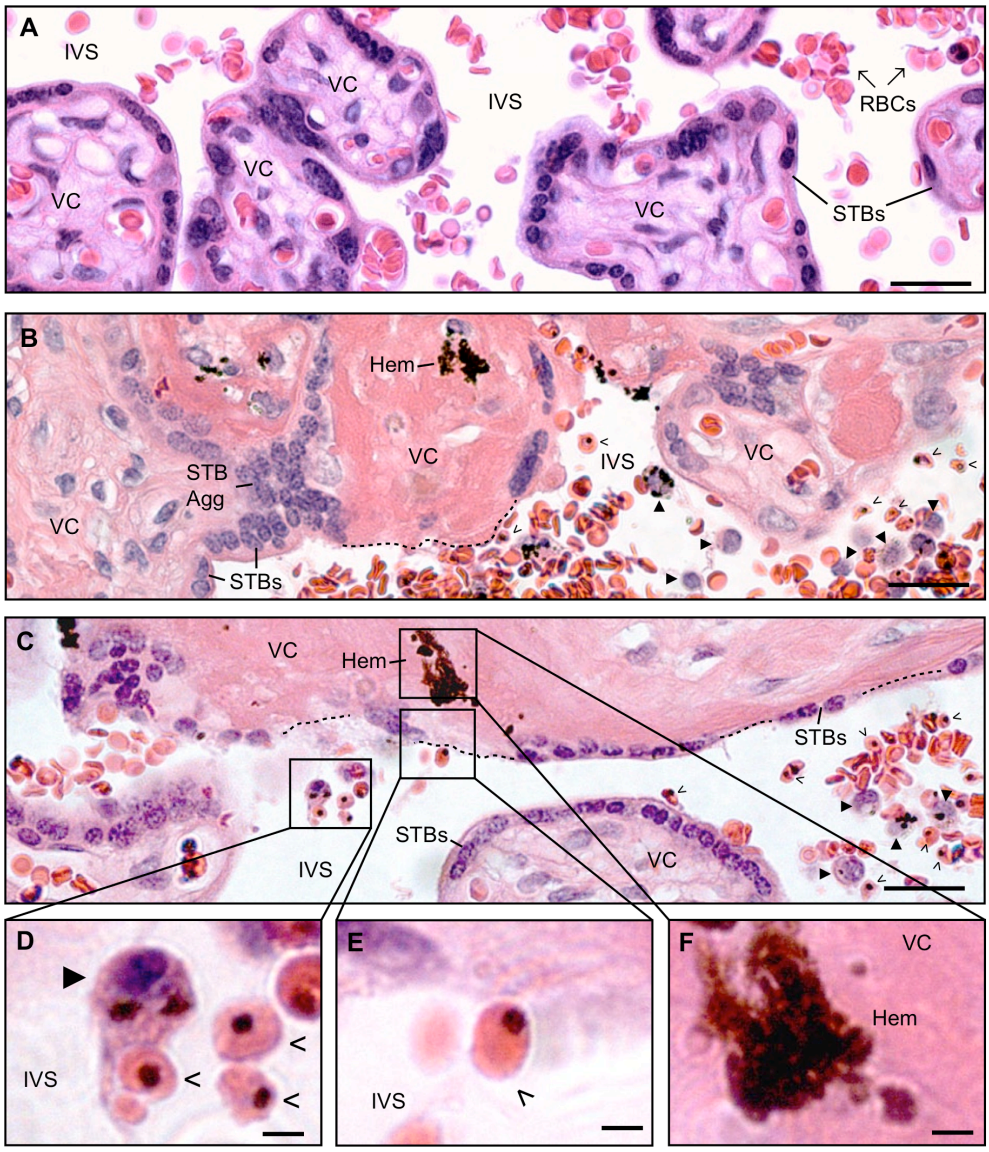

Figure 2.1 STB loss is a prominent histopathological feature of placental malaria.

In all instances, tissue sections of the placenta were stained with hematoxylin and eosin. 17 cases and an equal number of control samples from Kinshasa, the Democratic Republic of the Congo were analyzed. (A) In control, uninfected placentas, the villous core (VC), which contains stromal cells and fetal blood vessels, is covered by a continuous layer of multinucleated STBs. Maternal blood cells, primarily RBCs, occupy the intervillous space (IVS). (B-C) In *P. falciparum*-infected placentas, STB denudation (dotted lines) brought the VC into direct contact with the intervillous space. Some denuded villi were acellular and eosinophilic (intravillous fibrinoid) (B). In other instances, the exposed VCs resembled normal stroma (C). Additionally, STB aggregation (STB Agg) was commonly observed. Villi that displayed these pathological alterations often contained hemozoin (Hem). These regions were reservoirs for iRBCs (open arrowheads) and maternal leukocytes (closed arrowheads). (D) Cells, with the morphological appearance of monocytes (closed arrowhead) contained hemozoin and were found in close association with iRBCs (open arrowheads). (E) iRBCs were also observed adjacent to the VCs of denuded villi (F), which often contained hemozoin. Scale bars, 50μm A-C and 10μm D-F.

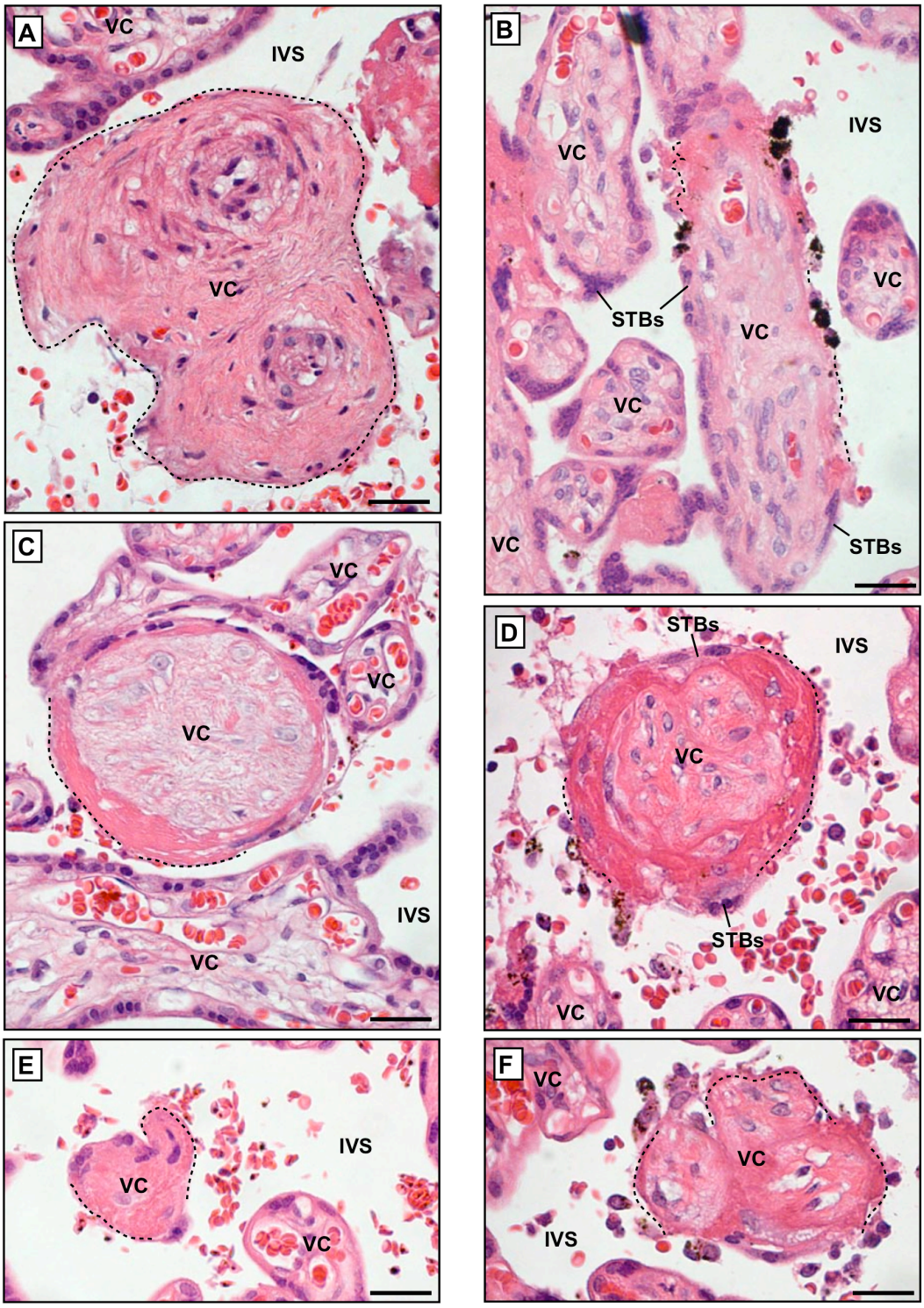

Figure 2.2 Additional examples of STB denudation.

Tissue sections of *P. falciparum*-infected placentas were stained with hematoxylin and eosin. In rare cases, villi were completely denuded of the STB layer (dotted lines, A). More commonly, STB denudation was focal (dotted lines, B-F). Some villous cores (VCs) resembled normal stroma (A). In other cases, the denuded villi were largely acellular and eosinophilic, consistent with intravillous fibrinoid (B-F). Perivillous fibrinoid was occasionally observed in association with STB loss. Scale bars, 40μm.

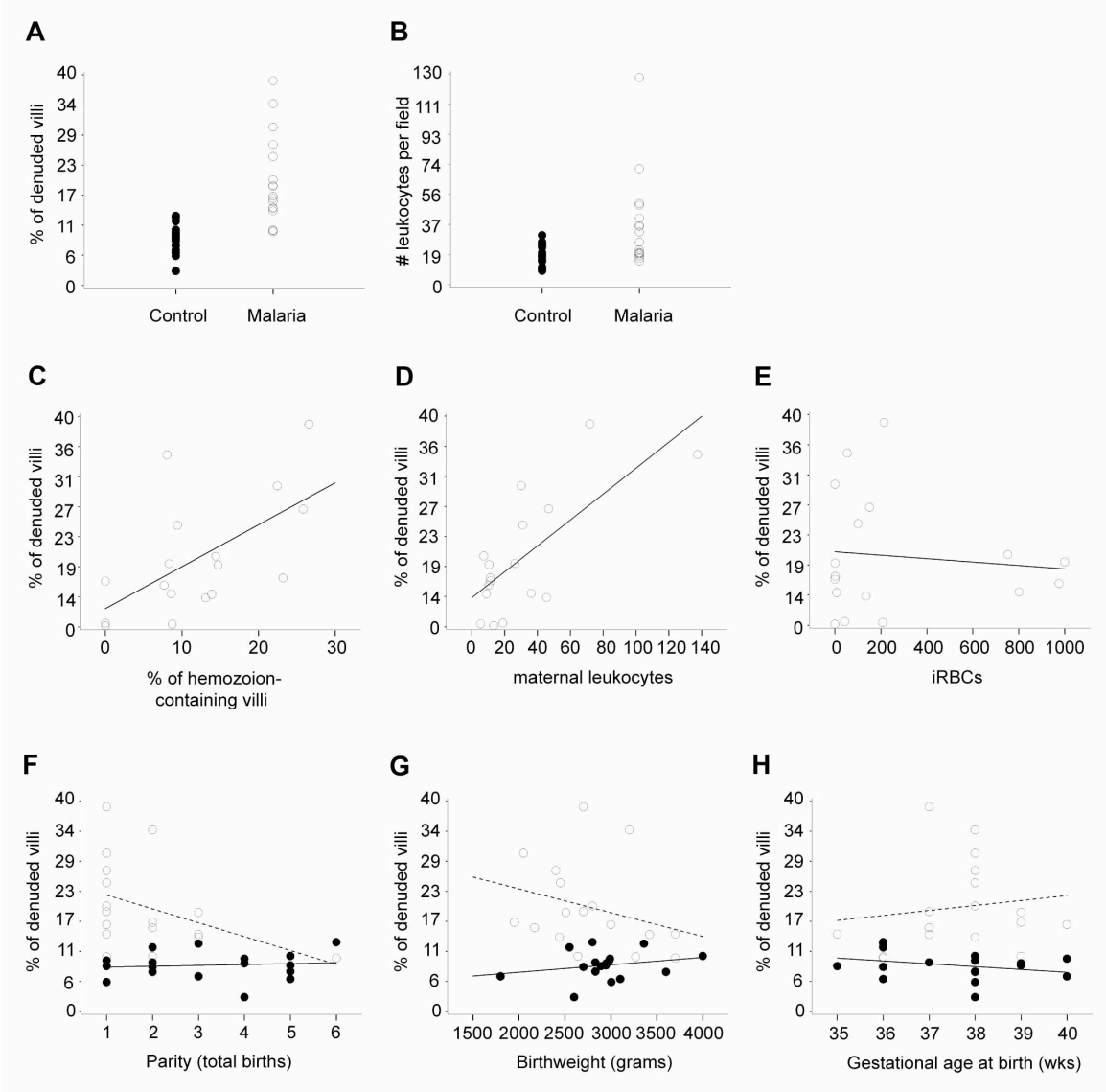

Figure 2.3 STB denudation was more common in placentas from primigravidae and associated with lower birthweights.

Controls and cases (n=17/group, 5 biopsies/organ collected from Kinshasa) were scored for histological changes. (A) STB denudation (# of denuded villi/total villi) was 11% higher in the cases versus controls (SE=2.2%, p<0.0001). The mean percentage of STB loss was 9.0% in controls (closed circles; range 3.0 to 13.0) and 17.0% in the malaria group (open circles; range 10.0 to 39.0). (B) Maternal leukocyte infiltration was 18% higher in the cases versus controls (SE=7.0%, p=0.01). The mean number of maternal leukocytes per 400x field was 18.0 in the controls (closed circles; range 8.6 to 30.5) and 26.3 in the malaria group (open circles; range 14.6 to 128.0). (C-E) Linear regression analysis was used to determine associations between STB denudation and infection or inflammation. STB loss was associated with (C) hemozoin (p=0.01) and (D) maternal leukocytes (p=0.001), but not with (E) iRBCs (p=0.88). (F-H) Linear regression analysis was also used to determine associations between STB denudation and clinical parameters. In the malaria group (open circles), STB loss decreased with (F) increasing parity (p=0.06) and (G) increasing birthweight (p=0.08). There was no relationship with (H) gestational age (p=0.81). These trends were not observed in control samples (closed circles).

Table 2.1. Characteristics of participants (Kinshasa, Democratic Republic of the Congo [-/+ malaria]).

	Control (-malaria) n=17	Infected (+malaria) n=17	
Characteristic	**Mean (SD)**		**P-value[1]**
Maternal age (years)	28.2 (6.2)	24.5 (4.4)	0.05
Gestational age at delivery (weeks)	37.5 (1.5)	37.6 (1.3)	0.81
Birthweight (grams)	2938 (464)	2771 (538)	0.34
	N (%)		**P-value[2]**
Preterm labor (<37 weeks)	6 (35%)	3 (18%)	0.44
Low birthweight (<2500 grams)	1 (6%)	6 (35%)	0.09
Primigravidae	3 (18%)	9 (53%)	0.07
Multigravidae	14 (82%)	8 (47%)	0.07

[1] For maternal age, gestational age at delivery, and birthweight, the p-values were derived from a T-test of differences in mean values in controls vs. malaria-infected cases.

[2] For preterm labor, low birthweight, and parity categories, the p-values were derived from a Fisher's exact test of differences of proportions in controls versus malaria-infected cases.

Table 2.2. Infection parameters and histopathological features (Kinshasa, Democratic Republic of the Congo [-/+ malaria]).

	Control (-malaria) n=17	Infected (+malaria) n=17	
Infection Parameters[1]	**Median (Min, Max)**		
iRBCs/400x field (#)	*na*	100.7 (0.07, 1000+)	
villi with hemozoin/total villi in a 400x field (%)	*na*	9.0 (0, 27.0)	
Histopathological Features[1]	**Median (Min, Max)**		**P-value**
leukocytes/400x field (#)	18.0 (8.6, 30.5)	26.3 (14.6, 128.0)	0.01
# villi with loss of STB/total villi in a 400x field (%)	9.0 (3.0, 13.0)	17.0 (10.0, 39.0)	<0.0001

[1] Descriptive statistics are based on means for 5 biopsies per placenta and 3 fields per biopsy

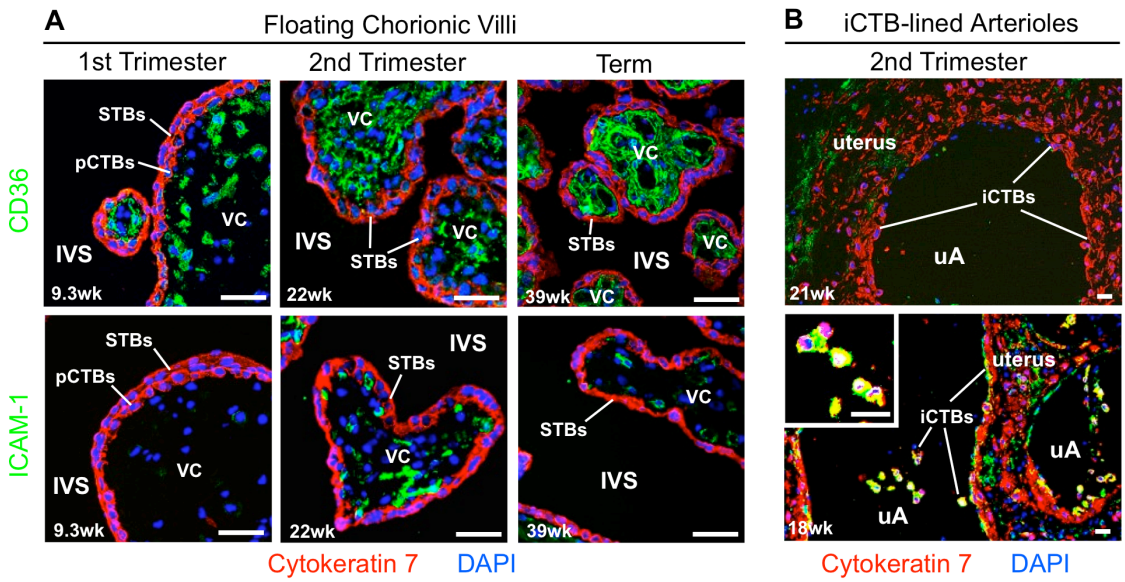

Figure 2.4 CD36 and ICAM-1 expression in relationship to the intervillous space during normal pregnancy.

Placental biopsies from uncomplicated pregnancies (first-trimester, second-trimester and term; n=3/group) were fixed in paraformaldehyde and frozen. Tissue sections corresponding to site 1 (panel A) and site 2 (panel B), as diagrammed in Figure 1.1 D, were analyzed. STBs and underlying pCTBs were visualized by staining with cytokeratin 7 (KRT7) (red). Nuclei were labeled with DAPI (blue). (A) In floating chorionic villi at all gestational ages, anti-CD36 Ab (green, top panels) reacted with the stromal villous cores (VCs); pCTBs and STBs failed to stain. ICAM-1 expression (green, bottom panels), which was more variable, was not detected in first-trimester samples. Patchy staining of the VCs was evident beginning in the second trimester. No staining of the trophoblast layers was observed. (B) iCTB invasion of uterine arterioles (uAs) peaks in the second trimester. Therefore, these analyses focused on 3 placental samples that were collected from this time period. In basal plate biopsies that contained iCTB-remodeled uAs, anti-CD36 Ab (top panel) and anti-ICAM-1 Ab (bottom panel) reacted with the uterine extracellular matrix (green). iCTBs that lined the uAs failed to express CD36 (top panel), but stained brightly for ICAM-1 (bottom panel), enlarged in inset. Scale bar, 40μm.

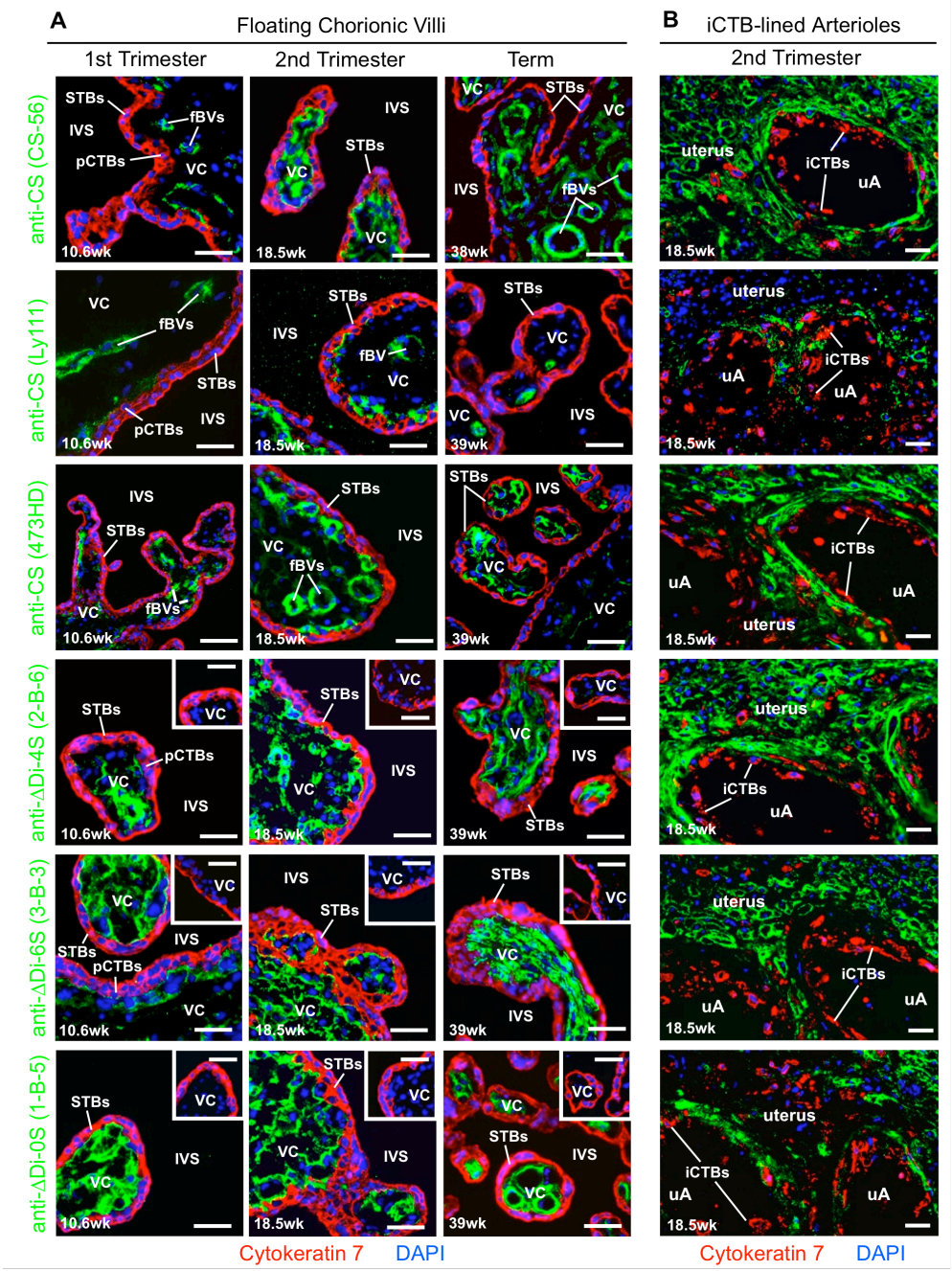

Figure 2.5 CS-A expression in relationship to the intervillous space during normal pregnancy.

Biopsies from two placental sites (see Figure 1.1 D) were analyzed using the experimental strategy described in Figure 2.4. At least three placentas were examined per trimester. (A) In floating chorionic villi, mAbs that specifically recognized CS-A (CS-56, LY111, 473HD), reacted with the villous cores (VCs) (green). Often times, intense immunostaining was observed in association with fetal blood vessels (fBVs). The stub mAbs (2-B-6, 3-B-3, 1-B-5), which recognized epitopes exposed by chondroitinase ABC digestion, also reacted with the VCs (green). In general, control tissue sections that were not digested with chondroitinase ABC, did not stain (insets). None of the mAbs stained STBs or pCTBs, which were labeled with an anti-KRT7 mAb (red). (B) In second-trimester basal plate biopsies that contained iCTB-remodeled uterine arterioles (uAs), the anti-CS-A mAb panel reacted with the uterine extracellular matrix, but failed to stain iCTBs that lined the uAs. Scale bar, 40μm.

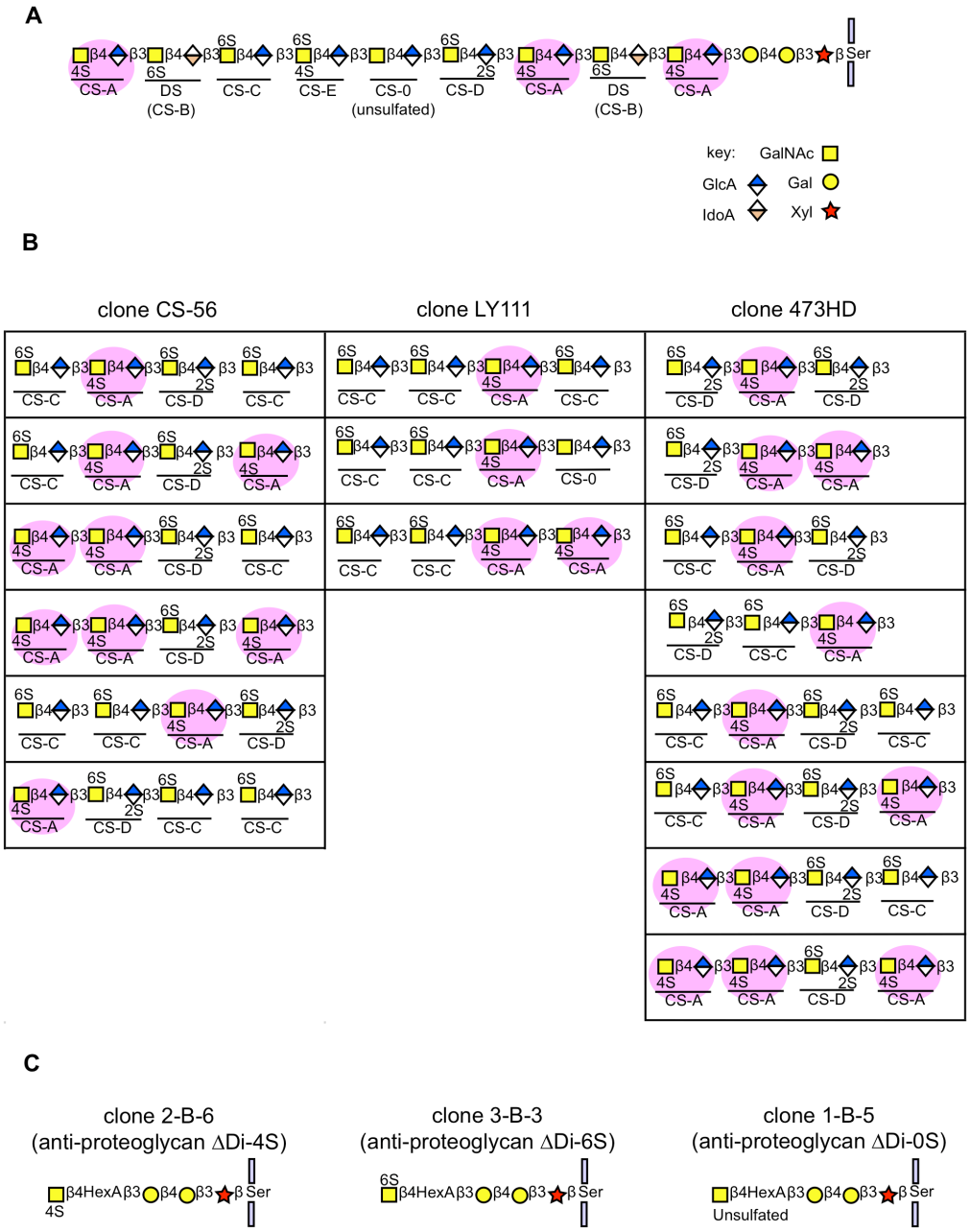

Figure 2.6 Specificities of anti-chondroitin sulfate mAbs.

(A) CS-GAGs are unbranched polysaccharides of variable length consisting of repeating disaccharide units of D-glucuronic acid (GlcA) and *N*-acetyl-D-galactosamine (GalNAc). CS-GAGs contain a heterogeneous mixture of CS and dermatan sulfate (DS) disaccharides. CS disaccharides are named according to the position of sulfation: C-4 of GalNAc (*i.e.*, chondroitin-4-sulfate/CS-A), C-6 of GalNAc (*i.e.*, chondroitin-6-sulfate/CS-C), both substituents of GalNAc (*i.e.*, chondroitin-4,6-sulfate/CS-E) and C-6 of GalNAc plus C-2 of GlcA (*i.e.*, CS-D). (B) Oligosaccharides recognized by CS-56, LY111, and 473HD mAbs. CS-56 and 473HD recognize epitopes that contain the A-D core tetrasaccharide (47, 95, 190); Ly111 reacts with chains that contain a CS-A motif (47, 190). CS-A disaccharides are marked with pink circles. (C) Stub epitopes, created by chondroitinase ABC digestion, are recognized by mAbs 2-B-6 (left), 3-B-3 (middle) and 1-B-5 (right) (37 *the specificity of 2-B-6 is the same as 9-A-2, 145). Hexuronic acid (HexA) represents glucuronic acid if it was a CS chain, or iduronic acid if it was a DS chain. Additional information regarding these mAbs can be found on the Seikagaku website: http://www.seikagaku.co.jp/english/.

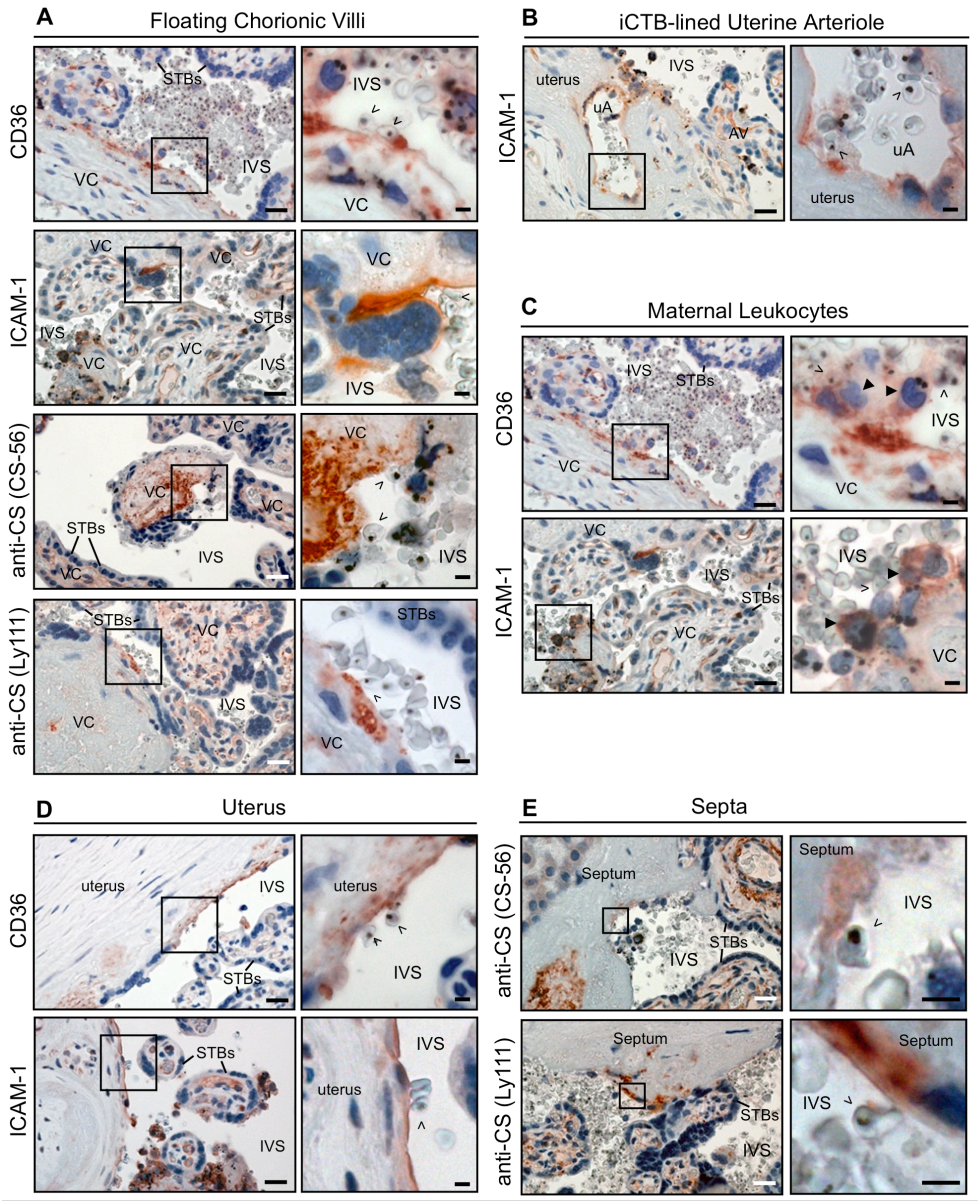

Figure 2.7 CD36, ICAM-1 and CS-A expression in relationship to the intervillous space during malaria infection.

P. falciparum-infected term placentas (n=4) were formalin-fixed and paraffin-embedded. Binding of primary antibodies was detected with biotin-conjugated secondaries followed by ABC-peroxidase, and visualized using a 3-amino-9-ethylcarbazole (AEC) substrate (red color). Sections were counterstained with hematoxylin (blue). Boxed area in left panel is enlarged as right panel. (A) In floating chorionic villi, villous core (VC) regions that were denuded of STBs expressed CD36. STBs exhibited patchy ICAM-1 immunoreactivity. Antibodies that specifically recognized CS-A (CS-56 and Ly111) also reacted with denuded VC regions (bottom panels). (B) As shown for normal samples collected in San Francisco (see Figure 4B), iCTBs that lined uterine arterioles (uAs) expressed ICAM-1. Anchoring villus, AV. (C) Maternal leukocytes in the intervillous space (IVS) with the morphological appearance of monocytes (closed arrowheads) stained for CD36 (top panel) and ICAM-1 (bottom panel). Often, these cells formed a bridge between iRBCs (open arrowheads) and STBs. (D) The portion of the uterus that lines the intervillous space expressed CD36 (top panel) and ICAM-1 (bottom panel). (E) Uterine septa (see Figure 1B) that were continuous with the intervillous space, stained for CS-A, which was detected with the CS-56 and LY111 antibodies. Scale bars, 50μm for lower magnification and 10 μm for higher magnification micrographs.

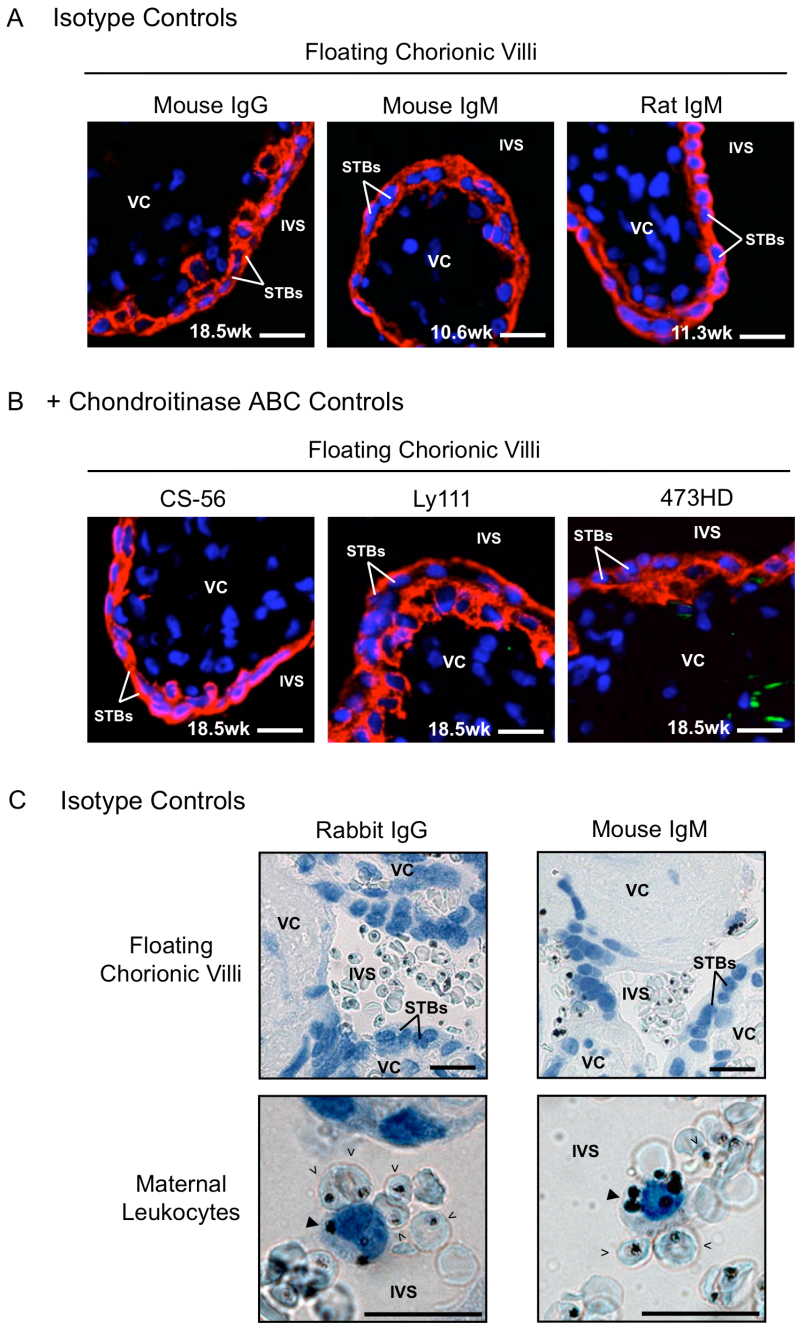

Figure 2.8 Staining controls

(A-B) Biopsies were analyzed using the experimental strategy described in Figure 2.4 (A & B) or Figure 2.7 (C). (A) In frozen sections, mouse IgG (left), mouse IgM (middle) and rat IgM (right) isotype control antibodies were used to monitor binding via fetal Fc receptors. (B) Antibody specificity for CS-GAGs was monitored by digesting sections with chondroitinase ABC prior to staining with CS-56 (left), Ly111 (middle) and 473HD (right). (C) In paraffin-embedded sections, rabbit IgG (left) and mouse IgM (right) isotype control antibodies were used to monitor binding via fetal Fc receptors on chorionic villous cells (top) and maternal leukocytes (bottom). Scale bars, 40μm.

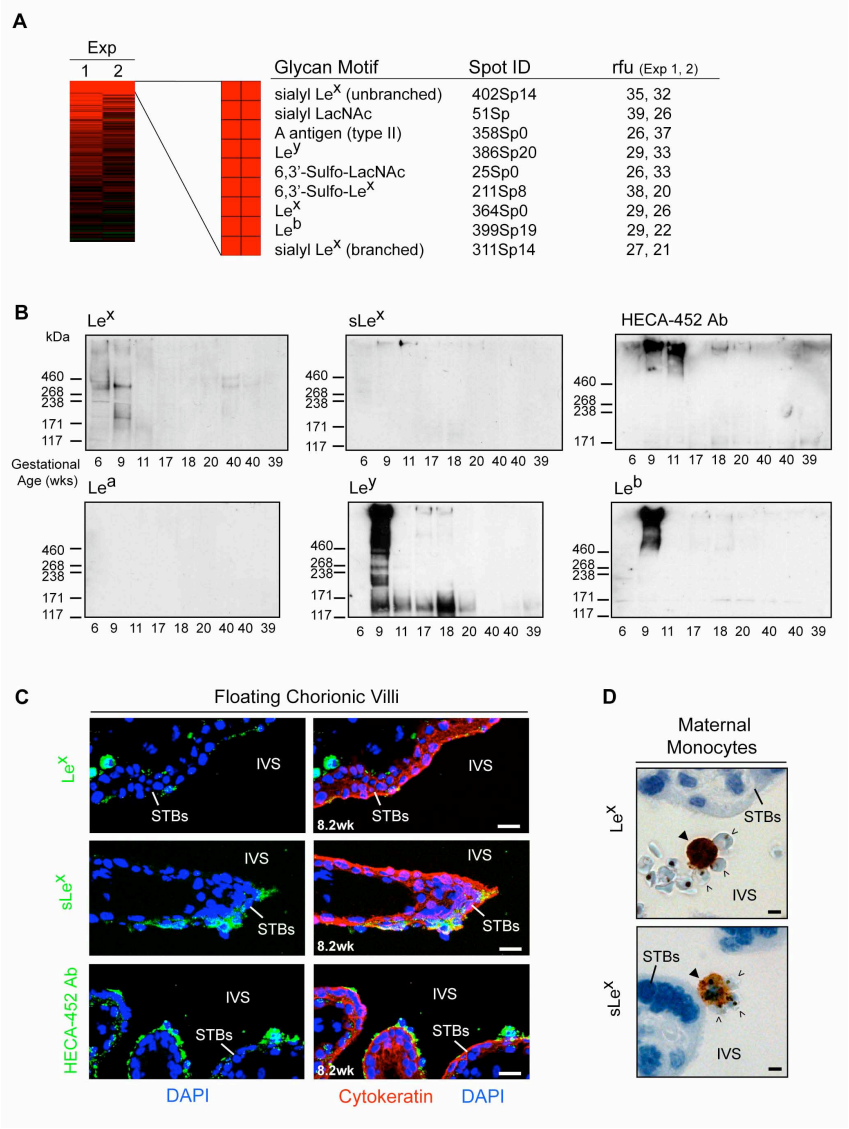

Figure 2.9 A glycan binding screen reveals a role for Lewis carbohydrate antigens in cytoadhesion.

(A) Fluorescently-labeled iRBCs were bound to a glycan array that contained 377 structures. An annotated heat map of potential *P. falciparum* binding partners that were detected in both experiments (Exp 1, 2) is shown. These included a preponderance of Lewis blood group structures. Relative fluorescent units (rfu) were computed as the foreground minus background intensity. B) STB plasma membrane fractions (n=9) were isolated from placentas of the gestational ages shown, separated by SDS-PAGE, and probed with mAbs that recognized the glycans that iRBCs bound on the arrays. First-trimester placentas had appreciable levels of Le^x, sLe^x, and sulfated Le^x (detected with HECA-452 Ab) expression (top blots). Ab reactivity declined with advancing gestational age. In contrast, Le^a expression was not detected (bottom, left). Le^y (bottom, middle) immunoreactivity was observed in most samples collected during the first half of pregnancy, while Le^b (bottom, right) expression was primarily confined to a 9-week preparation. (C) First-trimester placental biopsies from uncomplicated pregnancies (n=4) were fixed in paraformaldehyde, frozen, and analyzed using the experimental strategy described in Figure 4. In floating chorionic villi, STBs exhibited patchy Le^x (top panel) and sLe^x (middle panel) expression (green). STBs uniformly stained for sulfated sLe^x (green, bottom panel). Scale bar, 20μm. (D) *P. falciparum*-infected, term placentas (n=4) were formalin-fixed and paraffin-embedded, and analyzed as described in Figure 6. Maternal leukocytes closed arrowheads), expressed Le^x (top panel) and sLe^x (bottom panel). iRBCs (open arrowheads) were found in close association with these cells. Scale bar, 10μm.

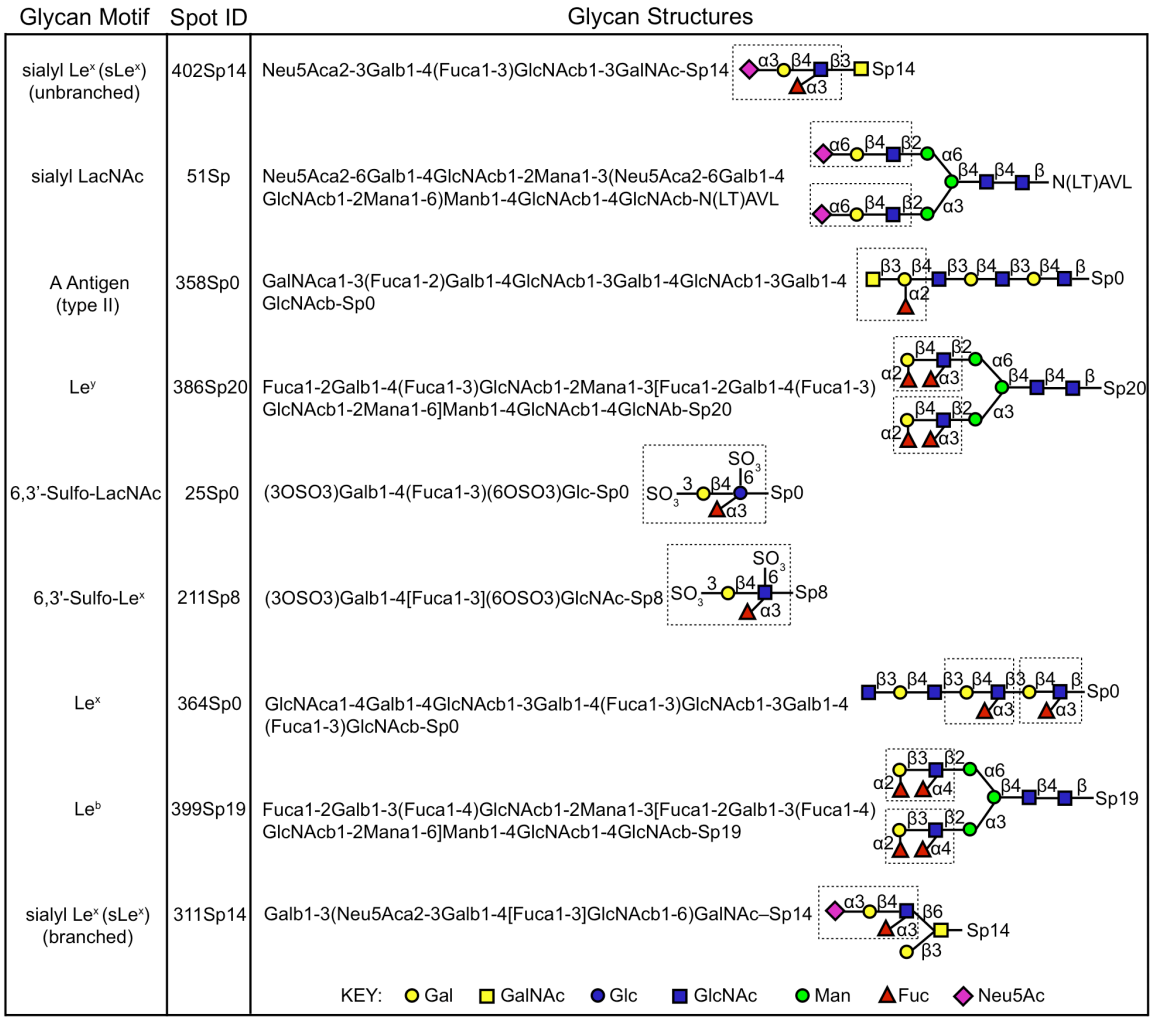

Figure 2.10 iRBC glycan binding partners.

iRBCs bound oligosaccharides that contained Lewis (Le) antigens and related lactosamine (LacNAc) motifs. Spot identities (spot ID column) were assigned by the Consortium for Functional Glycomics. The structures that were spotted on the array are listed in the third column; boxes outline specific carbohydrate motifs. Galactose, Gal. N-acetyl galactosamine, GalNAc. Glucose, Glc. N-acetyl glucosamine, GlcNAc. Mannose, Man. Fucose, Fuc. Sialic acid, Neu5Ac.

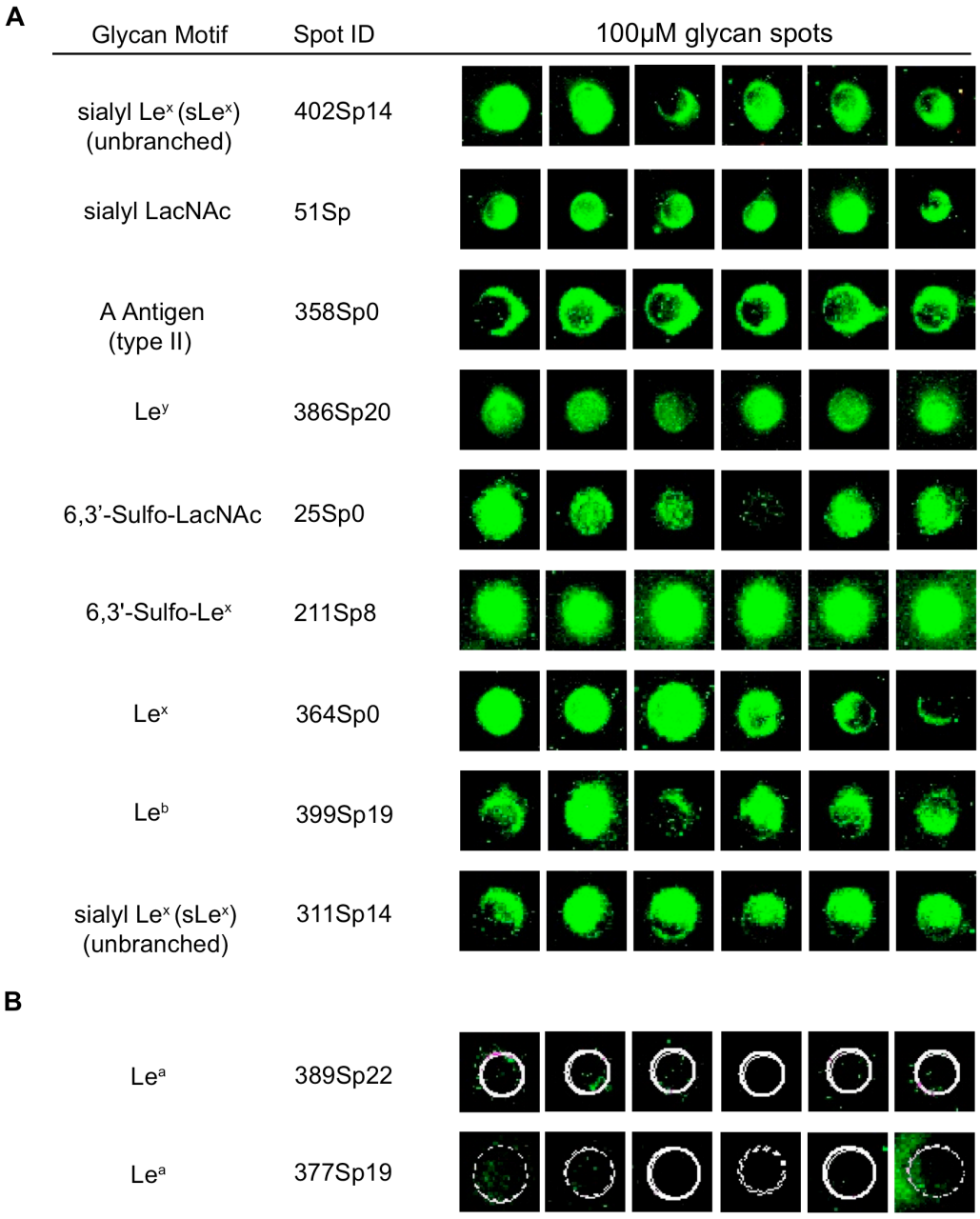

Figure 2.11 iRBCs bound reproducibly to glycan spots.

(A). The same oligosaccharide was spotted in six locations on each slide. Data are representative of two independent binding experiments. In general, iRBCs bound in a reproducible manner to the glycans shown. (B) iRBCs failed to bind two spots that contained Le^a, which was not expressed by STBs (see Figure 2.9).

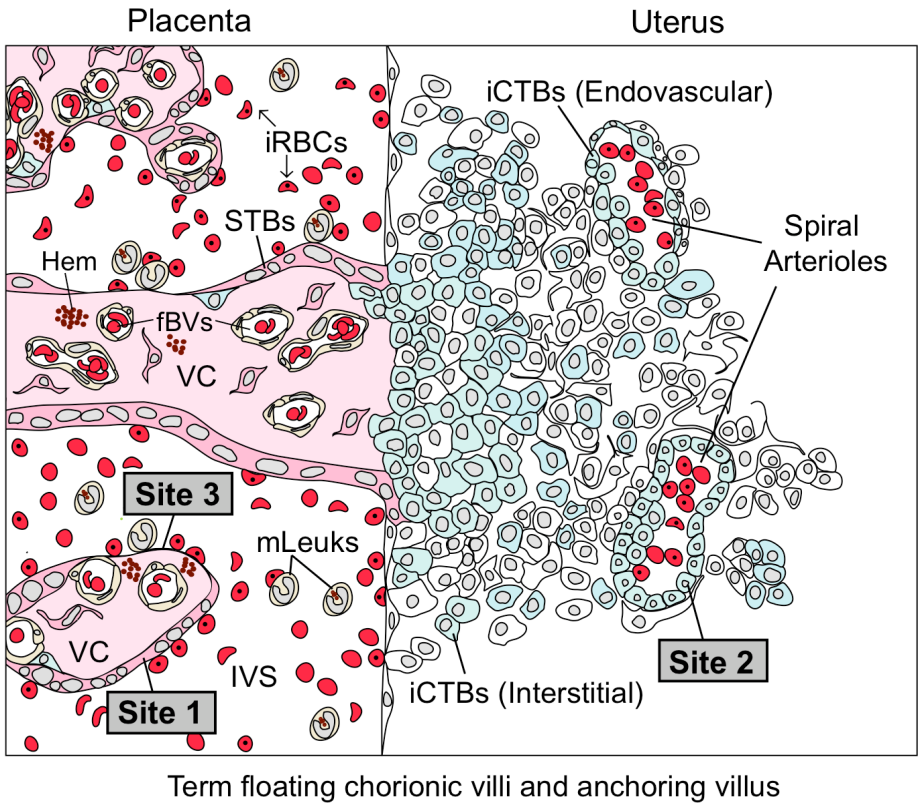

Figure 2.12 A model for *P. falciparum* sequestration by the human placenta.

At a microanatomical level, *P. falciparum* infection changes the repertoire of placental tissues that are in direct contact with maternal blood. In this context, binding to syncytiotrophoblasts (STBs; site 1) and/or invasive cytotrophoblasts that line uterine vessels (iCTBs; site 2) initiates infection. At later stages, STB denudation brings site 3, the villous core (VC), into direct contact with maternal blood. At a molecular level, our findings suggest that infection is initiated when iRBCs adhere to STBs via Lewis (Le) blood group antigens (site 1), which support *P. falciparum* adhesion in vitro, and/or to endovascular iCTBs that line uterine arterioles and express ICAM-1 (site 2). As infection progresses, cytoadherence to STBs might also occur via ICAM-1, which is upregulated in other settings by the pro-inflammatory cytokines TNF-α and IL-1. Advanced stages of placental malaria are associated with hemozoin (Hem) and STB denudation, which exposes villous CD36 and CS-A to maternal blood (site 3). Placenta-associated maternal leukocytes (mLeuk) could also participate in adherence because they express CD36, ICAM-1, and Le antigens.

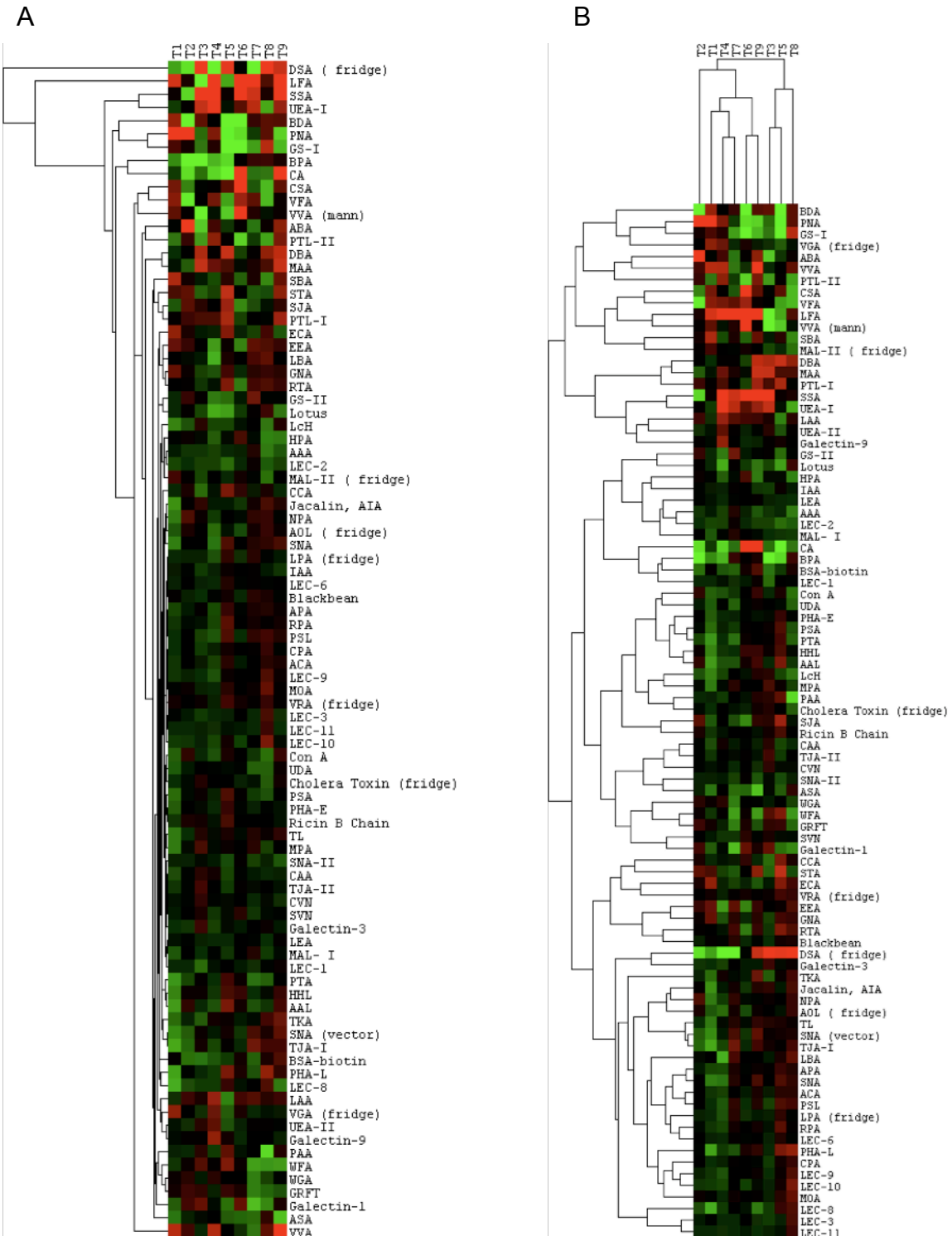

Figure 2.13 Glycopattern of STB plasma membranes as revealed by lectin blotting.

STB plasma membrane preparations were labeled with Cy3 and Cy5 mono-reactive dyes and profiled on lectin microarrays. (A) Data were normalized, but not clustered. (B) Data were normalized and clustered.

Table 2.3 Lectin Specificities (generously provided by Dr. Mahal)

Lectin	Abbreviation	Specificity
Aleuria aurantia	AAL	αFuc
Amaranthus Caudatus	ACA	GalNAc or clusters of Galb1,3GlcNAc
Aspergillus oryzae	AOL	αFuc 1,6 preferred (core fucosylation), some recognition of 1,2 off of Gal
Anguilla anguilla	AAA	αFuc
Agaricus bisporus	ABA	Galb1-3GalNAc
Artocarpus intergrifolia (Jacalin)	AIA	αGalNAc not substituted at C-6 (*e.g.*, core 1, 3, T-antigen but not core 2).
Abrus precatorius	APA	Galb-1,3GalNAc (TF antigen) > Gal (LacNAc on N-linked core)
Aegopodium podagaria	APP	GalNAc
Allium sativa	ASA	High mannose chains (Man9-GlcNAc2..)
Bryonia dioica	BDA	GalNAc
Black Bean	Black Bean-Crude	GalNAc
Bauhinia purpurea		Primarily Gal b1,3or 1,4 but will also bind b-GalNAc more weakly
Colchicum autumnale	CA	Terminal Galb-OR? (GalNac alpha and beta-CFG)
Caragana arborescens	CAA	GalNAc/Gal (monosaccharides best)
Cancer antennarius	CCA	9-O-Acetyl Sia and 4-O-Acetyl Sia
Canavalia ensiformis	Con A	branched and terminal mannose, terminal GlcNAc
Cicer arietinum	CPA	Complex
Cicer arietinum	CPA	Complex
Cystisus scoparius	CSA	b-GalNAc, terminal
Dolichos biflorus	DBA	GalNAca-OR
Datura stramonium	DSA	GlcNAcb-1,4GlcNAc oligomers and LacNAc
Erythrina cristagalli	ECA	Galb1,4GlcNAc
Euonymus eurpaeus	EEA	Blood Groups B and H
Galanthus nivalis	GNA	terminal a-1,3 mannose
Griffonia simplicifolia I	GS-I	αGal
Griffonia simplicifolia II	GS-II	terminal GlcNAc
Amarylis Lectin	HHL	αMan not Glc (1,3 and 1,6)
Homaris americanus	HMA	sialic acid
Helix pomatia	HPA	αGalNAc terminal
Iberis Amara	IAA	GalNAc
Laburnum alpinum	LAA	GlcNAc oligomers
Phaseolus lunatus	LBA	GalNAcα1,3[Fucα1,2]Gal
Lens culinaris	LcH	Complex (Man/GlcNAc core with or without α1,6 Fuc)
Lypersicon esculentum	LEA	β1,4GlcNAc oligomers

Limax flavus	LFA	αSia (O-glycans)
Lotus tetragonolobus	Lotus (LTL)	Terminal αFuc, Lex
Limulus polphemus	LPA	α sialic acid
Maackia amurensis	MAA	α2,3 sialic acid
Maackia amurensis -I	MAL-I	LacNAc (1-4) structures that can contain sialic acid
Maackia amurensis -II	MAl-II	α2,3 sialic acid-LacNAc structures
Macluria Pomifera	MPA	GalNAcalpha1-->Ser/Thr (Tn) and Galbeta1-->3GalNAcalpha1-->Ser/Thr (T alpha)
Marasimus oreades	MOA	Ga1α1,3Ga1-containing sugar epitopes, including but not limited to Ga1α1,3Ga1β1,4G1cNAc. (blood group B)
Narcissus pseudonarcissus	NPA	terminal and internal Mannose
Persea Americana	PAA	unknown
Pisum sativum	PEA, PSA	mannose
Phaseolus vulgaris-L	PHA-E	Gal
Phaseolus vulgaris-L	PHA-L	β1,6 branched trimannosyl core N-linked glycans
Arachis hyogaea	PNA	terminal Galb-OR
Polyporus Squamosus	PSL	α2,6 sialic acid
Psophocarpus tetragonolobus	PTL-I	αGalNAc, A-antigen, Fucα1,2Gal(NAc preferred)α1,3Gal, Galα1,3GalNAc
Psophocarpus tetragonolobus	PTL-II	βGalNAc (Vector), Fuc alpha 1,2 Gal beta 1,4 GlcNAc (CFG, like UEA-I)
Psophocarpus tetragonolobus	PTA galactose	Gal
Robinia pseudoacacia	RPA	complex
Trifolium repens	RTA	2-deoxy-Glu
Glycine max	SBA	terminal GalNAc
Sophora japonica	SJA	GalNAc
Sambucus nigra	SNA	α2,6 sialic acid or 6-sulfation on gal (Lac core)
Sambucus nigra	SNA-II	The lectin's binding site appears to be most complementary to Gal-NAc linked alpha to the C-2, C-3, or C-6 hydroxyl group of galactose.
Sambucus sieboldiana	SSA	Siaα2-6Gal/GalNAc
Solanus tuberosum	STA	GlcNAc oligomers (LacNAc,or LacdiNAc where both gal and glc have Nac, can be substituted, residual high mannose-CFG)
Trichosanthes kirilowii	TKA	βGal, LacNAc but Siaα2,3 or 2,6 inhibits best
Trichosanthes japonica	TJA-I	Siaα2,6LacNAc or 6-sulfo LacNAc
Trichosanthes japonica	TJA-II	Fuca1,2 Galb1,3/4-GlcNAc or GalNAcb1,4-Galb1- A series of oligosaccharides possessing Fuca1,2Galbl3/4 or GalNAcbl+ groups at their nonreducing terminals showed stronger binding ability than ones with Galb1-GlcNAc (Glc) groups
Tulipa sp.	TL	GlcNAc/Man
Uritica dioica	UDA	GlcNAcβ1,4GlcNAc oligomers, LacNAc, high mannose
Ulex europaaeus I	UEA-I	αfucose
Viscum album	VAA	Gal
Vicia fava	VFA	Man>Glc>GlcNAc

Vicia graminea	VGA	O-linked Galb-1,3GalNAc clusters
Vigna radiata	VRA	αGal
Vicia villosa	VVA (man)	Man
Vicia villosa	VVA (VVL on array?)	GalNAc
Wisteria floribunda	WFA	GalNAc
Tritiicum vulgare	WGA	βGlcNAc, sialic acid, GalNAc

CHAPTER 3. HEMOZOIN-POSITIVE SYNCYTIOTROPHOBLASTS AND CD68+ CELLS ARE INCREASED IN PLACENTAS FROM PRIMIGRAVIDAE AND SECUNDIGRAVIDAE

3.1. INTRODUCTION

3.1.1 Introduction to hemozoin as a marker of placental malaria

P. falciparum infection during pregnancy is most common in primigravid mothers and reduces infant birthweights (163). Histological signs of infection include the accumulation of *P. falciparum*-infected erythrocytes in the maternal blood spaces of the placenta (*i.e.*, the intervillous space) and the deposition of hemozoin, the byproduct of intraerythrocytic heme digestion by *Plasmodium* parasites. Malarial pigment is an inert crystalline molecule, which accumulates for an unknown period of time and can be used to determine prior malaria infection (reviewed by 192). The pigment is observed within maternal macrophages/monocytes, which are recruited to the intervillous space during infection (165, 204), and within eosinophilic, acellular material consistent with intravillous and perivillous fibrinoid (28, 41, 71, 204).

Numerous groups have also described punctate parasite pigment within villous cells, including fetal syncytiotrophoblasts (STBs) and mesenchymal cells (28, 41, 71, 72, 108, 204, 215). STBs cover the chorionic villi and form a transport epithelium. These cells clearly display hemozoin in their cytoplasm (110) and it is well documented that they exhibit micropinocytotic activity, which allows them to uptake material (15). It has been suggested that the hemozoin-positive mesenchyme may be Hofbauer cells (72, 108), the fetal/embryonic macrophage, but this has not been confirmed by immunostaining. Hofbauer cells reside within the villous core and are phagocytic. To our knowledge, it has not been determined whether pigment engulfment by villous cells is

focal or widespread.

In addition to being a histological marker of infection, there is some indication that hemozoin adversely affects pregnancy outcome. For example, hemozoin in intervillous monocyte/macrophages has been associated with lower infant birthweights (165, 209). As to a mechanism of action, there is evidence that hemozoin impairs effector function (177, 178) and influences chemokine and cytokine production in monocytes/macrophages (122). Recently, an *in vitro* study demonstrated that term trophoblasts also secreted chemokines in response to hemozoin (110). Finally, hemozoin and associated free radicals might be directly toxic (138).

Here, we co-localized hemozoin with cytokeratin 7 (KRT7)+ STBs and mesenchymal cells that expressed CD68—in this location, a marker of fetal Hofbauer cells. Next, we determined the frequency of hemozoin uptake by villous cells and carried out regression analyses to determine associations with parity, infant birthweight, and gestational age. Finally, we showed that total numbers of CD68+ mesenchymal cells were significantly increased in *P. falciparum*-infected placentas as a function of parity.

3.2 RESULTS AND DISCUSSION

3.2.1 Characterization of hemozoin-positive villous cells

Villous KRT7+ STBs and CD68+ cells contain parasite pigment.

Initially, we carried out a morphological analysis of *P. falciparum*-infected placentas (see Chapter 2 for more details). Samples were collected from Kinshasa, Democratic Republic of the Congo (n=17 cases and 17 uninfected controls) and consisted of five full-depth biopsies, two from the center and three from the periphery of each placenta. Control term placentas had the expected cellular composition, *i.e.*, a

villous core composed of stromal cells and fetal blood vessels completely surrounded by a covering of multinucleated STBs (see Figure 1.1). As previously reported (28, 41, 71, 72, 108, 204, 215), pigment-containing STBs and mesenchymal cells were observed in the *P. falciparum*-infected placentas, but not in the controls. When we immunolocalized KRT7, a marker for STBs, we confirmed that in some cases, hemozoin was present in these cells (Figure 3.1 A-C). Staining for CD68, which marks macrophages/monocytes, demonstrated that pigment was also associated with these cells (Figure 3.1 D-E). It is generally accepted that CD68+ mesenchymal cells are Hofbauer cells, the fetal/embryonic macrophage of the placenta (15). Together, these results demonstrated that STBs and CD68+ cells in the chorionic villi engulf hemozoin.

Pigmented STBs and CD68+ cells are increased in placentas from primigravidae and secundigravidae.

Next, we quantified the observed pigmentation and carried out regression analyses to determine associations with clinical parameters. The mean number of pigmented STBs per 400x field was 2.5, range of 0 to 6 (Figure 3.1 G). Hemozoin-positive STBs were associated with placentas from primigravidae and secundigravidae (linear trend p=0.01, 2 vs. 1 p=0.06, > 2 vs. 1 p=0.0004; Figure 3.1 H). No association was detected with birthweight or gestational age (data not shown). The mean number of pigmented mesenchymal cells per 400x field was 1.2, range of 0 to 2.8 (Figure 3.1 I). Similarly, hemozoin-positive mesenchymal cells were associated with placentas from primigravidae and secundigravidae (linear trend p=0.04, 2 vs. 1 p=0.07, > 2 vs. 1 p=0.02; Figure 3.1 J). No relationship with birthweight or gestational age was observed (data not shown). As expected, pigmented villous cells were not observed in uninfected control placentas. Together, these results suggested that pigmented STBs and CD68+ cells are more commonly observed in placentas from primigravidae and secundigravidae

than multigravidae.

3.2.2 Analysis of total numbers of villous CD68+ cells

CD68+ cells are increased in infected placentas from primigravidae and secundigravidae.

Our CD68 immunolocalization studies led us to hypothesize that total numbers of Hofbauer cells might be increased in the setting of malaria. To address this question, we immunostained infected and uninfected placentas and quantified the number of CD68+ cells. As shown in Figure 3.2, these cells were more prevalent in some *P. falciparum*-infected placentas (panel B) as compared to controls (panel A). When we separated our findings based on parity, we found that CD68+ cells were significantly increased in infected placentas from primigravidae and secundigravidae (red bars) compared to controls (black bars) ($p<0.05$; 1 & 2 bars, Figure 3.2 C). No difference was found between cases and controls in samples from multigravidae (> 2 bars, Figure 3.2 C). Together, these data suggested that CD68+ cells were increased in groups that are known to be susceptible to severe forms of malaria.

3.2.3 Discussion of findings

It is well appreciated that hemozoin accumulates in *P. falciparum*-infected placentas for an unknown period of time. In addition, pigment has been observed in villous cells, which based on location and morphology, are consistent with STBs (110) and Hofbauer cells (72, 108). Here, we used immunostaining to confirm that the pigment-containing cells are STBs and CD68+ macrophages (Figure 3.1). We also showed that hemozoin engulfment by these cells occurs more frequently in placentas from primigravidae and

secundigravidae than in multigravidae. We suspect that these phenomena signify severe infection, which is more prevalent in lower parity groups.

Our data suggested that STBs micropinocytosed free pigment and/or iRBCs. *In vitro* infection experiments with cultured villous explants could be used to determine if both events occur. Since hemozoin may be toxic and inflammatory (see Introduction), it is intriguing to speculate that STB engulfment of pigment and/or iRBCs might directly harm these cells. Galbraith *et al*. (72) suggested that this phenomenon could be toxic, and it is intriguing to speculate that pigmentation might promote STB necrosis and denudation, a histopathological change that I discussed in Chapter 2.

CD68+ Hofbauer cells, the fetal/embryonic version of the macrophage, are by definition phagocytic. However, it is unclear how these cells gain access to malarial pigment, which should theoretically be restricted to the intervillous space and to a lesser extent, to STBs (see Figure 3.1). One possibility is that Hofbauer cells survey STBs that form the outer perimeter of the villi and engulf hemozoin-containing material within these cells. Subsequently, they might migrate back to the villous core. Thus, large deposits of hemozoin, which are often observed in association with fibrinoid necrosis, might be remnants of pigmented CD68+ Hofbauer cells.

Here, we demonstrated that placentas from primigravidae and secundigravidae contained increased numbers of villous CD68+ cells (Figure 3.2). It is intriguing to speculate that this may represent the fetal immune system response to infection. The origin of Hofbauer cells is not fully understood. It has been suggested that these cells differentiate from mesenchymal cells in the first part of pregnancy before the fetal circulation is established (for review see 15). More recently, Barcena *et al*. showed that the human placenta is a source of multipotent hematopoietic progenitors throughout gestation (5). In addition, they could also be mobilized from the fetal bloodstream as gestation advances (15). Interestingly, maternal cells have been reported to traffic

across the placenta (98); therefore, we cannot exclude the possibility that some of the CD68+ villous cells are maternal macrophages. Genotyping experiments would address this possibility. Either way, it would be extremely interesting to investigate this phenomenon further.

3.3 MATERIAS AND METHODS

Human subjects

This study was approved by the Kinshasa School of Public Health Ethics Committee and the University of California, San Francisco Committee on Human Research. Written informed consent was obtained from all participants.

Recruitment of participants

Patients were recruited as described in Chapter 2.

Tissue sampling and handling

Placentas were collected and biopsied as described in Chapter 2.

Immunolocalization

Tissue sections were deparaffinized and rehydrated in a series of graded ethanol solutions. Antigens were retrieved by heating for 30 min at 95°C in 10 mM sodium citrate and 0.05% Tween 20 (pH 6.0). Endogenous peroxidase activity was blocked by incubation in 0.3% H_2O_2 (30 min at RT). Signals from native IgG bound to fetal Fc receptors were blocked by incubation with goat or donkey anti-human IgG (1.0 µg/ml; Jackson ImmunoResearch; 1 hr at RT). To block unoccupied Fc receptors, samples were incubated in 1.5% serum from the species in which the secondary antibody was produced. Tissues sections were incubated overnight at 4°C with mouse anti-KRT7 (OV-

TL 12/30; 1:100 cell culture supernatant; Dako) or mouse anti-CD68 (KP1; 9.4 µg/ml; Zymed). Binding of primary antibodies was detected with species-specific, biotin-conjugated, secondaries (Jackson ImmunoResearch) plus ABC-peroxidase (Vector Laboratories). The reaction was developed with the 3-amino-9-ethylcarbazole (AEC) substrate (Vector Laboratories) and sections were counterstained with hematoxylin. For controls, mouse IgG (BioLegend) or PBS was substituted for the primary antibodies. The staining pattern of each antibody was evaluated in 3 to 17 independent experiments. To evaluate hemozoin deposition relative to antigen expression, the sections were viewed with polarized light, which illuminates this pigment (166).

Histology

34 cases and controls (n=17/group) were randomly selected based on the sample sizes of previous studies in which we analyzed the effects of preterm labor or preeclampsia on gene expression patterns in the basal plate region of the placenta (219). H&E-stained sections were examined by transmission light microscopy. Three randomly chosen fields per biopsy were scored at 400x for the number of pigmented mesenchymal cells and STBs. In general, there was good agreement among the scores for each of the 15 400x fields that were examined per placenta.

Statistical tests

Statistical analyses were performed as described in Chapter 2.

3.4 CONCLUDING REMARKS

In this chapter, I demonstrated by immunostaining that hemozoin co-localizes with villous STBs and CD68+ cells. Based on location, the CD68+ cells are Hofbauer cells, the fetal/embryonic macrophage. I showed that pigmentation of these cells is

associated with primigravidae and secundigravidae as compared to multigravidae, groups that are susceptible to severe forms of infection. However, these events were not associated with infant low birthweight or preterm labor. I also showed that total numbers of villous CD68+ cells are increased in the setting of malaria. To my knowledge, this may be one of the first examples of a fetal immune cell response to malaria infection. Future experiments could include understanding the molecular cues that recruit fetal Hofbauer cells to the villi. It would also be interesting to determine if all the CD68+ cells are of fetal origin or if maternal macrophages also traffic into the villi during placental malaria.

3.5 FIGURES AND FIGURE LEGENDS

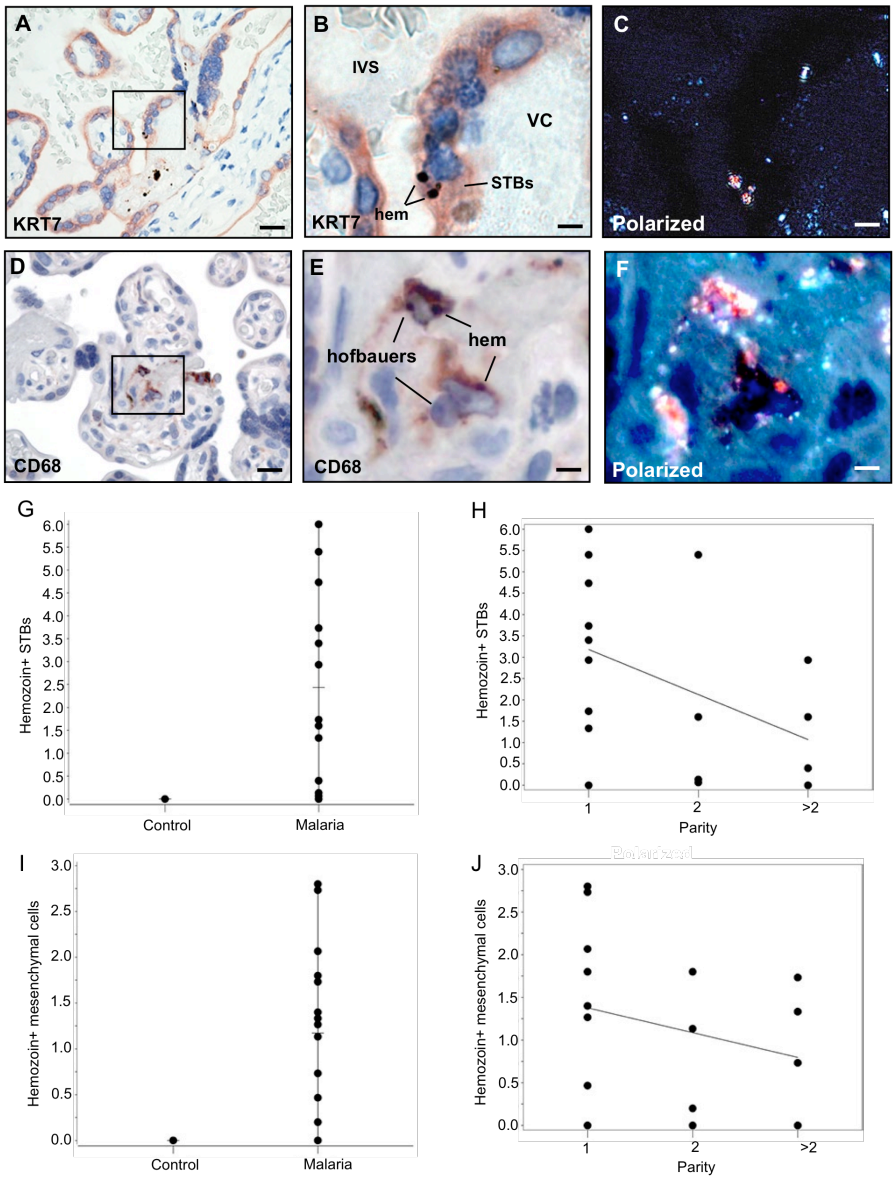

Figure 3.1 Pigmented STBs and CD68+ mesenchymal cells are associated with placentas from primigravidae.

P. falciparum-infected term placentas were formalin-fixed and paraffin-embedded. Binding of primary antibodies was detected with biotin-conjugated secondaries followed by ABC-peroxidase, and visualized using a 3-amino-9-ethylcarbazole (AEC) substrate (red color). Sections were counterstained with hematoxylin (blue). (A-C) Hemozoin (hem) co-localized with KRT7+ syncytiotrophoblasts (STBs) (left panel and enlarged in B). Polarized light confirmed the presence of hemozoin (C). (D-F) Hemozoin co-localized with CD68+ Hofbauer cells (left panel and enlarged in E). Polarized light confirmed the presence of hemozoin (F). Scale bars, 40μm for lower magnification and 10 μm for higher magnification. (G) The mean number of hemozoin+ STBs per 400x field ranged from zero to six in +malaria samples. (H) Hemozoin+ STBs were associated with placentas from primigravidae and secundigravidae (linear trend p=0.01, 2 vs. 1 p=0.06, > 2 vs. 1 p=0.0004). (I) The mean number of hemozoin+ mesenchymal cells per 400x field ranged from zero to three in +malaria samples. (J) Hemozoin+ mesenchymal cells were associated with placentas from primigravidae and secundigravidae (linear trend p=0.04, 2 vs. 1 p=0.07, > 2 vs. 1 p=0.02).

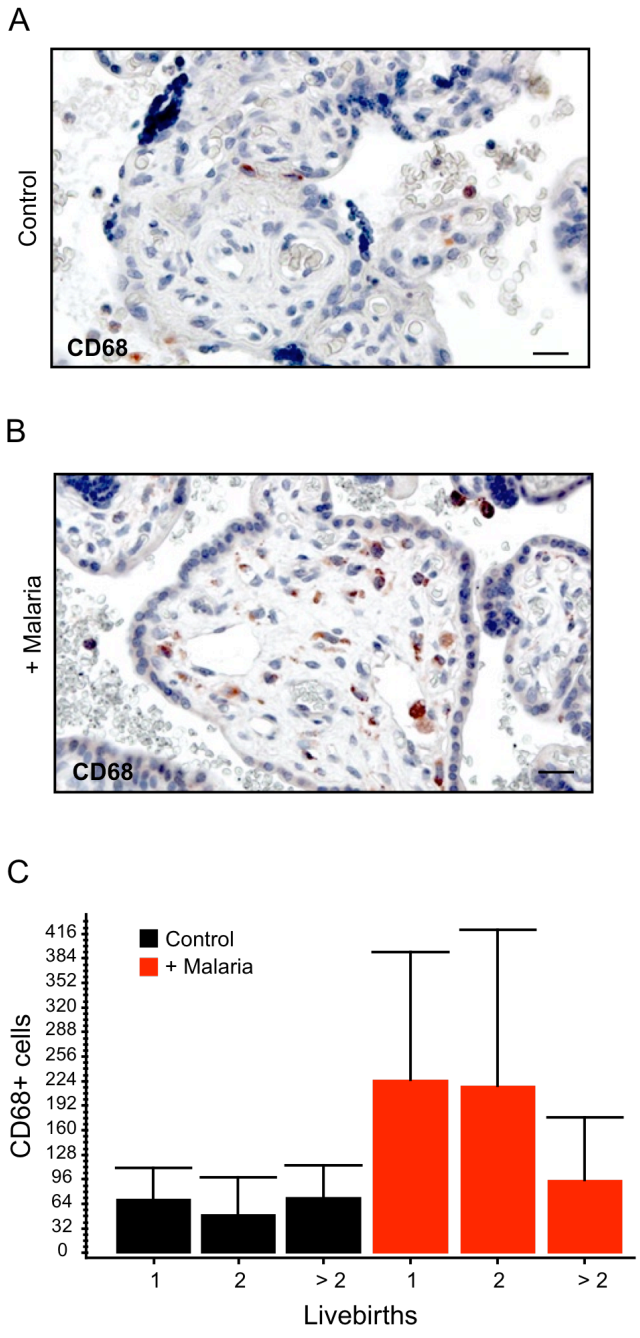

Figure 3.2 Villous CD68+ cells are increased in *P. falciparum*-infected placentas.

(A-B) *P. falciparum*-infected and -uninfected term placentas (n=17/group) were processed and analyzed as described in Figure 3.1. Fewer CD68+ villous cells were present in controls (panel A) as compared to infected placentas from primigravidae (panel B). (C) The mean number of CD68+ cells per 400x field was significantly higher in infected placentas from primigravidae and secundigravidae (red bars) compared to parity-matched controls (black bars; $p < 0.05$). No difference in numbers of CD68+ cells was observed in placentas from multigravidae (red bar, livebirths > 2) as compared to controls (black bar, livebirths > 2; $p > 0.05$). Error bars represent SD.

CHAPTER 4. POLYSIALIC ACID IS ASSOCIATED WITH DESMOSOMES IN THE HUMAN PLACENTA AND ENHANCES CYTOTROPHOBLAST MIGRATION AND INVASION

4.1 ABSTRACT AND INTRODUCTION

4.1.1 Abstract

Polysialic acid (polySia) is a large, cell-surface linear homopolymer composed of α2,8-linked sialic acid residues. Best studied in the nervous system, this unique glycan modulates development by enhancing progenitor cell migration and regulating cell differentiation. PolySia also functions in the developing and adult immune systems and is a signature of many cancer cells. Here, we demonstrated that human placental trophoblasts also display this glycan. Cytotrophoblasts (CTBs) and syncytiotrophoblasts (STBs) expressed polySia in the first trimester and downregulated it during the course of pregnancy. Immunoprecipitation of polySia and subsequent mass spectrometry-based protein identification suggested that placental forms of this glycan are associated with desmosomes, intercellular junctions that enable strong adhesion between cells. Immunoprecipitation followed by immunoblotting demonstrated that polySia was associated with desmoglein 1 (DSG1), a glycosylated desmosomal cadherin that faces the extracellular space, and with intracellular complex members including plakoglobin (JUP) and plakophilin 3 (PKP3). Together, these results revealed that placental polySia is part of a high molecular weight desmosome complex**.** As to functional roles, polySia promoted CTB migration in an explant model of chorionic villous growth. Removal or perturbation of this glycan also reduced CTB penetration of basement membranes in an *in vitro* model of invasion. Finally, we showed that polySia was overexpressed in biopsies from patients with gestational trophoblastic diseases, including benign molar

pregnancies and malignant choriocarcinomas. These results demonstrated, for the first time, functional roles for desmosome-associated polySia during normal human placental development and implicate these unusual oligosaccharides in the unrestrained invasion of trophoblast tumors.

4.1.2 Introduction

Polysialic acid (polySia) is a cell-surface linear homopolymer composed of α2,8-linked sialic acid residues. This unique glycan modulates cell-cell interactions through its unusual physical properties—a long chain length, typically hundreds of negatively charged sialic acid residues, with a much larger hydration volume than most other cell-surface molecules. As a result polySia modulates the distance between apposing membranes of neighboring cells (169). PolySia, a post-translational modification that is added in the Golgi apparatus, is the product of polysialyltransferases, ST8SiaII (STX), which is largely restricted to the nervous system, or ST8SiaIV (PST1), which is more broadly expressed, for example in the immune system and the human placenta (2). Unlike most glycans, polySia modifications have thus far been identified on a limited number of protein scaffolds. These include the neural cell adhesion molecule (NCAM/CD56) (58, 90), neuropilin-2 (NRP2) (43), CD36 (213), the α-subunit of the voltage-sensitive sodium channel (96), and SynCAM-1 (CADM1) (73). Autocatalytic polysialylation of ST8SiaII and ST8SiaIV has also been reported (127).

NCAM is by far the best studied of the known scaffolds and the impact of polysialylation on brain development and function is well understood. Interestingly, polySia functions through at least two distinct mechanisms. The first is steric hindrance, which inhibits binding of homo- and heterotypic adhesion molecules (reviewed by 169). The second is charge-mediated binding of small cationic molecules such as cytokines

and chemokines, thus modulating their interactions with cell surface receptors, a phenomenon that is observed with other large anionic molecule including glycosaminoglycans such as heparan sulfate. As to functional consequences, NCAM-polySia influences the migration of neuronal progenitors (92, 139, 179) and some populations of mature neurons (129). It also modulates contact-dependent differentiation; removal of polySia results in premature maturation (142). NCAM-polySia may also promote viability; its removal increases apoptosis without affecting proliferation (78, 202). Finally, this unusual glycan influences cell signaling by increasing responses to a number of growth factors (49, 128, 200, 201, 218).

PolySia is also expressed outside of the nervous system, most notably in the immune system, where it is carried by NCAM on human natural killer (NK) cells and murine monocytes (50), and by NRP2 on human and murine dendritic cells (43). In some cases, polySia enhances the migratory ability of these cells. For example, in the mouse, NCAM-polySia is required for the mobilization of hematopoietic progenitors from the bone marrow to the thymus (51). NRP2-polySia enhances CCL21-dependent migration (*i.e.*, chemotaxis) of dendritic cells to secondary lymphoid organs (10, 158, 159). This unusual glycan is also expressed by many human tumors including lung carcinomas, myelomas, neuroblastomas, gliomas, and Wilm's tumor (88, 101, 113, 167, 195). On cancer cells, polySia may promote invasion (193), and in some cases, its expression has been correlated with tumor progression (88). PolySia is also transiently expressed in the developing embryo (169). With the exceptions noted above, expression is lost in most adult organs. Overall, the published evidence suggests that polySia is critical to enhancing cell movement during periods of rapid growth, for example, as progenitors migrate great distances (52, 92, 139, 179), and during tumorigenesis and metastasis (101). In the adult, this homopolymer may also regulate plasticity, promoting cell migration to new locations in response to environmental cues (10, 158, 159).

Here, we provide evidence that polySia modulates human placentation, which requires explosive growth, cellular plasticity in terms of phenotypic changes, and invasion. During this process, trophoblast cells initiate and maintain a physical connection to the mother, setting up an exchange system that supports embryronic/fetal development (106, 155). Placental architecture at the histological level reveals how this connection is established (Figure 4.1 J). Both human trophoblast cell types, invasive cytotrophoblasts (iCTBs) and syncytiotrophoblasts (STBs), are derived from a common progenitor cytotrophoblast (pCTB). In one pathway, pCTBs fuse to form a multinucleate layer of STBs (*i.e.,* syncytium), which cover the villi, the fundamental subunits of the human placenta. These cells mediate nutrient, oxygen, and waste exchange between maternal and fetal blood, and respond to maternal cues through their expression of receptors for small molecules (*e.g.*, epidermal growth factor [EGF] (160)). In the other pathway, pCTBs differentiate into iCTBs, which form columns of cells that migrate away from the placenta and invade the uterus, forming an “anchor” between the mother and the embryo/fetus. A subpopulation of iCTBs go on to remodel maternal uterine arterioles, widening the vessel bore and replacing the resident endothelial cells. During this invasive process, iCTBs modulate the expression of cell adhesion molecules, down-regulating integrin $\alpha 6\beta 4$ and epithelial cadherin as they exit the villi, and upregulating vascular-endothelial cadherin, IgG family members VCAM-1 and PECAM-1, and integrins $\alpha V\beta 3$ and $\alpha 1\beta 1$ as they move into the uterus (154). Glycan expression is also regulated as a function of iCTB differentiation, for example, integrin glycosylation (123) and the expression of L-selectin carbohydrate ligands (148). In many respects, iCTB penetration of the uterus resembles cancer cell invasion. However, during normal pregnancy, this phenomenon is tightly regulated. As a result, iCTBs invade only as far as the inner third of the myometrium. However, uncontrolled iCTB invasion can occur, most notably in the form of trophoblast-derived tumors (*e.g.,* choriocarcinomas).

Given polySia's ability to regulate cellular movement and plasticity, we investigated its involvement in the formation of the human maternal-fetal interface. First, we showed that, in the placenta, polySia was exclusively expressed by trophoblasts. We also observed regulation as a function of gestational age. PolySia, which was very abundant early in pregnancy, was nearly absent at term. Immunoprecipitation (IP) with a polySia-specific antibody and mass spectrometry-based identification of captured species, revealed desmosomal components as possible carriers. Subsequent IP/immunoblot (IB) experiments suggested that desmoglein 1 (DSG1), a type I cadherin that faces the extracellular space, carried polySia. As to functional roles, removal or perturbation of polySia diminished iCTB migration and invasion. Finally, we showed that polySia was overexpressed in biopsies from patients with gestational trophoblastic disease, which included benign molar pregnancies and malignant choriocarcinomas. These results demonstrated, for the first time, functional roles for desmosome-associated polySia during human placental development.

4.2 RESULTS AND DISCUSSION

4.2.1 Characterization of placental polySia

Placental polySia is expressed by trophoblasts and the levels are regulated as a function of gestational age

We localized polySia in placental biopsies with two mAbs that specifically recognize α2-8 linked sialic acid chains: 735 and 12F8. In first-trimester formalin-fixed, paraffin-embedded samples, mAb 735 reacted with STBs that cover the chorionic villi, underlying pCTBs, and iCTBs in cell columns (Figure 4.1 A, cell column at higher magnification in Figure 4.1 B). In first-trimester paraformaldehyde-fixed, frozen biopsies,

mAb 12F8 showed the same pattern of staining (Figure 4.1 C, green). Starting around week 15, both anti-polySia mAbs failed to stain syncytium and immunoreactivity was restricted to pCTBs, which are depleted as pregnancy advances (Figures 4.1 D&E, green). However, immunoreactivity in extravillous iCTBs was observed beyond 15 weeks. iCTBs in cell columns, which are transiently present during the first and second trimesters as cells migrate into the uterus, stained (Figure 4.1 F, green). In addition, anti-polySia mAbs reacted with iCTBs that had invaded the uterus; a signal was detected on some interstitial iCTBs (Figure 4.1 G) and also in association with endovascular iCTBs that lined the uterine spiral arterioles (Figure 4.1 H). Cytokeratin 7 (KRT7)-negative uterine NK (uNK) cells, which express NCAM, were also reactive, a result that is in accord with previous studies demonstrating that human NK cells carry polySia (50). Immunoblotting with mAb 735 confirmed that STBs and iCTBs expressed polySia (Figure 4.1 I). Treatment with endoneuraminidase N (Endo N), which removes polySia, abrogated immunoreactivity on tissue sections and immunoblots (Figure 4.2). Together, these results demonstrated that trophoblasts displayed polySia at the early stages of pregnancy and downregulated its expression as gestation advanced (summarized in Figure 4.1 J).

In the placenta, ST8SiaIV adds polySia to N-linked carbohydrates

Expression of ST8SiaII (STX) or ST8SiaIV (PST1) is sufficient for polysialylation of glycan precursors. However, ST8SiaII expression appears to be restricted to the brain, while ST8SiaIV is more broadly expressed (2). To determine whether ST8SiaII or ST8SiaIV synthesized placental polySia, we interrogated global gene expression profiling data that was produced in our laboratory (manuscript in preparation) to measure mRNA levels of these transcripts in CTBs that were isolated from villi (pCTBs) or from

iCTBs that migrated from explanted cell columns. Both populations expressed ST8SiaIV (black bars), but not ST8SiaII (Figure 4.3 A; white bars).

Next, we investigated whether polySia was attached to its carrier protein(s) via an *N*- or *O*-linked glycan. Placental lysates were digested with peptide *N*-glycosidase F (PNGase F), which specifically removes glycans that are attached to asparagine. Control and enzymatically treated lysates were separated by SDS-PAGE and transferred to nitrocellulose blots, which were probed with anti-polySia mAb 735 (Figure 4.3 B). Immunoreactivity was completely abrogated by PNGase F treatment, suggesting that placental polySia was attached via an *N*-linkage to its carrier protein(s) (left blot). Mouse brain, which predominately expresses polySia *N*-linked to NCAM, served as a positive control (right blot). Together, these results are evidence that ST8SiaIV added polySia to *N*-linked core carbohydrate structures in the human placenta.

Placental polySia is associated with the desmosomal cadherin, desmoglein 1

To date, only a few proteins are known to carry polySia: NCAM isoforms (58, 90), the α-subunit of the voltage-gated sodium channel (96), CD36 (213), NRP2 (43), and SynCAM-1 (73). Of these, NCAM is by far the most abundant and best studied. To identify the scaffold for polySia in trophoblast cells we immunoprecipitated lysates of chorionic villi (12 wk) with the anti-polySia mAb 735. Then, we desialylated the precipitates by treatment with Endo N, which specifically removes polySia. Next, the samples were separated by SDS-PAGE and stained with Coomassie Blue (Figure 4.4 A). A high molecular weight band was observed in the experimental immunoprecipitate (right lane), but not in a sample that had been processed in parallel with an isotype control antibody (middle lane). The band and the analogous region of the control lane were excised and analyzed by LC-MS/MS. A number of desmosome components were identified, including desmoglein 1 (DSG1), desmocollin 1 (DSC1), desmoplakin (DSP),

and junction plakoglobin (JUP, also called γ-catenin) (Table 4.1). DSG1 and DSC1 are transmembrane desmosomal cadherins that mediate homophilic and/or heterophilic interactions on adjacent cells. Their cytoplasmic tails interact with intracellular components such as JUP and plakophilin isoforms. DSP anchors the desmosome complex to cytokeratin intermediate filaments (84), which were also identified in the excised band (data not shown). Together, these results suggested that placental polySia was associated with a component(s) of a high molecular weight desmosome complex.

To determine if the cell-surface glycoproteins DSG1 or DSC1 carried polySia, mAb 735 immunoprecipitates ± PNGase digestion were separated by SDS-PAGE on low percentage gels to better resolve higher molecular weights proteins. Nitrocellulose transfers of the gels were probed with antibodies that specifically reacted with one or the other molecules (Figure 4.4 B). When precipitates were treated with PNGase F prior to blotting, we observed an ~ 500 kDa immunoreactive band with anti-DSG1, but not anti-DSC1. Interestingly, anti-DSG1 mAbs failed to react with glycosylated precipitates (*i.e.,* samples that had not been treated with PNGase F), which suggested that polySia and/or additional modifications obscured the epitopes that this antibody recognizes. As controls, nitrocellulose transfers of immunoprecipitates were also probed with NCAM and NRP2, which are expressed by some trophoblast populations (61, 149) and are polysialylated in other human cell types (see Introduction). These proteins failed to immunoprecipitate with polySia (Figure 4.5). Finally, attempts to perform the reverse experiment—immunoprecipitation of DSG1 and immunoblotting for polySia—failed (data not shown), perhaps due to masking of the peptide epitopes. Together, these results demonstrated that placental polySia associated with desmosome complexes and suggested that DSG1 was the carrier.

4.2.2 Functional roles for placental polySia

PolySia promotes CTB migration in a human placental explant model of iCTB migration

PolySia facilitates the movement of neural precursors in the brain (92, 139, 179) and multipotent hematopoietic progenitors from the mouse bone marrow (52). To investigate if this unusual form of glycosylation also modulates placental cell movement, we used an *in vitro* organ culture system that models CTB differentiation along the invasive pathway (82). Cell columns of anchoring chorionic villi were dissected from 5- to 7-wk placentas and cultured on Matrigel-coated wells in the presence or absence of Endo N, which removes polySia (Figure 4.6). Over several days, untreated controls gave rise to iCTB outgrowths, which migrated away from the villi (Figure 4.6 A, top panels), a process that was inhibited by Endo N treatment (Figure 4.6A; bottom panels). A quantitative analysis of migration (from 48 to 144 hr) demonstrated an approximate 60% reduction in Endo N-treated samples as compared to untreated controls, $p < 0.0001$ (Figure 4.6 B). Together, these results demonstrated that polySia promoted iCTB migration.

Removal or perturbation of polySia reduces iCTB invasion

Next, we investigated whether polySia promoted iCTB invasion (93). Freshly isolated CTBs were plated in the upper portions of Matrigel-coated transwell inserts ± Endo N or mAb 735. After 40 hrs, invasion was quantified by counting the number of KRT7-positive trophoblasts that migrated to the underside of the filter (Figure 4.7). Compared to untreated cultures (black bars) and cells that were incubated with an isotype control Ab (light grey bars), Endo N digestion (white bars) significantly reduced iCTB invasion. While mAb 735 (dark grey bars) also diminished iCTB invasion compared to the untreated control cultures, the reduction was only marginally different from

treatment with an isotype control Ab (light grey bars). These data demonstrated that polySia facilitated iCTB invasion. The results of these experiments also suggested that mAb 735 does not have robust function perturbing activity.

PolySia also promotes the viability of newly generated neurons and removal of polySia can induce apoptosis (79). To ensure that the reduced migration and invasion were not attributable to apoptosis, we cultured iCTBs ± Endo N, mAb 735 or an IgG2a isotype control Ab for 24 or 48 hrs, and immunostained the cells for activated caspase 3 (CASP3) (Figure 4.8). Enzyme levels identical to those used in the migration (1:100 in Matrigel, 1:1000 in medium) and invasion (1:50 in Matrigel, 1:500 in medium) experiments did not induce apoptosis, although some staining was observed in cultures that were treated with two- to four-fold higher concentrations (1:25 in Matrigel, 1:250 in medium). Likewise mAb 735 did not induce CASP3 expression. Together, these results demonstrated that removal or perturbation of polySia diminished iCTB migration and invasion, and that the observed reductions were not the result of cell death.

4.2.3 Dysregulation of polySia during pregnancy complications

PolySia is overexpressed in biopsies from patients with gestational trophoblastic disease

We hypothesized that polySia levels would be increased in placental pathologies that are characterized by uncontrolled trophoblast invasion (*e.g.,* gestational trophoblastic disease). To address this question, we investigated polySia expression by the placental-derived choriocarcinoma cell lines BeWo, JEG-3, and Jar (75). BeWo and JEG-3 were isolated from cerebral metastases, while Jar was established from a placental site tumor. Immunostaining with the polySia-specific mAb 12F8 showed that these cell lines stained brightly for polySia (Figure 4.9). Nearly every cell exhibited cell-

surface polySia expression and the observed fluorescence was brighter than in primary CTBs.

Based on these results, we hypothesized that biopsies of choriocarcinomas and other gestational trophoblastic disease tumors would also stain for polySia. This diverse group of disorders arises from trophoblasts at various stages during the differentiation process. Some are benign (*e.g.,* placental site nodules), while others present as aggressive cancers (*e.g.,* choriocarcinomas, placental site and epithelioid trophoblastic tumors). Many such lesions arise from partial or complete hydatidiform moles, abnormal growths of trophoblasts that contain at least two paternal X chromosomes. To determine if polySia was overexpressed in gestational trophoblastic disease, we immunostained tissue microarrays of biopsies and compared the results with the staining patterns of first trimester placentas (Figure 4.10 A). The intensity of polySia immunoreactivity was scored on a scale of 0 (no signal) to 3 (intense staining). The mean score for first-trimester placental site biopsies was < 1. All the gestational trophoblastic tumors stained more intensely, averaging 1.5 - 2 (Figure 4.10 B). These data revealed that trophoblast transformation and uncontrolled invasion are associated with a significant increase in polySia levels ($p < 0.001 - 0.01$).

4.2.4 Discussion of findings

This is the first description of placental polySia. Here, we showed that iCTBs, STBs, and their common progenitor expressed this unusual glycan (Figures 4.1 and 4.2), which is incorporated into *N*-linked carbohydrates by ST8SiaIV (PST1) (Figure 4.3). Our results suggested that placental polySia is associated with desmosomes, high molecular weight membrane complexes that provide mechanical support for cell-cell adhesion. Desmosomes are comprised of at least three protein families (207):

transmembrane cadherins, armadillo proteins, and plakins. Immunoprecipitation, SDS-PAGE separation and mass spectrometry identification demonstrated that members of each family were associated with polySia (Table 4.1). Specifically, the cadherins DSG1 and DSC1, the armadillo family member plakoglobin (JUP), the plakin protein desmoplakin (DSP), and cytokeratin intermediate filaments co-immunoprecipitated with polySia. Peptide generation required deglycosylation, additional evidence that polySia resided in a complex glycan structure that was resistant to trypsin digestion.

Based on the mass spectrometry results, we hypothesized that DSG1 and/or DSC1 carried polySia because they are plasma membrane glycoproteins. As shown in Figure 4.4 B, DSG1, but not DSC1, co-immunoprecipitated with polySia. Although DSG1, a protein of 1049 amino acids, has a predicted molecular weight of 165 kDa, we observed a > 500 kDa band. The results of this work was evidence that the discrepancy could be explained, at least in part, by polysialylation. However, the very large difference suggested that DSG1 resided in a high molecular weight desmosome complex, which was not solubilized under the conditions that we used for cell lysis (medium salt plus 1% NP-40 and 0.01% SDS) and electrophoresis (SDS-PAGE). This finding was consistent with reports that desmosomes are difficult to resolve (203) and require strong detergents (2% SDS plus 1% 2-mercaptoethanol) for solubilization (185), conditions that are not appropriate for immunoprecipitation. DSG1 has 3 *N*-linked consensus sequences (all extracellular) at N36, N110, and N180; however, only N110 has been experimentally shown to be occupied (150). Currently, we do not know which site(s) is occupied by polySia. Interestingly, little is known regarding the molecular composition of trophoblast desmosomes (14, 86) and to our knowledge, this is the first description of DSG1 expression in the human placenta. Previously, human DSG1, the autoantigen of the skin blistering disease pemphigus foliaceus (207), was thought to be limited to the epidermis and thymus (124).

Our results suggested that polySia functions during critical processes that underlie human placentation. First, our immunolocalization experiments showed that iCTBs expressed polySia as they differentiated, migrated, and invaded the uterus, a process that occurs in the first half of pregnancy (Figure 4.1). The results of our explant experiments suggested that polySia facilitates the group migration of iCTBs into cell columns (Figure 4.6). Additional data suggested that this unusual glycan might also promote iCTB invasion of the uterus (Figure 4.7). Together, these findings resonate with a large body of literature demonstrating that polySia (on the NCAM scaffold) enhances the migration of neural (92, 139, 179) and immune (51) progenitors. We also found that STBs, which cover the chorionic villi and display receptors for small molecules, also expressed polySia during the early stages of placentation. Although we do not know the role of polySia on these cells, it is intriguing to speculate that syncytial polySia may facilitate focal pCTB transmigration through the STB layer, thereby promoting cell column formation. Alternatively, STB-associated polySia might act as a web to capture small molecules (*e.g.*, growth factors, hormones and cytokines), which are abundant at the maternal-fetal interface.

This study adds to a body of literature describing polySia expression during cancer. For example, this unusual glycan is expressed by many human tumors (see Introduction). Here, we used tissue microarrays to screen a library of biopsies from gestational trophoblastic disease tumors. Our results demonstrated that polySia was significantly overexpressed in malignant and benign lesions as compared to first-trimester placental site biopsies (Figure 4.10). At this point, we do not know if DSG1 is also the scaffold for polySia in trophoblast-derived tumors. To our knowledge, the scaffold(s) for polySia in the aforementioned cancers (see above) has not been identified, but one report suggested that breast cancer and leukemia cells (113) had a

high molecular weight glycoprotein that carried polySia. Future experiments will investigate if polySia is also associated with desmosomes in cancer cells.

In summary, our findings suggested a new role for polySia in desmosomes. We propose that through steric hindrance, polySia blocks or decreases the strength of DSG1-mediated heterophilic and homophilic adhesive interactions and possibly, desmosome assembly. In doing so, polySia could enhance iCTB migration and invasion. Once the cells have reached their destination within the uterine wall, polySia is downregulated and tight desmosome adhesion can occur (Figure 4.11). Thus, modulating polySia expression might be one of the elusive “stop” signals that circumscribe the uterine boundaries of CTB invasion. In this way, trophoblast polySia may regulate formation of the maternal-fetal interface.

4.3 MATERIALS AND METHODS

Placental collection

Normal placentas were obtained from patients undergoing elective terminations of pregnancy (5-22 wks) or from women who had uncomplicated deliveries in San Francisco, California. The University of California, San Francisco Committee on Human Research approved this study and informed written consent was obtained from all participants.

Cell isolation and culturing

CTBs were isolated from pools of first- or second-trimester human placentas by published methods (59, 100). Briefly, placentas were subjected to a series of enzymatic digests, which detached pCTB from the stromal cores of the chorionic villi. Then the cells were purified over a Percoll gradient and resuspended in serum-free medium: Dulbecco's modified Eagle's media, 4.5 g/l glucose (Sigma Chemical) with 2%

Nutridoma (Boehringer Mannheim Biochemicals), 1% penicillin/streptomycin, 1% sodium pyruvate, 1% HEPES and 1% gentamicin (UCSF Cell Culture Facility). Isolated CTBs (2.5×10^5 cells in 250 µl serum-free media) or choriocarcinoma cells (1×10^5 cells in 250 µl MEM supplemented with 10% fetal calf serum) were cultured on Matrigel-coated (BD Biosciences) tissue culture plates or cover slips for 24 to 48 hr.

Immunolocalization

For histochemical detection, biopsies were fixed in 10% formalin for 24 hr, transferred to 70% ethanol, paraffin-embedded, and sectioned (5 µm). Tissue sections were deparaffinized in xylene and rehydrated in a series of graded ethanol solutions. Endogenous peroxidase activity was blocked by incubation in 0.3% H_2O_2 for 30 min at room temperature (RT). Signals from maternal IgG bound to fetal Fc receptors were blocked by incubation with goat or donkey anti-human IgG (1.0 µg/ml; Jackson ImmunoResearch; 1 hr at RT). To block binding of immune IgG to unoccupied Fc receptors, samples were incubated in 1.5% serum from the species in which the secondary Ab was produced. Tissue sections were incubated overnight (O/N) at 4°C with an anti-polySia mAb (735; 20µg/ml; generously provided by Dr. Rita Gerardy-Schahn), which was detected with a species-specific, biotin-conjugated, secondary Ab (Jackson ImmunoResearch) and ABC-peroxidase (Vector Laboratories). The reaction was visualized using 3,3-diaminobenzidine (DAB, Vector Laboratories) and sections were counterstained with hematoxylin. For controls, mouse IgG2a (BD Pharmingen) or PBS was substituted for the primary antibody.

For fluorescence detection, biopsies were fixed in 3% paraformaldehyde, embedded in optimal cutting temperature (OCT) medium, and frozen as previously described (219). Then, they were cryosectioned (5 µm), and permeabilized with ice-cold

methanol/acetone (2:1) for 5 min. Nonspecific reactivity was inhibited by incubating the sections for 1 hr in blocking buffer (1% BSA, 0.1% fish gelatin, 0.1% Triton-X-100, and 0.05% Tween-20). Tissue sections were incubated O/N at 4°C with the following Abs (singly or in combinations) diluted in blocking buffer: rat anti-polySia (12F8; 5 μg/ml; BD Pharmingen), mouse anti-KRT7 (OV-TL 12/30; 1:100; Dako), and rabbit anti-ACTIVE CASP3 (polyclonal; 1:250; Promega). Binding of primary Abs was detected with fluorescein isothiocyanate- or tetramethylrhodamine isothiocyanate-conjugated, species-specific, secondary Abs (Jackson ImmunoResearch). In some cases, sections were pre-incubated with Endo N O/N at 37°C (1:500-1:1000 in PBS, pH 8.0; generously provided by Dr. Rita Gerardy-Schahn), which specifically cleaves the α2-8 linkages of polySia. As controls, irrelevant rat IgM (BD Pharmingen), mouse IgG1 (BioLegend), or PBS was substituted for the primary antibody. Sections were mounted with DAPI-containing Vectashield (Vector Laboratories) and imaged with a Leica CTR5000 upright microscope.

Immunoblotting

Placental lysates of chorionic villi or decidua/basal plate were prepared by homogenizing 2 mm pieces of tissue in medium salt lysis buffer (20 mM Tris-Cl pH 8.0, 140 mM NaCl, 10% glycerol, 1% Nonidet P-40 [NP-40], 2 mM EDTA, 10mM NaF, 0.1% SDS, and proteinase inhibitor cocktail [Pierce]), followed by periodic vortexing on ice for 1 hr. STB plasma membrane preparations were isolated as previously described (187) with minor modifications. Briefly, placental chorionic villi were manually dissected into 5-10 mm pieces, resuspended in ice-cold PBS containing a proteinase inhibitor cocktail (Pierce) and stirred for 1 hr. The samples were passed through a 70 μm filter and the membrane fraction was isolated by a series of centrifugation steps:1000 x g (10 min), 14,000 x g (20 min) and 100,000 x g (1 hr). Pellets were resuspended in PBS and solubilized by

repeated aspiration through a 26-gauge needle. iCTB or BeWo lysates were prepared on ice with medium salt lysis buffer. Protein concentrations were determined using the Bradford assay (Bio-Rad). The samples were resuspended in NuPAGE lithium dodecyl sulfate (LDS) sample buffer (pH 8.4; Invitrogen) with NuPAGE reducing agent (Invitrogen), which contains 500 mM dithiothreitol (DTT), then heated at 70°C for 10 min. The lysates were separated (40 µg/lane) on 4-12% Bis-Tris gels in MOPS SDS running buffer (Invitrogen) or on 3-8% NuPAGE Tris-Acetate gels in Tris-Acetate SDS buffer (Invitrogen), and transferred to nitrocellulose (Bio-Rad). In some cases, the membranes were pre-incubated with Endo N (1:500-1:1000 in PBS pH 8.0) O/N on a shaker at 37°C. Nonspecific reactivity was blocked by incubating the membranes for 1 hr in PBS containing 0.05% Tween 20 (PBST) and 5% nonfat dried milk (blocking buffer). Then the blots were incubated O/N at 4°C with the following mAbs diluted in blocking buffer: anti-polySia (735; 1.4 µg/ml), anti-DSG1 (3G131; 2 µg/ml; GeneTex), anti-DSG1 (27B2; 3 µg/ml; Invitrogen), anti-DSG1 (129204; 4 µg/ml; R&D Systems), anti-DSG (62; 0.25 µg/ml; BD Biosciences), anti-DSC1 (polyclonal; 1:200; Sigma), anti-PKP3 (23E3/4; 2 µg/ml; Invitrogen), anti-JUP (15F11; 1:2000 ascites; Sigma-Aldrich), anti-NRP2 (polyclonal; 1:500; Santa Cruz Biotechnology), anti-NCAM (123C3.D5; 1:200 ascites; Chemicon), and anti-β-actin (C4) (polyclonal; 1:1000; Santa Cruz Biotechnology). After washing three times for 5 min in PBST, the transfers were incubated for 1 hr at RT with the appropriate peroxidase-conjugated, species-specific, secondary Abs (1:2500; Jackson ImmunoResearch). Finally, they were washed three times for 5 min in PBST and antibody reactivity was detected with ECL Plus (GE Healthcare).

Immunoprecipitation

Placental chorionic villous lysates (1 mg/ml) were pre-cleared by incubating with 100 µl (packed volume) of protein A-coupled Sepharose beads O/N at 4°C with constant

agitation by means of a rocker platform. Immunoprecipitation was performed at RT for 2 hr with mAb 735 or an IgG2a isotype control Ab (BioLegend). The bound species were captured with 30 µl (packed volume) protein A-coupled Sepharose beads. Subsequently, the immunoprecipitates were washed two times with each of the following: 1) HSA reagent (12.5 mM K_2HPO_4 pH 7.4, 0.6 M NaCl, 0.02% NaN_3); 2) MDB reagent (0.1% SDS, 0.05% NP-40, 0.3 M NaCl, 10 mM Tris pH 8.3); 3) SA reagent (12.5 mM K_2HPO_4 pH 7.4, 0.3 M NaCl, 0.02% NaN_3); and 4) Tris-wash buffer (20 mM Tris pH 8.3). In some cases, the immunoprecipitates were treated with PNGase F (New England Biolabs) O/N at 37°C according to the manufacturer's instructions.

Antibody Capture, Protein Digestion and Mass Spectrometry-Based Protein Identification

10 mg of 12.5 wk placental chorionic villous lysates were immunoprecipitated as described above, pooled and concentrated 10-fold with a microcon centrifugal filter device (Millipore), separated on a 4-12% Bis-Tris gel in MOPS SDS running buffer (Invitrogen), and stained with Coomassie blue (Pierce). A ~500 kDa MW band and an unstained region of the same MW from the control precipitate lane were excised from the gel. The pieces were destained with 25 mM NH_4HCO_3/50% acetonitrile, reduced with 10 mM DTT, and alkylated with 55 mM iodoacetamide. Then, the samples were dehydrated with 100 µL acetonitrile, and rehydrated with 50 µL of a solution containing a commercially available cocktail of glycosidases (New England Biolabs) according to the manufacturer's instructions for denatured proteins. Endo N (6% vol/vol) was added and the samples were incubated O/N at 37°C. Then, the gel pieces were dehydrated with 100 µL acetonitrile, rehydrated with 50 µL of 25 ng/µL sequencing grade Lys C in 25 mM NH_4HCO_3 (Promega), and incubated O/N at 37°C. The following day, the supernatant was collected. Next, the samples were dehydrated with 100 µL acetonitrile, rehydrated

with 50 μL of 12.5 ng/μL sequencing grade trypsin in 25 mM NH_4HCO_3 (Promega) and incubated O/N at 37°C. The supernatant was collected, and peptides were extracted in 50 μL of 50% acetonitrile/0.1% formic acid. The extracted peptides and supernatants were combined and analyzed by ESI-LC-MS/MS using a QSTAR Elite mass spectrometer (AB Sciex). Peptide sequences (and hence protein identity) were determined by matching protein databases with the acquired fragmentation patterns using the software programs ProteinPilot™ (AB Sciex) and Mascot (Matrix Science). Only highly confident spectral matches (*i.e.,* a ProteinPilot peptide confidence cut-off value of 99 or a Mascot expectation value of ≤0.016) were accepted.

Villous Explant Culture as a Measure of CTB Migration

Using methods developed in our laboratory (82, 93), human placental villous explants were cultured on undiluted Matrigel (BD Biosciences) in the presence or absence of Endo N (1:100 [vol/vol] in Matrigel, 1:1000 [vol/vol] in medium). Briefly, cell columns were isolated by manual dissection and plated on the Matrigel substrates. Medium was refreshed daily and phase contrast photographs of the explants were taken at regular intervals using a Nikon Eclipse TE2000-S microscope. Explants were maintained for a minimum of one week. Outgrowths were quantified by using an area index (AI) defined as the area 144 or 168 hr post plating divided by the initial area of the leading front at 48 hr. AI values were expressed in relative units and the mean control AI was set to 100%. Each experiment was performed with two to three explants per condition, and repeated with five placentas. The data were analyzed with an unpaired Student's *t*-test using InStat statistical software.

Quantifying CTB Invasion

Transwell inserts (8 μm pore size, Corning Costar) were coated by incubating with 8 μl of diluted Matrigel (2:1 v/v in serum-free medium BD Biosciences) for 30 min at 37°C. CTBs (2.5 x 10^5 cells in 250 μl serum-free media) were added to the upper compartments, and the inserts were placed in 24-well plates that contained 600 μl medium +/- Endo N (1:50 [vol/vol] in Matrigel, 1:500 [vol/vol] in medium), mAb 735 (2 μg/ml in medium), or mouse IgG2a isotype control (2 μg/ml in medium). The cells were incubated for 40 hr at 37°C, washed in PBS and fixed with 3% paraformaldehyde. Invasion was quantified by microscopy; iCTBs that had migrated to the underside of the filter were labeled with anti-KRT7 mAb as previously described, and counted in five randomly chosen fields. Invasion was expressed as a percentage of control values, which were set to 100%. Each experiment was performed with four replicates per condition, and repeated with CTBs isolated from four placentas. One-way ANOVA followed by Tukey's post-hoc comparisons tests were performed using InStat statistical software.

Quantifying Apoptosis

Freshly isolated iCTBs cultured on Matrigel, primary placental fibroblasts propagated on gelatin, and A549 lung adenocarcinoma cells grown on tissue culture-treated plates were exposed to Endo N, mAb 735, a mouse IgG2a isotype control Ab, or medium alone (n=2 CTB preparations from different placentas/treatment group). Primary placental fibroblasts and the A549 cell line, which do not express polySia, were used to control for apoptosis. Endo N concentrations (vol/vol) were as follows: (1:25 in Matrigel, 1:250 in medium), (1:50 in Matrigel, 1:500 in medium), and (1:100 in Matrigel, 1:1000 in medium). mAb 735 and IgG2a isotype control Ab concentrations were as follows: (16 μg/ml in medium) and (2 μg/ml in medium). Cells were cultured for 24 or 48 hr and fixed in 3% paraformaldehyde. Immunofluorescence was performed as previously described with

anti-ACTIVE CASP3 and the number of positive/total cells was quantified. One-way ANOVA followed by Tukey's post-hoc comparisons tests were performed using InStat statistical software.

Tissue Microarrays for analyzing polySia expression by Gestational Trophoblastic Disease tumors

Tissue microarrays containing biopsies from patients with gestational trophoblastic disease were prepared as described (197). Tumors and normal placental tissues from paraffin-embedded biopsies were retrieved from the archival files in the Department of Pathology at the Johns Hopkins Hospital and were arranged into tissue microarrays. Three representative cores (1.5 mm diameter) from each lesion were included. All of the cases were anonymous and the institutional review board approved the use of archival tissues. Immunohistochemistry with mAb 735 was performed as described above. Staining intensity was scored in a subset of the biopsies (n=4-30/group) by light microscopy according to the following system: 0-detectable, 0.5-very weak, 1-weak, 2-moderate, and 3-bright. The data were analyzed by one-way ANOVA followed by Tukey's post-hoc comparisons tests performed using InStat statistical software.

4.4 CONCLUDING REMARKS

In this chapter, I described investigations into the expression and function of polysialic acid at the maternal-fetal interface. Although it was previously known that ST8SiaIV, a polysialyltransferases, is expressed in the human placenta (2), to my knowledge, this is the first description of the modification of placental proteins with polysialic acid. Here, I demonstrated that polySia is expressed by trophoblasts, incorporated into *N*-linked carbohydrates by ST8SiaIV (PST1), and is associated with

desmosomes. With regard to function, it promotes cytotrophoblast migration and invasion, and is upregulated in biopsies from patients with gestational trophoblastic disease.

Although my data suggested that DSG1 is a scaffold for polySia (Figure 4.4F), additional experiments are required for definitive proof. There are also a few discrepancies that I need to account for. For example, unpublished gene expression profiling using an Affymetrix platform suggested that CTBs express DSG2, but not DSG1, 3 or 4. However, our mass spectrometry data suggested that DSG1 co-immunoprecipitated with polySia. We identified two peptides with exact matches to this protein isoform (Table 4.1). Previously, human DSG1 expression was thought to be limited to the epidermis and thymus. Therefore, in addition to being the first characterization of placental polySia, this report is also the first description of DSG1 in the human placenta. In these studies, I employed three anti-DSG1 antibodies that should not have reacted with the other isoforms. However, since I have not immunoblotted for DSG2, I cannot formally exclude this isoform as a scaffold. Although I have considered the possibility that DSG1 is a skin contaminant (introduced by poor sample handling), I do not think this is the case, because polySia consistently immunoprecipitated with DSG1 in samples from three different donors. In addition, anti-polySia mAb 735 did not react with primary keratinocytes (data not shown); therefore, keratinocytes do not appear to express DSG1-polySia.

DSG1 is a transmembrane glycoprotein with a predicted molecular weight of 165 kDa. In chorionic villous lysates prior to immunoprecipitation, I observed > 500 kDa DSG1 reactivity with two antibodies that recognize intracellular epitopes (clones 3G131 and 27B2) (data not shown). In the same lysates, another anti-DSG1 antibody (clone 129204), which is thought to bind an extracellular epitope, reacted with a ladder from ~ 170 – 280 kDa (data not shown). Intriguingly, the pattern of reactivity appeared strikingly

similar to polySia. In addition, clone 129204 recognized STB plasma membranes components at ~ 170 kDa (data not shown). As described earlier, when I immunoprecipitated villous lysates with polySia mAb 735, performed SDS-PAGE and then probed for DSG1, I did not observe reactivity. However, if I deglycosylated the immunoprecipitates with PNGase F, then I consistently observed > 500 kDa DSG1 immunoreactivity with clones 3G131 and 27B2, which recognize intracellular domains. Preliminary experiments suggested that two additional desmosomal proteins, JUP and PKP3, also co-immunoprecipitated with polySia (data not shown). Together, these data suggested that polySia is associated with a high molecular weight desmosome protein/glycan complex. Therefore, glycans (polySia and/or others) appear to be masking some protein epitopes. Perhaps not surprisingly, none of the anti-DSG1 antibodies worked for immunoprecipitation, although clones 3G131 and 27B2 are supposed to.

Desmosomes are notoriously difficult to dissociate and solubilize. However, it is clear that solubilization of this complex would simplify my experiments. Up until this point, I used a medium salt lysis buffer that contains 0.1% SDS. Earlier experiments demonstrated that SDS was required for isolation of placental polySia. Currently, I am employing a buffer that contains Empigen BB, a detergent that should solubilize desmosome complexes while preserving protein epitopes (203).

Finally, there is an additional matter that I am currently addressing. As shown in Figure 4.5, I performed experiments to determine if placental polySia was also carried by NRP2 and NCAM, which are known scaffolds in other organs and are expressed by select trophoblast populations. While NRP2 never co-immunoprecipitated with polySia, NCAM appeared to co-immunoprecipitate with one of my patient samples (data not shown). When I repeated the experiment with a different donor lysate, the association was not observed (Figure 4.5 B). Currently, I do not know if the observed association in

the first sample was due to an NCAM-polySia contaminant (perhaps from immune cells) or non-specific reactivity. I am currently employing an additional anti-NCAM antibody and testing immunoprecipitates from multiple placentas to resolve this issue.

4.5 FIGURES AND TABLES

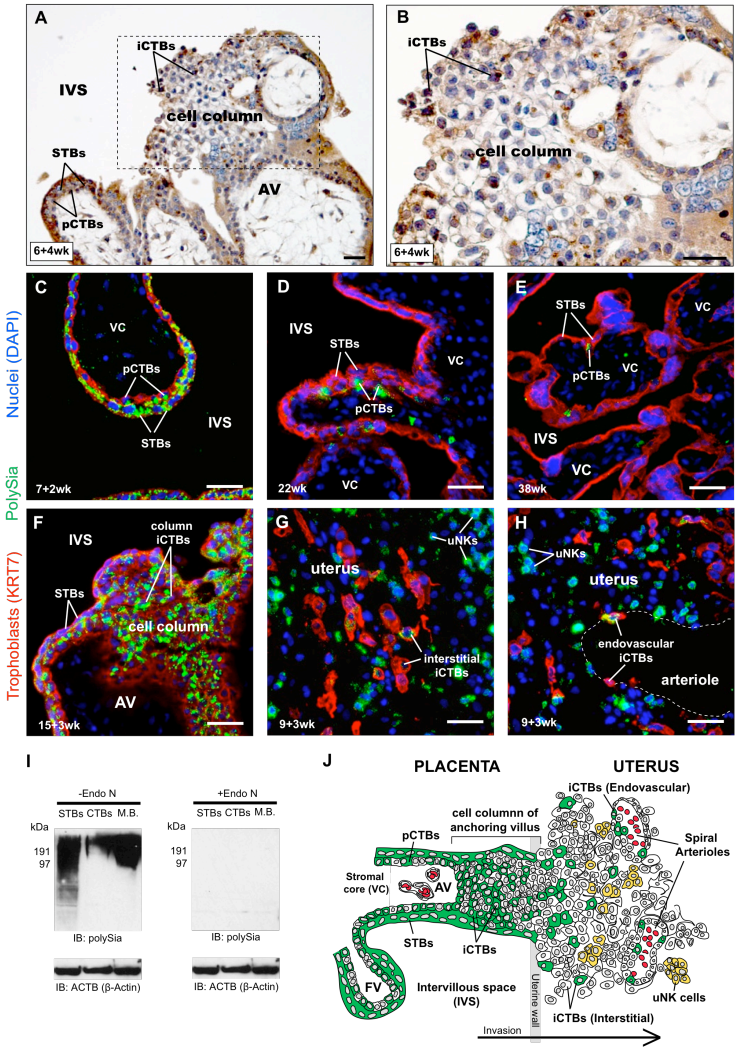

Figure 4.1 PolySia is expressed as a function of gestational age in STBs and CTBs.

(A-B) PolySia was detected with mAb 735 and visualized using 3,3-diaminobenzidine (DAB, brown color). Sections were counterstained with hematoxylin (blue). (A) In first-trimester chorionic villi, mAb 735 reacted with STBs, which cover the villi, underlying progenitor CTBs (pCTBs), and invasive CTBs (iCTBs) in cell columns. Box enlarged in panel B. Cell-surface polySia appeared light brown, while Golgi polySia was punctate and dark brown. (C-H) Placental sections reacted with anti-KRT7 mAb (red, to visualize trophoblast), DAPI (blue, to visualize nuclei), and anti-polySia mAb 12F8 (green). (C-E) 12F8 reacted with STBs and underlying pCTBs. PolySia signal was highest in first-trimester samples (panel C) and declined in second-trimester biopsies (panel D), such that the glycan's expression was restricted to pCTBs at term (panel D). In cell columns (F), intense immunoreactivity was observed on iCTBs. In the uterus (G-H), staining was detected on some interstitial iCTBs (panel G) and endovascular iCTBs (panel H) that lined the uterine arterioles. Uterine natural killer (uNK) cells, which express NCAM, were also reactive with mAb 12F8. (A-H) Scale bars, 40μM. (I) First-trimester STB plasma membrane fractions, CTB lysates, and mouse brain preparations (M.B.) were separated by SDS-PAGE, and treated with (right) or without (left) Endo N to remove polySia prior to immunoblotting with mAb 735. An identical blot was also probed with anti-actin to demonstrate loading (bottom). (J) Localization pattern of human placental polySia. In floating chorionic villi, placental polySia expression was restricted to pCTBs, STBs, and iCTBs (green). In the uterus, polySia was detected on interstitial and endovascular iCTBs (green) and uNK cells (yellow).

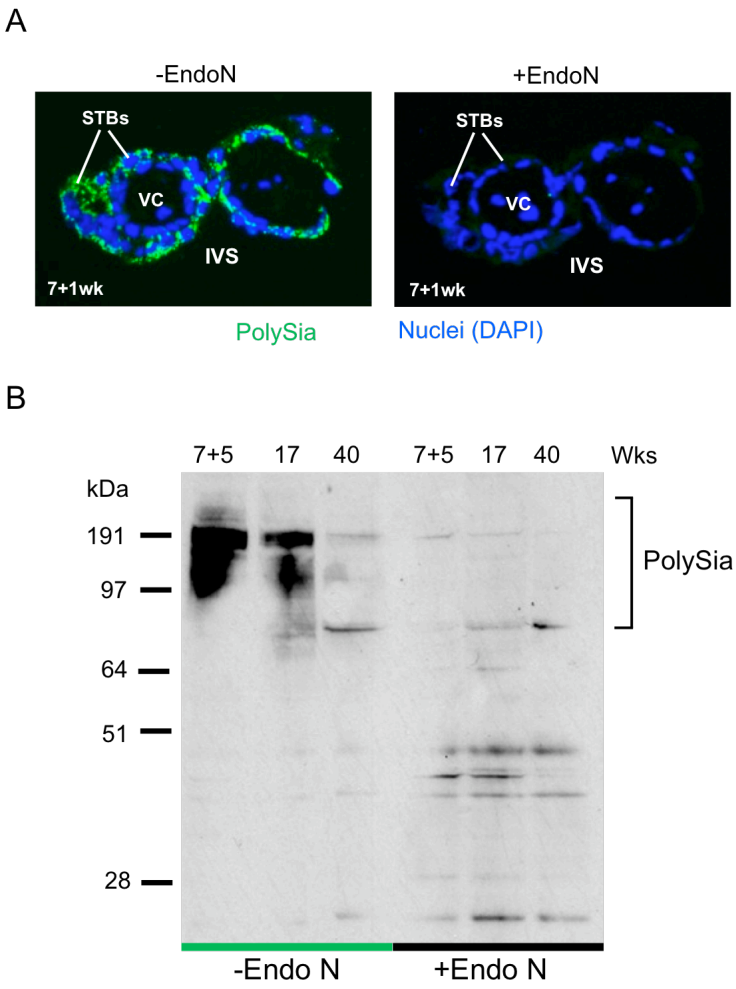

Figure 4.2 Endo N treatment abrogates placental polySia immunoreactivity.

(A) Paraformaldehyde-fixed, frozen sections of placental biopsies were stained with the anti-polySia mAb 12F8 followed by a fluorescently-conjugated secondary Ab (green; left panel). DAPI was used to label nuclei. As a negative control, sections were pretreated with Endo N to remove polySia (right panel). IVS; intervillous space. VC; villous core. (B) STB plasma membrane fractions were isolated from first- and second-trimester and term placentas, separated by SDS-PAGE (4-12% Bis-Tris gels), and immunoblotted using the anti-polySia mAb 735 (left lanes). As a negative control, membranes were treated with Endo N prior to blotting (right lanes).

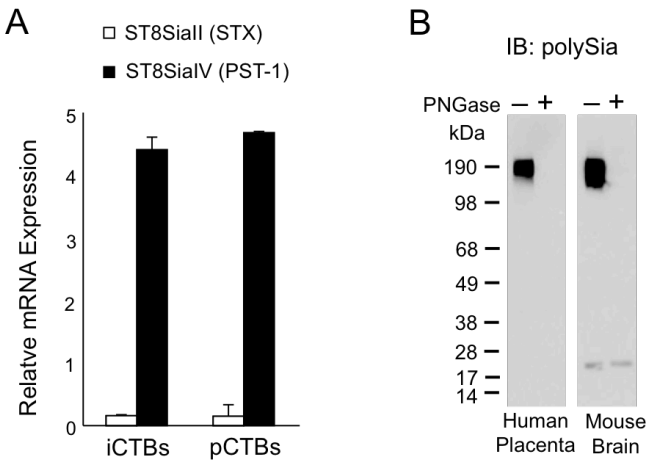

Figure 4.3 ST8SiaIV synthesizes *N*-linked polySia in the human placenta.

(A) Trophoblast-specific expression of the two polysialyltransferase enzymes, ST8SiaII and ST8SiaIV, was determined by relative RNA quantification using the Affymetrix Gene ST 1.0 exon array platform. iCTBs; invasive cytotrophoblasts. pCTBs; progenitor cytotrophoblasts. (B) Human placental lysates were treated with PNGase F, separated by SDS-PAGE (4-12% Bis-Tris gels) and immunoblotted with anti-polySia mAb 735 (left). Mouse brain lysates were included as a positive control (right).

Table 4.1 Mass spectrometry peptide sequences and scores

Gene Name	Protein Name	Peptide	Modifications/Cleavages	Protein Pilot Confidence Value	Mascot Score	Mascot Expect Value
DSG1	Desmoglein 1	VGDFVATDLDTGRPSTTVR	None	99	55	0.00045
DSG1	Desmoglein 1	VMGNNPADLLAVDSR	Cleaved Y-V @ N-term	99	Not observed	Not observed
DSP	Desmoplakin	TMIQSPSGVILQEAADVHAR	None	99	24	0.53
DSP	Desmoplakin	LASLEELK	None	62	40	0.016
DSC1	Desmocollin 1	VTATDLDEPDTLHTR	None	99	55	0.00039
JUP	Plakoglobin	LLNDEDPVVVTK	None	Not observed	52	0.0008

Desmoglein 1 (DSG1)

A VMGNNPADLLAVDSR

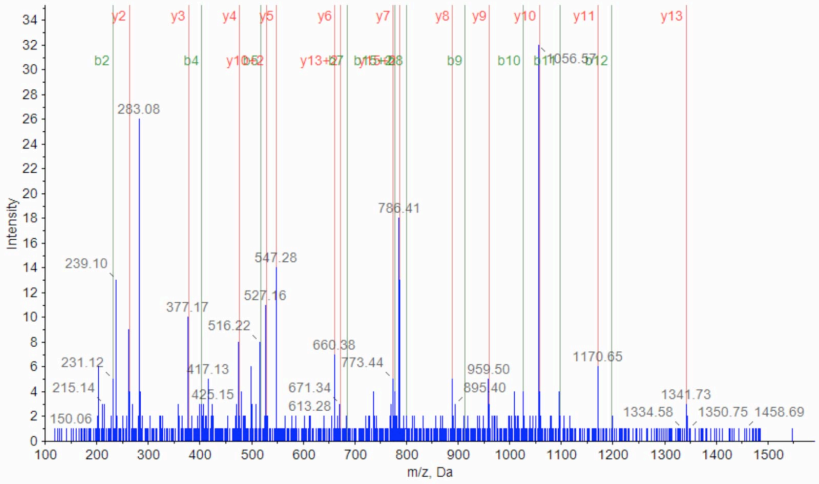

B VGDFVATDLDTGRPSTTVR

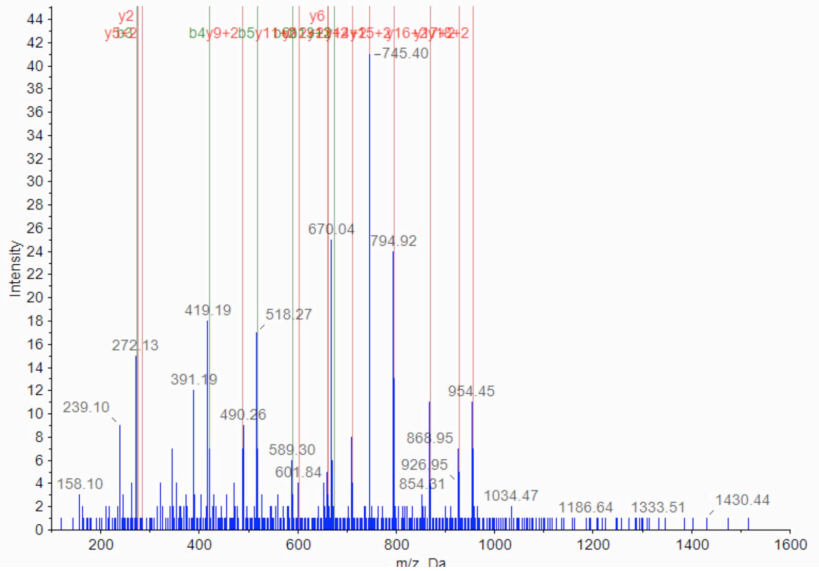

Figure 4.4 Mass spectrometry spectra for desmoglein 1 (DSG1).

Desmoplakin (DSP)

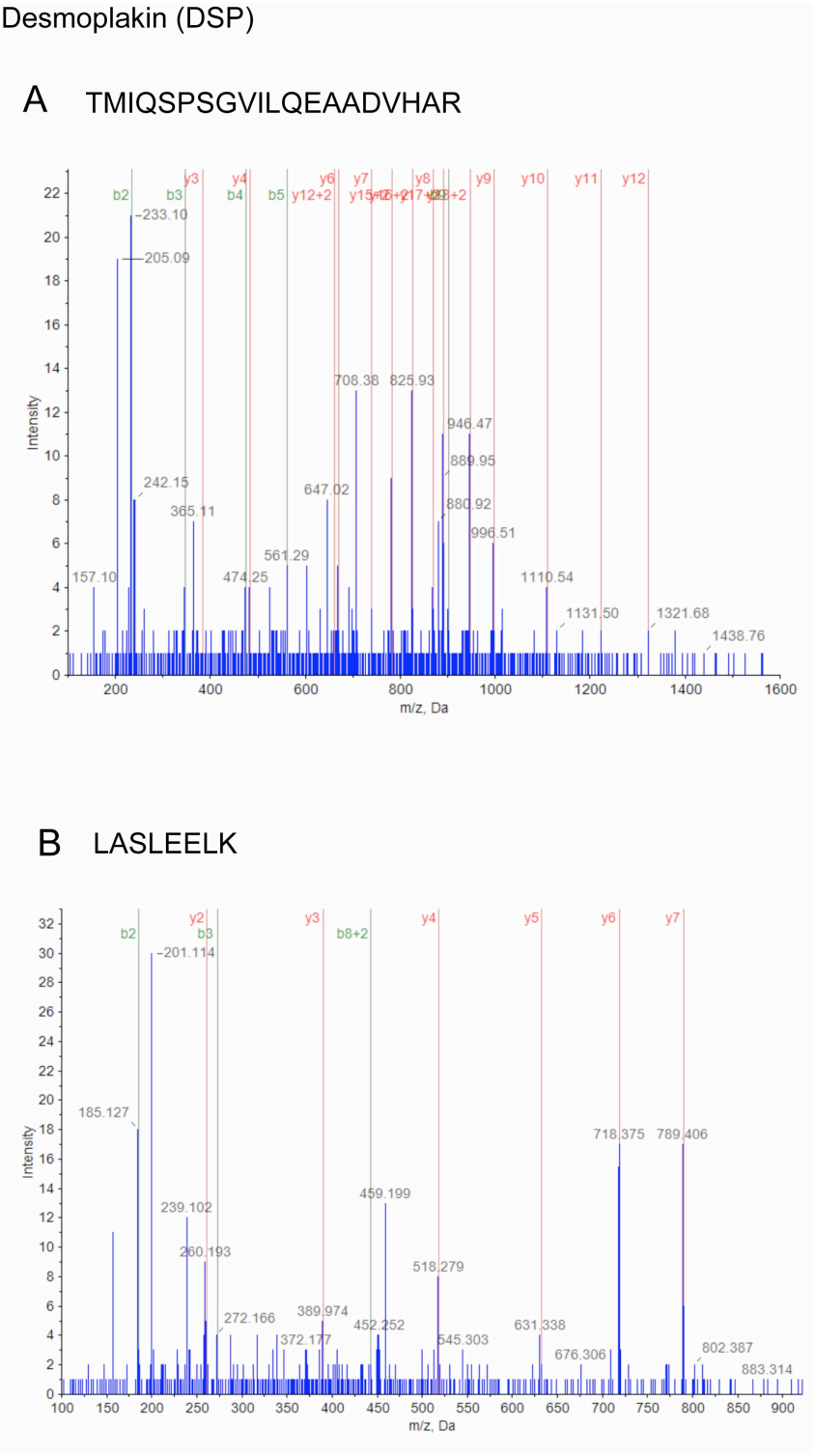

Figure 4.5 Mass spectrometry spectra for desmoplakin (DSP).

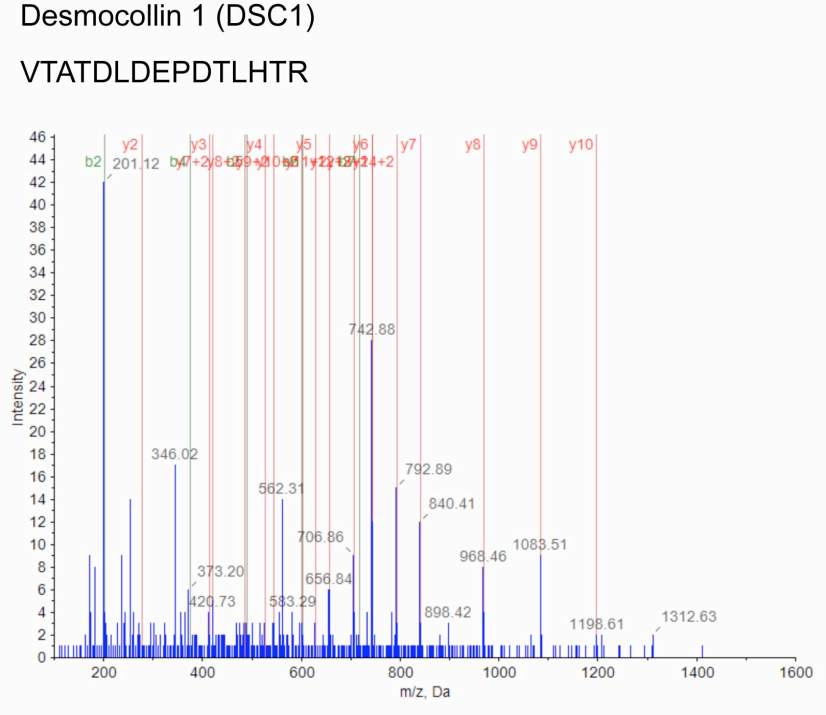

Figure 4.6 Mass spectrometry spectra for desmocollin 1 (DSC1).

Junction plakoglobin (JUP)

LLNDEDPVVVTK

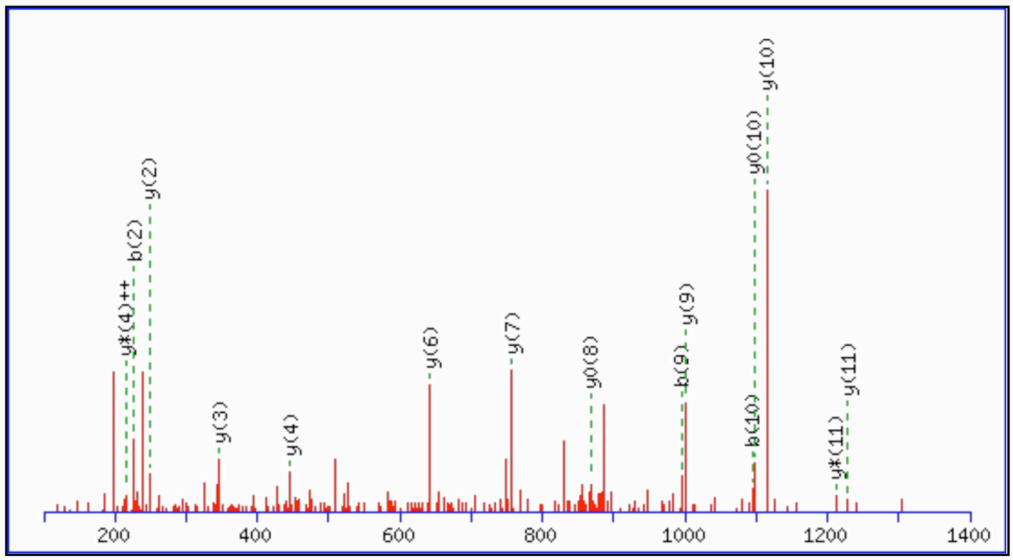

Figure 4.7 Mass spectrometry spectra for junction plakoglobin (JUP).

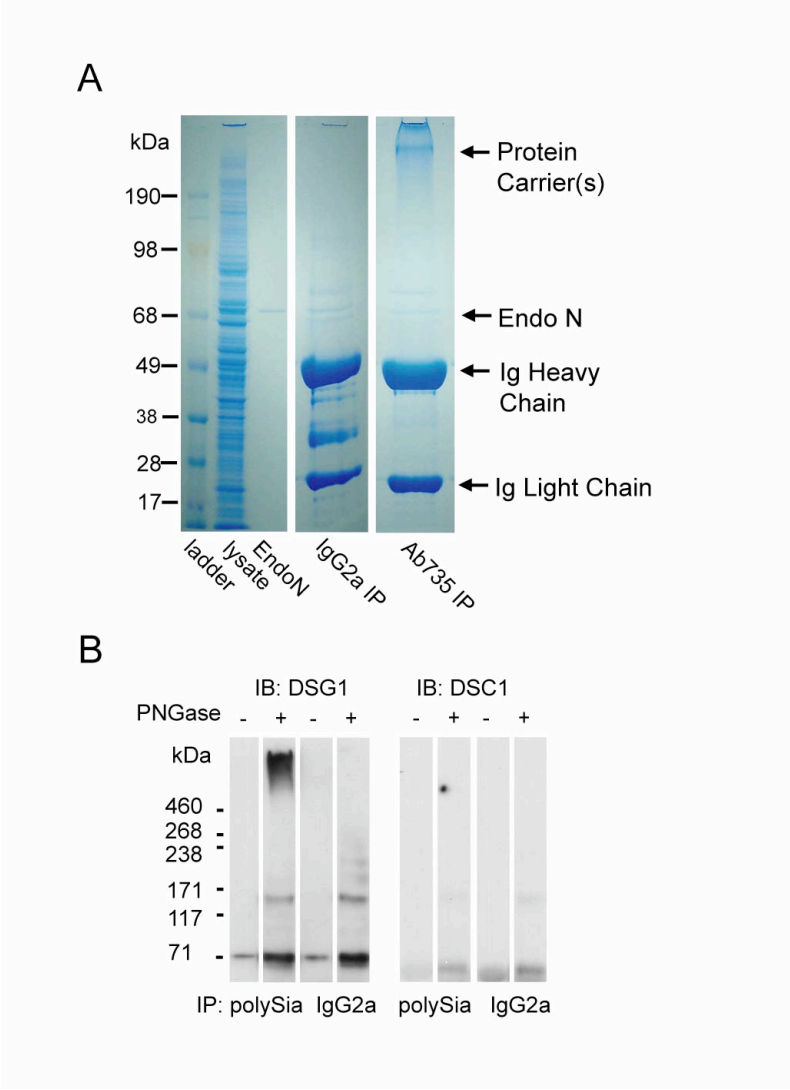

Figure 4.8 Placental polySia is associated with high molecular weight desmosome complexes.

(A) 12.5-wk chorionic villous lysates were immunoprecipitated with mAb 735 or an IgG2a isotype control, treated with endoneuraminidase (Endo N), and separated by SDS-PAGE (4-12% Bis-Tris gels). (B-C) Chorionic villous lysates were immunoprecipitated, treated with (+) or without (-) PNGase F, separated by SDS-PAGE (3-8% Tris-Acetate gels), and transferred to nitrocellulose. Membranes were then immunoblotted with antibodies that reacted with (B) the desmosomal cadherins, desmoglein 1 (DSG1) and desmocollin 1 (DSC1).

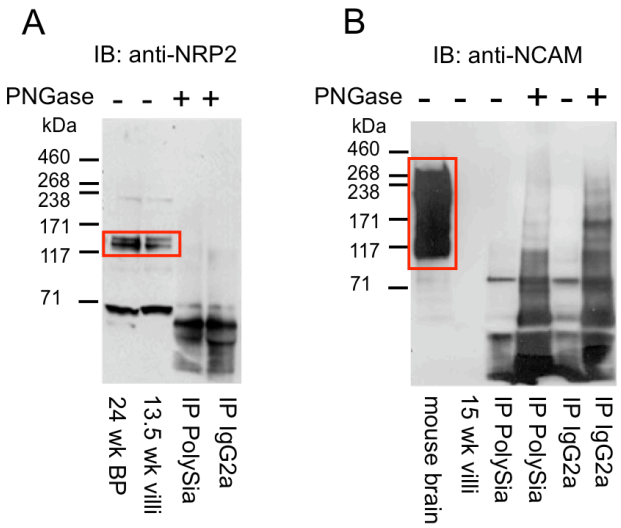

Figure 4.9. Placental polySia is not carried by NRP2 or NCAM1.

13.5- (A) or 15-wk (B) chorionic villous lysates were immunoprecipitated with mAb 735 or an IgG2a isotype control antibody and incubated with (+) or without (-) PNGase F. Control, untreated (-PNGase F) lysates, consisting of 24 wk-basal plate (BP),13.5- or 15-wk chorionic villi, or mouse brain, were also prepared. Samples were separated by SDS-PAGE (3-8% Tris-Acetate gels) and transferred to nitrocellulose. Then, NRP2 (A) and NCAM (B) proteins were detected by immunoblotting.

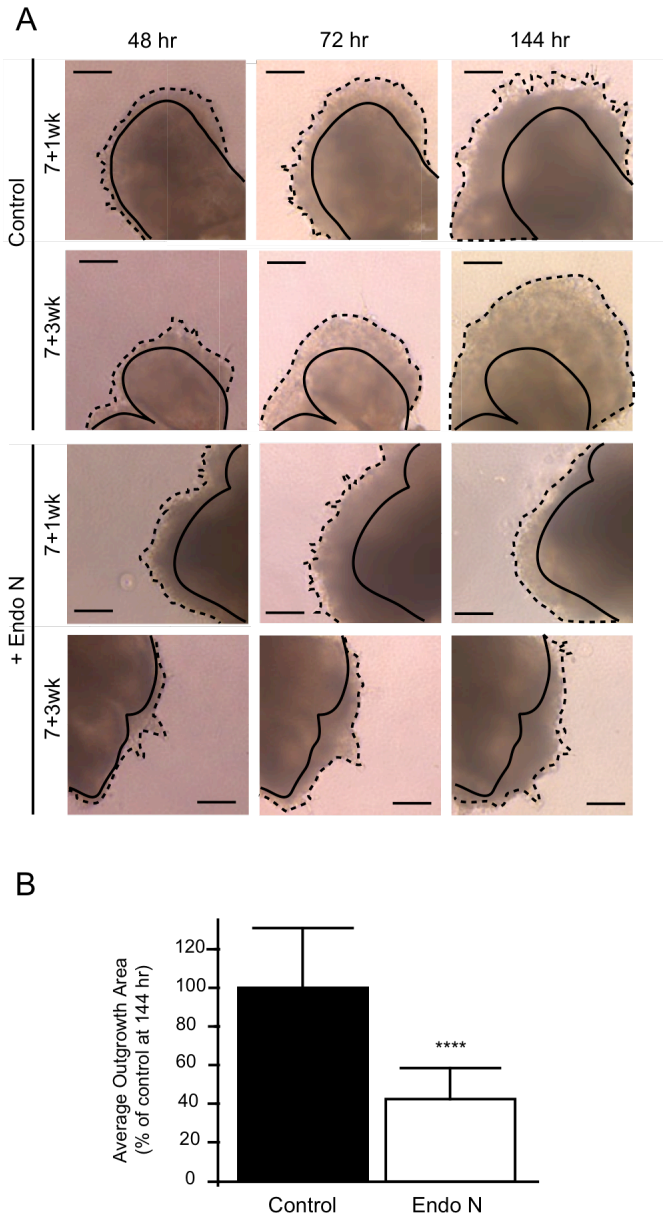

Figure 4.10 Removal of placental polySia reduces chorionic villous outgrowths.

(A) 5- to 7-wk placental anchoring villi were plated on Matrigel in the absence (top panels) or presence (bottom panels) of Endo N to remove polySia. At ~ 48 hr, cellular outgrowths, which depict cell columns giving rise to iCTBs, could be detected. Villi were cultured through 172 hr, and imaged every 24 hr. Scale bars, 200μM. (B) Explant lateral spread was quantified using a relative area index (AI), which was defined as the area 144-172 hr post-plating (hatched lines), divided by the area of the initial leading front at 48 hr (solid lines). Endo N treatment significantly reduced explant areas by 60% (white bar) compared to control (black bar), $p < 0.0001$ (****). Error bars represent SD.

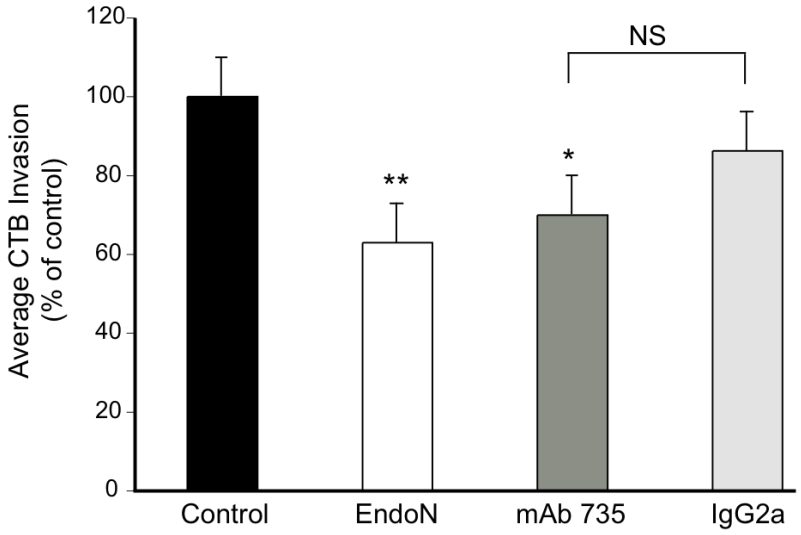

Figure 4.11 Removal and perturbation of polySia reduces CTB invasion of Matrigel.

10-12 wk iCTBs were monitored for their ability to invade Matrigel (n=16 invasion experiments/treatment group). Removal of polySia with Endo N (white) significantly reduced invasion as compared to an untreated control (black), $p < 0.01$ (**). Perturbation with mAb 735 (dark grey) also reduced invasion as compared to an untreated control, $p < 0.05$ (*), but the reduction was not significantly different than treatment with an IgG2a isotype control Ab (light grey). Error bars represent SD.

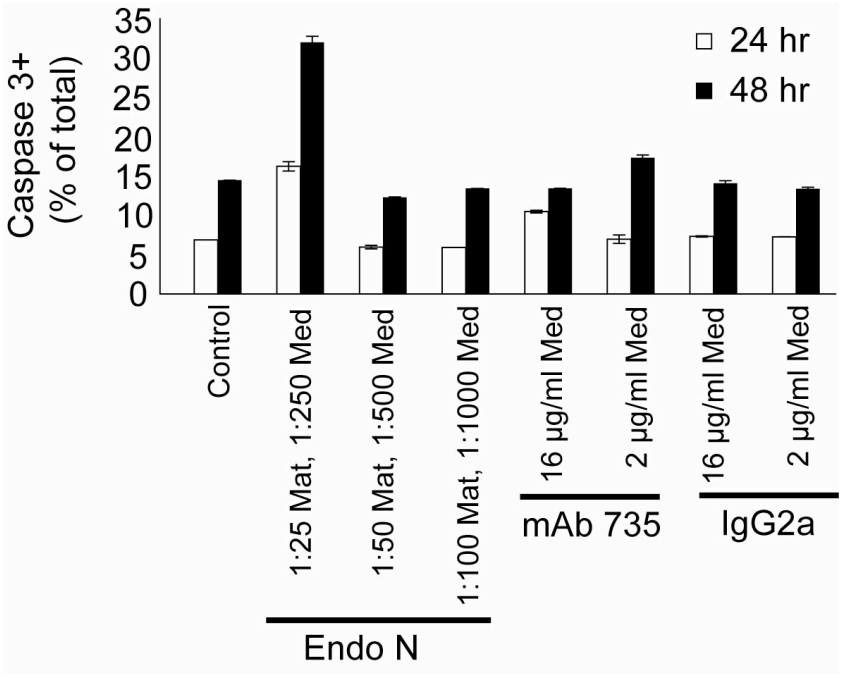

Figure 4.12 Effect of polySia removal or perturbation on apoptosis.

Primary iCTBs were seeded on Matrigel and exposed to different concentrations of Endo N, mAb 735, IgG2a, or left untreated as a negative control. Cells were grown for 24 or 48 hr, paraformaldehyde-fixed, and stained with anti-ACTIVE CASP3 Ab. The number of CASP3-positive/total cells was quantified. Endo N concentrations were as follows: 1) 1:25 in Matrigel (Mat), 1:250 in medium (Med), 2) 1:50 in Mat, 1:500 in Med, and 3) 1:100 in Mat, 1:1000 in Med. 735 mAb and IgG2a isotype control Ab concentrations were16 µg/ml in Med and 2 µg/ml in Med. Error bars represent SD.

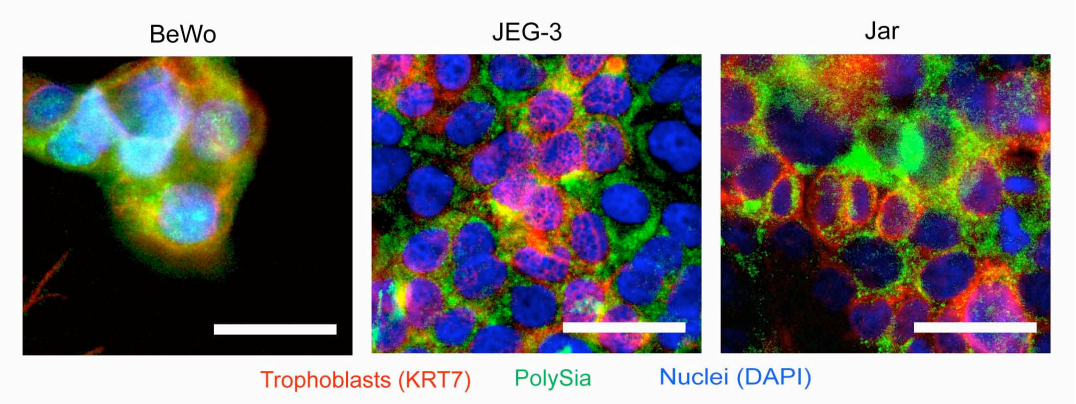

Figure 4.13 Choriocarcinoma cell lines express polySia.

Choriocarcinoma cell lines were seeded on Matrigel-coated coverslips, grown to 50-80% confluency, paraformaldehyde-fixed, and stained with anti-polySia mAb 12F8. Cells were visualized by staining with anti-KRT7 mAb (red). Nuclei were labeled with DAPI (blue). Anti-polySia immunoreactivity (green) was observed on the majority of BeWo (left), JEG-3 (center), and Jar (right) cells. Scale bars, 40μM.

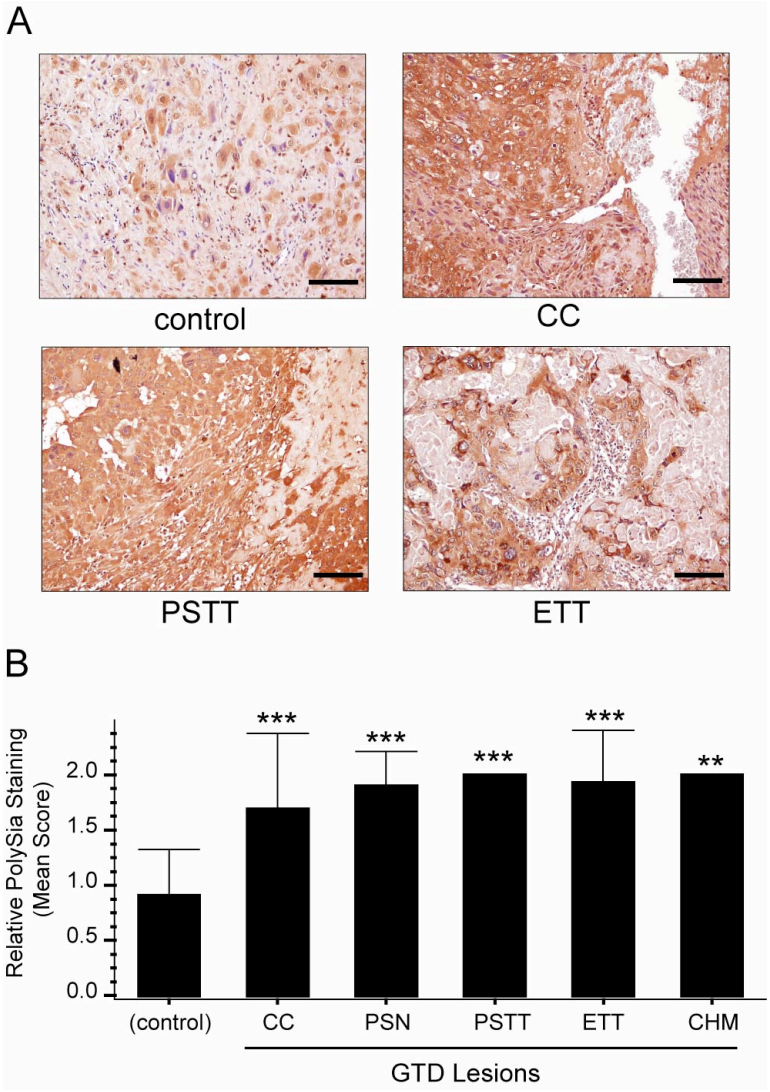

Figure 4.14 PolySia is overexpressed in gestational trophoblastic disease biopsies.

Biopsies of trophoblastic tumors and first-trimester normal placentas (controls) were paraffin-embedded and arranged into tissue microarrays. PolySia was detected with mAb 735 and visualized using 3,3-diaminobenzidine (DAB, brown color). (A) Malignant tumors (choriocarcinomas [CC], placental site trophoblastic tumors [PSTT], and epithelioid trophoblastic tumors [ETT]) stained brightly for polySia as compared to controls (normal first-trimester placental biopsies). Benign tumors (placental site nodules [PSN] and complete hydatidiform moles [CHM]) also stained (data not shown). Scale bars, 40μM. (B) The mean intensity of polySia immunoreactivity was significantly higher in biopsies from patients with gestational trophoblastic disease (GTD) as compared to controls, $p < 0.001$ (***) or $p < 0.01$ (**). Error bars represent SD.

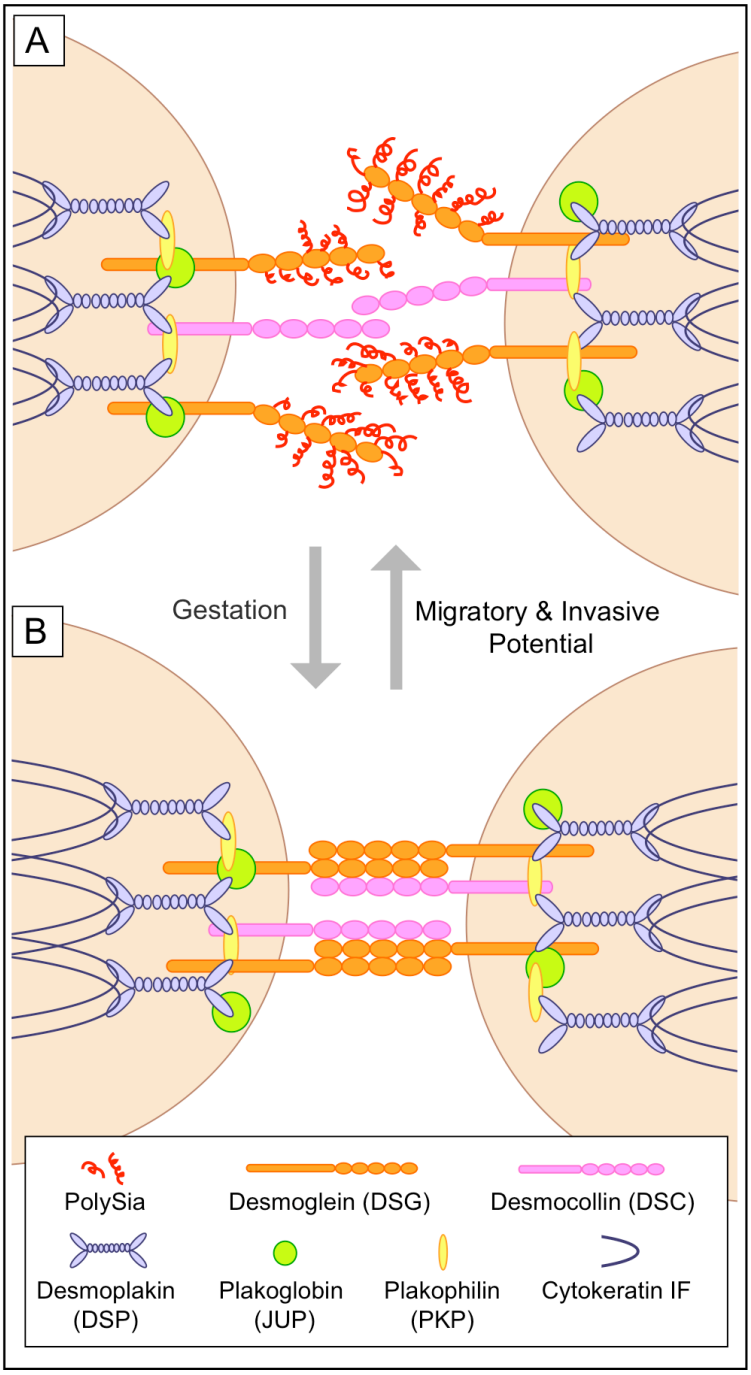

Figure 4.15 A model for polySia inhibition of trophoblast desmosome formation.

Desmosome cell adhesion with (A) and without (B) polySia. Desmoglein 1 (DSG1) and desmocollin 1 (DSC1) are glycosylated transmembrane desmosomal cadherins that form homophilic and/or heterophilic interactions on adjacent cells. The cytoplasmic tails of the cadherins interact with plakoglobin (JUP) and plakophilin isoforms (*e.g.,* PKP3). Desmoplakin (DSP) anchors the complex to the cytokeratin intermediate cytoskeleton (cytokeratin IF). Polysialylation of DSG1 promotes iCTB migration and invasion. Both the polySia modification and iCTBs' invasive capacity decrease with advancing gestational age.

CHAPTER 5: FUTURE DIRECTIONS

5.1 EXPLORATION OF IRBC ADHESION TO STBS AND CTBS

5.1.1 In vitro confirmation of glycan array screen

As described in Chapter 2, I carried out a glycan adhesion screen to identify novel receptors for *P. falciparum*. The screen was performed twice and RBCs that were infected with the CS2 parasite line reproducibly bound a number of related carbohydrate motifs. I also showed that Lewis blood group antigens, which also supported iRBC adhesion on the array, were expressed by first- and second-trimester STBs and maternal leukocyte infiltrates (Figure 2.9). To confirm these interactions, CS2-infected RBC adhesion to individual glycans under flow conditions should be assessed. Biotinylated versions of the glycans that were spotted on the arrays are available without cost from the Consortium for Functional Glycomics. These motifs can be chemically linked to streptavidin-coated cover slips. Then, the slides can be placed in a parallel flow chamber and iRBCs (in either medium or PBS) could be flowed over the immobilized glycans. In this way, one can visualize cell adhesion under well-defined, well-defined conditions that include shear stress as a variable. Function-perturbing reagents such as antibodies and lectins could be used to mask the glycan receptors. Alternatively, anti-parasite antibodies could be employed to block the ligand. Finally, free glycans or peptides could be used for competitive binding. Although these experiments would be very technically challenging, they are within the capabilities of our group and the results would provide extremely useful information.

5.1.2 Verification of glycan receptors by assaying iRBC binding to placental cryosections

Experiments should also be performed to determine the physiological relevance of the observed iRBC-glycan interactions. Since the Fisher group routinely obtains first- and second-trimester and term placentas, adhesion at different gestational time points could be investigated. Specifically, fluorescently-labeled iRBCs (*e.g.*, with Mitotracker dye) could be overlaid on frozen cryosections and adhesion could be assessed under flow conditions by rotation on a platform shaker. Binding could be perturbed with the reagents described earlier. The results could be imaged and quantified by using a fluorescence microscope.

5.1.3 Organ culture models for monitoring iRBC adhesion

Finally, binding to live placental cells should be investigated. At the inception of my graduate work, I experimented with a number of organ culture models. Specifically, I tested the explant model (118) as a binding partner for CS2-infected RBCs. In this model, freshly dissected 6 week-old chorionic anchoring villi are plated *ex vivo* on Matrigel, an extracellular matrix that supports trophoblast outgrowth. This model is ideal for investigating iRBC adhesion because it contains the two most relevant placental cell types—STBs and CTBs. Importantly, this model promotes CTBs to adopt an invasive phenotype that involves mimicry of the adhesion molecule profile of endothelial cells. One could overlay iRBCs on the explants and then gently rotate them on a platform shaker at 37ºC, 5% O_2, and 5% CO_2 to mimic shear stress at the maternal-fetal interface. To determine if parasitized erythrocytes adhered to the explants, they should be fixed, sectioned, and then visualized by light microscopy to score bound iRBCs. The aforementioned reagents could be employed to perturb adhesion.

5.2 OBSERVATIONS OF VACCINE TRIALS WITH VAR2CSA DOMAINS

VAR2CSA is commonly expressed by parasites isolated from the maternal blood

spaces of term placentas and is currently a vaccine target. It has been determined that VAR2CSA and CS-A function as a ligand-receptor pair (53, 170, 198). It has also been proposed that anti-VAR2CSA antibodies protect against infection. Pregnant women naturally develop protective VAR2CSA-specific antibodies during gestation; primigravid women have low levels and are most susceptible to placental malaria and poor birth outcomes, while higher titers are found in multigravidae and correlate with increased infant birthweights (161, 164). Many recent studies have been directed towards defining the portion of the 350 kDa VAR2CSA protein that is responsible for binding to CS-A (44). Overall, based on the published literature, many researchers believe that CS-A is the principal receptor for VAR2CSA-expressing parasites and that inducing VAR2CSA-specific antibodies will protect pregnant women at all stages of infection. Most researchers are proposing a vaccine that would induce antibodies that inhibit the interactions between VAR2CSA and CS-A (for review see 45). Although there are a number of challenges that must be overcome for vaccine development to be successful, the most immediate is that VAR2CSA is too large and thus smaller epitopes, which will induce a broad anti-adhesive antibody response, must be defined.

Based on my CS-A staining results, I can envision two outcomes for a VAR2CSA vaccine. First, since CS-A is not exposed to maternal blood in the uninfected state (*i.e.*, before the onset of STB denudation), the proposed vaccine would not neutralize the interactions that initiate infection, which in my estimation cannot be through CS-A. On the other hand, VAR2CSA is a very large protein and it could theoretically bind other placental molecules, which are exposed to maternal blood at the onset of infection. Thus, depending on which VAR2CSA domains are used as antigens, the resulting antibody response might or might not inhibit interactions with other placental molecules. If the antibodies blocked binding to molecules that initiated adhesion, then the vaccine would be protective. However, the reverse scenario seems more likely—the antibodies

would be specific for the VAR2CSA domains that bind CS-A and would, therefore, not be protective. However, if the vaccine induced opsonizing antibodies (*i.e*., the antibody bound VAR2CSA and marked the iRBC for ingestion by phagocytes), then it would theoretically protect against all stages of infection regardless of whether CS-A was available for parasite binding. It will be interesting follow the vaccine trials in light of the work that I presented in Chapter 2.

5.3 CHARACTERIZATION OF STB DENUDATION AS A HISTOPATHOLOGICAL READOUT FOR DRUG AND VACCINE TRIALS

Currently, a number of methods are used to determine severity of malaria infection at the maternal-fetal interface: 1) Gimsea-stained smears of maternal blood from the intervillous space; 2) PCR of *P. falciparum* DNA from maternal blood in the intervillous space; and 3) histological examination of placental biopsies. It is generally agreed that the latter provides the most accurate diagnosis. Three parameters of infection comprise the current histological grading scheme—iRBCs, hemozoin deposition, and inflammation (*i.e.*, maternal leukocytes at the placental surface). These readouts provide quantifiable evidence regarding the degree of active infection (*e.g.*, numbers of iRBCs) and past infection (*e.g.*, extent of hemozoin deposition), as well as information about the maternal immune response to infection. Importantly, both hemozoin and inflammation have been associated with lower infant birthweights (117, 165, 183). However, these histological features do not address the placental response, which should be monitored, since this organ nourishes the embryo/fetus and protects it from infection. Thus, in my opinion, it would be helpful to include a placental histological endpoint in addition to the aforementioned readouts.

In Chapter 2, I showed that STB denudation was associated with hemozoin and

maternal leukoctye infiltrates. It was also more common in placentas from primigravidae and secundigravidae, and in pregnancies that resulted in lower neonate birthweights. Thus, this histological lesion associates with parameters of severe infection. Importantly, this endpoint is easy to score—standard 400x magnification and H&E staining is sufficient for observation. In general, I found very little inter-biopsy differences, which suggested that this lesion is uniformly present across the placenta and not restricted to some cotyledons. However, I observed some inter-field variability within single biopsies. Thus, I recommend that at least 3, 400x fields per biopsy be scored. Finally, because STB denudation was present in both infected and uninfected placentas, multivariate analyses can be used to study its relationship with other outcomes and/or clinical parameters (*e.g.*, birthweight, other pregnancy complications, etc). My studies were carried out with a limited number of placentas (n=17 uninfected and 17 infected). Thus, to determine if this lesion is a useful histological readout, additional samples from different geographical regions should be analyzed.

5.4 HISTOPATHOLOGICAL ANALYSIS OF THE BASAL PLATE REGION OF *P. FALCIPARUM*-INFECTED PLACENTAS

Preeclampsia is a hypertensive complication of pregnancy. This condition presents clinically as hypertension, edema, and proteinuria. Histologically, preeclampsia is characterized by shallow iCTB invasion of the uterus and rudimentary remodeling of uterine spiral arterioles (for review see 15). Intriguingly, a few reports have suggested that placental malaria is associated with a preeclampsia-like syndrome (21). However, to my knowledge, a histological characterization of the basal plate—the uterine region that is attached to the placenta—of *P. falciparum*-infected placentas has not been performed. Thus, it would be very interesting to determine if shallow invasion and poor arteriole

remodeling are also features of placental malaria. Such a study could easily be performed with the biopsy library that I described in Chapters 2 and 3. Dr. Sadiki Ngeleza did an excellent job of collecting and processing these samples and ~ 95% of them contain a substantial piece of basal plate. All were full-depth biopsies that included the region lying between the maternal decidua and the fetal membranes. This valuable collection belongs to the Fisher laboratory, but will be shared with other researchers who might want to undertake this study. Since I already determined the degree of infection for each biopsy, it would be easy to measure statistical associations between basal plate histopathologies and infection status, clinical parameters (*e.g.,* parity) or outcomes (*e.g.,* birthweight). One could carry out a study similar to that described by Zhou *et al.* (220). This would include measuring the degree of invasion with particular focus on the endovascular compartment and studying the expression of molecules that are known to be dysregulated during preeclampsia.

5.5 FURTHER CHARACTERIZATION OF PLACENTAL POLYSIA

5.5.1 Effect of polySia on syncytialization

As discussed in Chapter 4, I demonstrated that polySia promoted CTB migration (Figure 4.6) and invasion (Figure 4.7). Since this glycan is also expressed by first-trimester STBs, it would be very interesting to explore functional roles in this location. Recently, the Fisher Lab generated human trophoblast progenitor cells (HTPCs) (81), which can be used to study syncytialization. This term refers to the formation of syncytium—multinucleate, fused cells. In preliminary staining experiments, I found that some of the hTPC lines expressed polySia (data not shown). Using these lines, it would be very interesting to induce syncytialization ± Endo N, which removes polySia, or mAb

735, which has been used as a function-perturbing antibody in other systems, but did not work that well with primary CTBs (see Chapter 4).

5.5.2 Effect of polySia on cytotoxicity

Another line of investigation involves determining if CTB- or STB-associated polySia influences cell tolerance or protection from pathogens. First, it would be interesting to investigate whether polySia protected trophoblasts from immunological attack by natural killer (NK) cells, so-called because they harbor cytotoxic molecules that "kill" cellular targets. It has been proposed that polySia, through its ability to bind small molecules, might shield cells from cytotoxic molecules. In fact, since NK cells express NCAM/CD56-polySia, it has been hypothesized that polySia could protect these cells from self-induced injury. A few years ago, Elizabeth Co, a former graduate student in our group, demonstrated that uterine NK cells are able to kill primary CTBs. Using a modified version of the cell culture model that she developed, it would be interesting to determine if polySia protected CTBs from immunological attack. In her assay, freshly isolated ^{51}chromium-labeled CTBs, which due to the purification procedure were stripped of their cell-surface polySia, were mixed with NK cells. Then, killing was assessed with a ^{51}chromium release assay. One could modify this approach, specifically culturing the CTBs *in vitro*—to allow them to re-express polySia—prior to incubation with NK cells. Endo N or mAb735 could be used for perturbation. In this way, it would be possible to determine whether polySia expression on target cells, or both target and effector cells, influences cytotoxicity. Human explants of chorionic villi could also be used to assess NK cell attack of STBs. In addition, bacterial pathogens could be substituted for NK cells to investigate whether polySia also shields trophoblasts from these cells.

5.6 CONCLUDING REMARKS

In summary, my thesis work resulted in many interesting findings that warrant follow-on studies. These include extending my studies of iRBC interactions with placental glycans to include more physiologic conditions that incorporate shear stress. Additional functional data are needed to bolster the novel conclusion that CS proteoglycans do not initiate iRBC adhesion to the intact placenta. I am also hopeful that my work will have translational aspects with regard to incorporating STB denudation into the scoring index that is used to assess placental malaria.

REFERENCES

1. **Achur, R. N., M. Valiyaveettil, A. Alkhalil, C. F. Ockenhouse, and D. C. Gowda.** 2000. Characterization of proteoglycans of human placenta and identification of unique chondroitin sulfate proteoglycans of the intervillous spaces that mediate the adherence of Plasmodium falciparum-infected erythrocytes to the placenta. J Biol Chem **275:**40344-40356.
2. **Angata, K., J. Nakayama, B. Fredette, K. Chong, B. Ranscht, and M. Fukuda.** 1997. Human STX polysialyltransferase forms the embryonic form of the neural cell adhesion molecule. Tissue-specific expression, neurite outgrowth, and chromosomal localization in comparison with another polysialyltransferase, PST. J Biol Chem **272:**7182-7190.
3. **Asch, A. S., J. Barnwell, R. L. Silverstein, and R. L. Nachman.** 1987. Isolation of the thrombospondin membrane receptor. The Journal of clinical investigation **79:**1054-1061.
4. **Baczyk, D., C. Dunk, B. Huppertz, C. Maxwell, F. Reister, D. Giannoulias, and J. C. Kingdom.** 2006. Bi-potential behaviour of cytotrophoblasts in first trimester chorionic villi. Placenta **27:**367-374.
5. **Barcena, A., M. O. Muench, M. Kapidzic, and S. J. Fisher.** 2009. A new role for the human placenta as a hematopoietic site throughout gestation. Reprod Sci **16:**178-187.
6. **Barnwell, J. W., C. F. Ockenhouse, and D. M. Knowles, 2nd.** 1985. Monoclonal antibody OKM5 inhibits the in vitro binding of Plasmodium falciparum-infected erythrocytes to monocytes, endothelial, and C32 melanoma cells. J Immunol **135:**3494-3497.

7. **Baruch, D. I., X. C. Ma, B. Pasloske, R. J. Howard, and L. H. Miller.** 1999. CD36 peptides that block cytoadherence define the CD36 binding region for Plasmodium falciparum-infected erythrocytes. Blood **94:**2121-2127.

8. **Baruch, D. I., X. C. Ma, H. B. Singh, X. Bi, B. L. Pasloske, and R. J. Howard.** 1997. Identification of a region of PfEMP1 that mediates adherence of Plasmodium falciparum infected erythrocytes to CD36: conserved function with variant sequence. Blood **90:**3766-3775.

9. **Baruch, D. I., B. L. Pasloske, H. B. Singh, X. Bi, X. C. Ma, M. Feldman, T. F. Taraschi, and R. J. Howard.** 1995. Cloning the P. falciparum gene encoding PfEMP1, a malarial variant antigen and adherence receptor on the surface of parasitized human erythrocytes. Cell **82:**77-87.

10. **Bax, M., S. J. van Vliet, M. Litjens, J. J. Garcia-Vallejo, and Y. van Kooyk.** 2009. Interaction of polysialic acid with CCL21 regulates the migratory capacity of human dendritic cells. PLoS ONE **4:**e6987.

11. **Beeson, J., S. Rogerson, B. Cooke, J. Reeder, W. Chai, A. Lawson, M. Molyneux, and G. Brown.** 2000. Adhesion of Plasmodium falciparum-infected erythrocytes to hyaluronic acid in placental malaria. Nat Med **6:**86-90.

12. **Beeson, J. G., G. V. Brown, M. E. Molyneux, C. Mhango, F. Dzinjalamala, and S. J. Rogerson.** 1999. Plasmodium falciparum isolates from infected pregnant women and children are associated with distinct adhesive and antigenic properties. The Journal of infectious diseases **180:**464-472.

13. **Beeson, J. G., S. J. Rogerson, S. R. Elliott, and M. F. Duffy.** 2005. Targets of protective antibodies to malaria during pregnancy. The Journal of infectious diseases **192:**1647-1650.

14. **Beham, A., H. Denk, and G. Desoye.** 1988. The distribution of intermediate filament proteins, actin and desmoplakins in human placental tissue as revealed by polyclonal and monoclonal antibodies. Placenta **9:**479-492.

15. **Benirschke, K., P. Kaufmann, and R. N. Baergen.** 2006. Pathology of the Human Placenta, 5 ed. Springer Science+Business Media, Inc., New York.

16. **Berendt, A. R., A. McDowall, A. G. Craig, P. A. Bates, M. J. Sternberg, K. Marsh, C. I. Newbold, and N. Hogg.** 1992. The binding site on ICAM-1 for Plasmodium falciparum-infected erythrocytes overlaps, but is distinct from, the LFA-1-binding site. Cell **68:**71-81.

17. **Berendt, A. R., D. L. Simmons, J. Tansey, C. I. Newbold, and K. Marsh.** 1989. Intercellular adhesion molecule-1 is an endothelial cell adhesion receptor for Plasmodium falciparum. Nature **341:**57-59.

18. **Bir, N., S. S. Yazdani, M. Avril, C. Layez, J. Gysin, and C. E. Chitnis.** 2006. Immunogenicity of Duffy binding-like domains that bind chondroitin sulfate A and protection against pregnancy-associated malaria. Infection and immunity **74:**5955-5963.

19. **Bonne, S., B. Gilbert, M. Hatzfeld, X. Chen, K. J. Green, and F. van Roy.** 2003. Defining desmosomal plakophilin-3 interactions. J Cell Biol **161:**403-416.

20. **Bonne, S., J. van Hengel, F. Nollet, P. Kools, and F. van Roy.** 1999. Plakophilin-3, a novel armadillo-like protein present in nuclei and desmosomes of epithelial cells. J Cell Sci **112 (Pt 14):**2265-2276.

21. **Brabin, B., and P. Johnson.** 2005. Placental malaria and pre-eclampsia through the looking glass backwards? J Reprod Immunol **65:**1-15.

22. **Brabin, B. J.** 1983. An analysis of malaria in pregnancy in Africa. Bull World Health Organ **61:**1005-1016.

23. **Brabin, B. J., M. Ginny, M. Alpers, L. Brabin, T. Eggelte, and H. J. Van der Kaay.** 1990. Failure of chloroquine prophylaxis for falciparum malaria in pregnant women in Madang, Papua New Guinea. Annals of tropical medicine and parasitology **84:**1-9.

24. **Brabin, B. J., and P. M. Johnson.** 2005. Placental malaria and pre-eclampsia through the looking glass backwards? J Reprod Immunol **65:**1-15.

25. **Brabin, B. J., C. Romagosa, S. Abdelgalil, C. Menendez, F. H. Verhoeff, R. McGready, K. A. Fletcher, S. Owens, U. D'Alessandro, F. Nosten, P. R. Fischer, and J. Ordi.** 2004. The sick placenta-the role of malaria. Placenta **25:**359-378.

26. **Bray, R., and R. Sinden.** 1979. The sequestration of Plasmodium falciparum infected erythrocytes in the placenta. Trans R Soc Trop Med Hyg **73:**716-719.

27. **Brown, A., and M. K. Higgins.** 2010. Carbohydrate binding molecules in malaria pathology. Current opinion in structural biology **20:**560-566.

28. **Bulmer, J. N., F. N. Rasheed, N. Francis, L. Morrison, and B. M. Greenwood.** 1993. Placental malaria. I. Pathological classification. Histopathology **22:**211-218.

29. **Bulmer, J. N., F. N. Rasheed, L. Morrison, N. Francis, and B. M. Greenwood.** 1993. Placental malaria. II. A semi-quantitative investigation of the pathological features. Histopathology **22:**219-225.

30. **Caniggia, I., S. Grisaru-Gravnosky, M. Kuliszewsky, M. Post, and S. J. Lye.** 1999. Inhibition of TGF-beta 3 restores the invasive capability of extravillous trophoblasts in preeclamptic pregnancies. J Clin Invest **103:**1641-1650.

31. **Casasnovas, J. M., C. Pieroni, and T. A. Springer.** 1999. Lymphocyte function-associated antigen-1 binding residues in intercellular adhesion molecule-2 (ICAM-2) and the integrin binding surface in the ICAM subfamily. Proceedings of

the National Academy of Sciences of the United States of America **96:**3017-3022.

32. **Chakravorty, S. J., and A. Craig.** 2005. The role of ICAM-1 in Plasmodium falciparum cytoadherence. Eur J Cell Biol **84:**15-27.

33. **Chassin, D., J. L. Benifla, C. Delattre, H. Fernandez, D. Ginisty, J. L. Janneau, M. Prade, G. Contesso, B. Caillou, M. Tournaire, and et al.** 1994. Identification of genes overexpressed in tumors through preferential expression screening in trophoblasts. Cancer Res **54:**5217-5223.

34. **Chen, Q., M. Schlichtherle, and M. Wahlgren.** 2000. Molecular aspects of severe malaria. Clinical microbiology reviews **13:**439-450.

35. **Cohen, M., A. Meisser, and P. Bischof.** 2006. Metalloproteinases and human placental invasiveness. Placenta **27:**783-793.

36. **Cooke, B. M., S. J. Rogerson, G. V. Brown, and R. L. Coppel.** 1996. Adhesion of malaria-infected red blood cells to chondroitin sulfate A under flow conditions. Blood **88:**4040-4044.

37. **Couchman, J. R., B. Caterson, J. E. Christner, and J. R. Baker.** 1984. Mapping by monoclonal antibody detection of glycosaminoglycans in connective tissues. Nature **307:**650-652.

38. **Craig, A., and A. Scherf.** 2001. Molecules on the surface of the Plasmodium falciparum infected erythrocyte and their role in malaria pathogenesis and immune evasion. Molecular and biochemical parasitology **115:**129-143.

39. **Creasey, A. M., T. Staalsoe, A. Raza, D. E. Arnot, and J. A. Rowe.** 2003. Nonspecific immunoglobulin M binding and chondroitin sulfate A binding are linked phenotypes of Plasmodium falciparum isolates implicated in malaria during pregnancy. Infection and immunity **71:**4767-4771.

40. **Crocker, I., O. Tanner, J. Myers, J. Bulmer, G. Walraven, and P. Baker.** 2004. Syncytiotrophoblast degradation and the pathophysiology of the malaria-infected placenta. Placenta **25:**273-282.

41. **Crocker, I. P., O. M. Tanner, J. E. Myers, J. N. Bulmer, G. Walraven, and P. N. Baker.** 2004. Syncytiotrophoblast degradation and the pathophysiology of the malaria-infected placenta. Placenta **25:**273-282.

42. **Cserti, C. M., and W. H. Dzik.** 2007. The ABO blood group system and Plasmodium falciparum malaria. Blood **110:**2250-2258.

43. **Curreli, S., Z. Arany, R. Gerardy-Schahn, D. Mann, and N. M. Stamatos.** 2007. Polysialylated neuropilin-2 is expressed on the surface of human dendritic cells and modulates dendritic cell-T lymphocyte interactions. J Biol Chem **282:**30346-30356.

44. **Dahlback, M., L. M. Jorgensen, M. A. Nielsen, T. M. Clausen, S. B. Ditlev, M. Resende, V. V. Pinto, D. E. Arnot, T. G. Theander, and A. Salanti.** 2011. The chondroitin sulfate A-binding site of the VAR2CSA protein involves multiple N-terminal domains. The Journal of biological chemistry **286:**15908-15917.

45. **Dahlback, M., M. A. Nielsen, and A. Salanti.** Can any lessons be learned from the ambiguous glycan binding of PfEMP1 domains? Trends in parasitology **26:**230-235.

46. **Damsky, C. H., M. L. Fitzgerald, and S. J. Fisher.** 1992. Distribution patterns of extracellular matrix components and adhesion receptors are intricately modulated during first trimester cytotrophoblast differentiation along the invasive pathway, in vivo. The Journal of clinical investigation **89:**210-222.

47. **Deepa, S. S., S. Yamada, S. Fukui, and K. Sugahara.** 2007. Structural determination of novel sulfated octasaccharides isolated from chondroitin sulfate

of shark cartilage and their application for characterizing monoclonal antibody epitopes. Glycobiology **17:**631-645.

48. **Desai, M., F. O. ter Kuile, F. Nosten, R. McGready, K. Asamoa, B. Brabin, and R. D. Newman.** 2007. Epidemiology and burden of malaria in pregnancy. Lancet Infect Dis **7:**93-104.

49. **Dityatev, A., G. Dityateva, V. Sytnyk, M. Delling, N. Toni, I. Nikonenko, D. Muller, and M. Schachner.** 2004. Polysialylated neural cell adhesion molecule promotes remodeling and formation of hippocampal synapses. J Neurosci **24:**9372-9382.

50. **Drake, P., J. Nathan, C. Stock, P. Chang, M. Muench, D. Nakata, J. Reader, P. Gip, K. Golden, B. Weinhold, R. Gerardy-Schahn, F. Troy, and C. Bertozzi.** 2008. Polysialic acid, a glycan with highly restricted expression, is found on human and murine leukocytes and modulates immune responses. J Immunol **181:**6850-6858.

51. **Drake, P., C. Stock, J. Nathan, P. Gip, K. Golden, B. Weinhold, R. Gerardy-Schahn, and C. Bertozzi.** 2009. Polysialic acid governs T-cell development by regulating progenitor access to the thymus. Proc Natl Acad Sci U S A **106:**11995-12000.

52. **Drake, P. M., C. M. Stock, J. K. Nathan, P. Gip, K. P. Golden, B. Weinhold, R. Gerardy-Schahn, and C. R. Bertozzi.** 2009. Polysialic acid governs T-cell development by regulating progenitor access to the thymus. Proc Natl Acad Sci U S A **106:**11995-12000.

53. **Duffy, M., A. Maier, T. Byrne, A. Marty, S. Elliott, M. O'Neill, P. Payne, S. Rogerson, A. Cowman, B. Crabb, and G. Brown.** 2006. VAR2CSA is the principal ligand for chondroitin sulfate A in two allogeneic isolates of Plasmodium falciparum. Mol Biochem Parasitol **148:**117-124.

54. **Duffy, M. F., A. G. Maier, T. J. Byrne, A. J. Marty, S. R. Elliott, M. T. O'Neill, P. D. Payne, S. J. Rogerson, A. F. Cowman, B. S. Crabb, and G. V. Brown.** 2006. VAR2CSA is the principal ligand for chondroitin sulfate A in two allogeneic isolates of Plasmodium falciparum. Molecular and biochemical parasitology **148:**117-124.

55. **Duffy, P. E., and R. S. Desowitz.** 2002. Pregnancy malaria throughout history: dangerous labors, p. 1-25. *In* P. E. Duffy and M. Fried (ed.), Malaria in pregnancy: deadly parasite, susceptible host. Taylor and Francis, New York, N.Y.

56. **Duraisingh, M. T., T. S. Voss, A. J. Marty, M. F. Duffy, R. T. Good, J. K. Thompson, L. H. Freitas-Junior, A. Scherf, B. S. Crabb, and A. F. Cowman.** 2005. Heterochromatin silencing and locus repositioning linked to regulation of virulence genes in Plasmodium falciparum. Cell **121:**13-24.

57. **Figdor, C. G., Y. van Kooyk, and G. J. Adema.** 2002. C-type lectin receptors on dendritic cells and Langerhans cells. Nature reviews **2:**77-84.

58. **Finne, J., U. Finne, H. Deagostini-Bazin, and C. Goridis.** 1983. Occurrence of alpha 2-8 linked polysialosyl units in a neural cell adhesion molecule. Biochem Biophys Res Commun **112:**482-487.

59. **Fisher, S. J., T. Y. Cui, L. Zhang, L. Hartman, K. Grahl, G. Y. Zhang, J. Tarpey, and C. H. Damsky.** 1989. Adhesive and degradative properties of human placental cytotrophoblast cells in vitro. J Cell Biol **109:**891-902.

60. **Fisher, S. J., and C. H. Damsky.** 1993. Human cytotrophoblast invasion. Semin Cell Biol **4:**183-188.

61. **Fitzpatrick, T. E., G. E. Lash, A. Yanaihara, D. S. Charnock-Jones, S. K. Macdonald-Goodfellow, and C. H. Graham.** 2003. Inhibition of breast carcinoma and trophoblast cell invasiveness by vascular endothelial growth factor. Exp Cell Res **283:**247-255.

62. **Flick, K., C. Scholander, Q. Chen, V. Fernandez, B. Pouvelle, J. Gysin, and M. Wahlgren.** 2001. Role of nonimmune IgG bound to PfEMP1 in placental malaria. Science (New York, N.Y **293:**2098-2100.

63. **Fraenkel, S., and Y. Bergman.** 2006. Variability and exclusion in host and parasite: epigenetic regulation of Ig and var expression. J Immunol **177:**5767-5774.

64. **Freitas-Junior, L. H., E. Bottius, L. A. Pirrit, K. W. Deitsch, C. Scheidig, F. Guinet, U. Nehrbass, T. E. Wellems, and A. Scherf.** 2000. Frequent ectopic recombination of virulence factor genes in telomeric chromosome clusters of P. falciparum. Nature **407:**1018-1022.

65. **Freitas-Junior, L. H., R. Hernandez-Rivas, S. A. Ralph, D. Montiel-Condado, O. K. Ruvalcaba-Salazar, A. P. Rojas-Meza, L. Mancio-Silva, R. J. Leal-Silvestre, A. M. Gontijo, S. Shorte, and A. Scherf.** 2005. Telomeric heterochromatin propagation and histone acetylation control mutually exclusive expression of antigenic variation genes in malaria parasites. Cell **121:**25-36.

66. **Fried, M., and P. Duffy.** 1996. Adherence of Plasmodium falciparum to chondroitin sulfate A in the human placenta. Science **272:**1502-1504.

67. **Fried, M., and P. E. Duffy.** 1996. Adherence of Plasmodium falciparum to chondroitin sulfate A in the human placenta. Science (New York, N.Y **272:**1502-1504.

68. **Fried, M., R. O. Muga, A. O. Misore, and P. E. Duffy.** 1998. Malaria elicits type 1 cytokines in the human placenta: IFN-gamma and TNF-alpha associated with pregnancy outcomes. J Immunol **160:**2523-2530.

69. **Fried, M., F. Nosten, A. Brockman, B. J. Brabin, and P. E. Duffy.** 1998. Maternal antibodies block malaria. Nature **395:**851-852.

70. **Galbraith, R., H. Fox, B. Hsi, G. Galbraith, R. Bray, and W. Faulk.** 1980. The human materno-foetal relationship in malaria. II. Histological, ultrastructural and immunopathological studies of the placenta. Trans R Soc Trop Med Hyg **74:**61-72.

71. **Galbraith, R. M., W. P. Faulk, G. M. Galbraith, T. W. Holbrook, and R. S. Bray.** 1980. The human materno-foetal relationship in malaria: I. Identification of pigment and parasites in the placenta. Trans R Soc Trop Med Hyg **74:**52-60.

72. **Galbraith, R. M., H. Fox, B. Hsi, G. M. Galbraith, R. S. Bray, and W. P. Faulk.** 1980. The human materno-foetal relationship in malaria. II. Histological, ultrastructural and immunopathological studies of the placenta. Transactions of the Royal Society of Tropical Medicine and Hygiene **74:**61-72.

73. **Galuska, S. P., M. Rollenhagen, M. Kaup, K. Eggers, I. Oltmann-Norden, M. Schiff, M. Hartmann, B. Weinhold, H. Hildebrandt, R. Geyer, M. Muhlenhoff, and H. Geyer.** Synaptic cell adhesion molecule SynCAM 1 is a target for polysialylation in postnatal mouse brain. Proc Natl Acad Sci U S A **107:**10250-10255.

74. **Gamain, B., J. D. Smith, N. K. Viebig, J. Gysin, and A. Scherf.** 2007. Pregnancy-associated malaria: parasite binding, natural immunity and vaccine development. International journal for parasitology **37:**273-283.

75. **Ganapathy, V., P. D. Prasad, and F. H. Leibach.** 1999. Choriocarcinoma, p. 141-147. *In* J. Masters and B. Palsson (ed.), Human Cell Culture, vol. 11. Kluwer Academic Publishers.

76. **Garcia, J. E., A. Puentes, and M. E. Patarroyo.** 2006. Developmental biology of sporozoite-host interactions in Plasmodium falciparum malaria: implications for vaccine design. Clinical microbiology reviews **19:**686-707.

77. **Garcia-Lloret, M. I., B. Winkler-Lowen, and L. J. Guilbert.** 2000. Monocytes adhering by LFA-1 to placental syncytiotrophoblasts induce local apoptosis via release of TNF-alpha. A model for hematogenous initiation of placental inflammations. J Leukoc Biol **68:**903-908.

78. **Gascon, E., L. Vutskits, B. Jenny, P. Durbec, and J. Z. Kiss.** 2007. PSA-NCAM in postnatally generated immature neurons of the olfactory bulb: a crucial role in regulating p75 expression and cell survival. Development **134:**1181-1190.

79. **Gascon, E., L. Vutskits, and J. Z. Kiss.** 2007. Polysialic acid-neural cell adhesion molecule in brain plasticity: from synapses to integration of new neurons. Brain research reviews **56:**101-118.

80. **Gatton, M. L., J. M. Peters, E. V. Fowler, and Q. Cheng.** 2003. Switching rates of Plasmodium falciparum var genes: faster than we thought? Trends in parasitology **19:**202-208.

81. **Genbacev, O., M. Donne, M. Kapidzic, M. Gormley, J. Lamb, J. Gilmore, N. Larocque, G. Goldfien, T. Zdravkovic, M. T. McMaster, and S. J. Fisher.** Establishment of Human Trophoblast Progenitor Cell Lines from the Chorion. Stem Cells.

82. **Genbacev, O., S. A. Schubach, and R. K. Miller.** 1992. Villous culture of first trimester human placenta--model to study extravillous trophoblast (EVT) differentiation. Placenta **13:**439-461.

83. **Grau, G. E., C. D. Mackenzie, R. A. Carr, M. Redard, G. Pizzolato, C. Allasia, C. Cataldo, T. E. Taylor, and M. E. Molyneux.** 2003. Platelet accumulation in brain microvessels in fatal pediatric cerebral malaria. The Journal of infectious diseases **187:**461-466.

84. **Green, K. J., and C. L. Simpson.** 2007. Desmosomes: new perspectives on a classic. J Invest Dermatol **127:**2499-2515.

85. **Guyatt, H. L., and R. W. Snow.** 2004. Impact of malaria during pregnancy on low birth weight in sub-Saharan Africa. Clinical microbiology reviews **17:**760-769, table of contents.

86. **Harris, L. K., C. J. Jones, and J. D. Aplin.** 2009. Adhesion molecules in human trophoblast - a review. II. extravillous trophoblast. Placenta **30:**299-304.

87. **Heimburg-Molinaro, J., X. Song, D. F. Smith, and R. D. Cummings.** 2011. Preparation and analysis of glycan microarrays. Curr Protoc Protein Sci **Chapter 12:**Unit12 10.

88. **Hildebrandt, H., C. Becker, S. Glüer, H. Rösner, R. Gerardy-Schahn, and H. Rahmann.** 1998. Polysialic acid on the neural cell adhesion molecule correlates with expression of polysialyltransferases and promotes neuroblastoma cell growth. Cancer Res **58:**779-784.

89. **Ho, M., M. J. Hickey, A. G. Murray, G. Andonegui, and P. Kubes.** 2000. Visualization of Plasmodium falciparum-endothelium interactions in human microvasculature: mimicry of leukocyte recruitment. The Journal of experimental medicine **192:**1205-1211.

90. **Hoffman, S., B. C. Sorkin, P. C. White, R. Brackenbury, R. Mailhammer, U. Rutishauser, B. A. Cunningham, and G. M. Edelman.** 1982. Chemical characterization of a neural cell adhesion molecule purified from embryonic brain membranes. The Journal of biological chemistry **257:**7720-7729.

91. **Horrocks, P., R. Pinches, Z. Christodoulou, S. A. Kyes, and C. I. Newbold.** 2004. Variable var transition rates underlie antigenic variation in malaria. Proceedings of the National Academy of Sciences of the United States of America **101:**11129-11134.

92. **Hu, H., H. Tomasiewicz, T. Magnuson, and U. Rutishauser.** 1996. The role of polysialic acid in migration of olfactory bulb interneuron precursors in the subventricular zone. Neuron **16:**735-743.

93. **Hunkapiller, N. M., and S. J. Fisher.** 2008. Chapter 12 Placental Remodeling of the Uterine Vasculature, p. 281-302. Methods in Enzymology, vol. Volume 445. Academic Press.

94. **Hviid, L., and A. Salanti.** 2007. VAR2CSA and protective immunity against pregnancy-associated Plasmodium falciparum malaria. Parasitology **134:**1871-1876.

95. **Ito, Y., M. Hikino, Y. Yajima, T. Mikami, S. Sirko, A. von Holst, A. Faissner, S. Fukui, and K. Sugahara.** 2005. Structural characterization of the epitopes of the monoclonal antibodies 473HD, CS-56, and MO-225 specific for chondroitin sulfate D-type using the oligosaccharide library. Glycobiology **15:**593-603.

96. **James, W. M., and W. S. Agnew.** 1987. Multiple oligosaccharide chains in the voltage-sensitive Na channel from electrophorus electricus: evidence for alpha-2,8-linked polysialic acid. Biochem Biophys Res Commun **148:**817-826.

97. **Jimenez, D., P. Roda-Navarro, T. A. Springer, and J. M. Casasnovas.** 2005. Contribution of N-linked glycans to the conformation and function of intercellular adhesion molecules (ICAMs). The Journal of biological chemistry **280:**5854-5861.

98. **Kay, H. H., D. M. Nelson, Y. Wang, H. S. Gammill, S. E. Peterson, and J. L. Nelson.** 2011. Maternal–Fetal Cell Trafficking and Microchimerism. The Placenta: From Development to Disease, From Development to Disease. Blackwell Publishing Ltd.

99. **Kishimoto, T. e. a., eds.** 1997. Leukocyte Typing VI. Garland Publishing, Inc, New York and London.

100. **Kliman, H. J., J. E. Nestler, E. Sermasi, J. M. Sanger, and J. F. Strauss, 3rd.** 1986. Purification, characterization, and in vitro differentiation of cytotrophoblasts from human term placentae. Endocrinology **118:**1567-1582.

101. **Komminoth, P., J. Roth, P. M. Lackie, D. Bitter-Suermann, and P. U. Heitz.** 1991. Polysialic acid of the neural cell adhesion molecule distinguishes small cell lung carcinoma from carcinoids. Am J Pathol **139:**297-304.

102. **Kraemer, S. M., and J. D. Smith.** 2006. A family affair: var genes, PfEMP1 binding, and malaria disease. Current opinion in microbiology **9:**374-380.

103. **Kristoffersen, E. K.** 2000. Placental Fc receptors and the transfer of maternal IgG. Transfus Med Rev **14:**234-243.

104. **Kwiatkowski, D., and M. Nowak.** 1991. Periodic and chaotic host-parasite interactions in human malaria. Proceedings of the National Academy of Sciences of the United States of America **88:**5111-5113.

105. **Lambros, C., and J. P. Vanderberg.** 1979. Synchronization of Plasmodium falciparum erythrocytic stages in culture. J Parasitol **65:**418-420.

106. **Larsen, W.** 2001. Fetal Development and teh Fetus as Patient. *In* L. P. Sherman, SS; Scott, WJ (ed.), Human Embryology, Third ed. Churchill Livingstone.

107. **Lawrence, M. B., and T. A. Springer.** 1991. Leukocytes roll on a selectin at physiologic flow rates: distinction from and prerequisite for adhesion through integrins. Cell **65:**859-873.

108. **Leopardi, O., W. Naughten, L. Salvia, M. Colecchia, A. Matteelli, A. Zucchi, A. Shein, J. A. Muchi, G. Carosi, and M. Ghione.** 1996. Malaric placentas. A quantitative study and clinico-pathological correlations. Pathology, research and practice **192:**892-898; discussion 899-900.

109. **Li, H. W., S. W. Tsao, and A. N. Cheung.** 2002. Current understandings of the molecular genetics of gestational trophoblastic diseases. Placenta **23:**20-31.

110. **Lucchi, N. W., D. Sarr, S. O. Owino, S. M. Mwalimu, D. S. Peterson, and J. M. Moore.** 2011. Natural hemozoin stimulates syncytiotrophoblast to secrete chemokines and recruit peripheral blood mononuclear cells. Placenta.

111. **Manchana, T., C. Ittiwut, A. Mutirangura, and J. J. Kavanagh.** 2010. Targeted therapies for rare gynaecological cancers. Lancet Oncol **11:**685-693.

112. **Marionneau, S., A. Cailleau-Thomas, J. Rocher, B. Le Moullac-Vaidye, N. Ruvoen, M. Clement, and J. Le Pendu.** 2001. ABH and Lewis histo-blood group antigens, a model for the meaning of oligosaccharide diversity in the face of a changing world. Biochimie **83:**565-573.

113. **Martersteck, C. M., N. L. Kedersha, D. A. Drapp, T. G. Tsui, and K. J. Colley.** 1996. Unique alpha 2, 8-polysialylated glycoproteins in breast cancer and leukemia cells. Glycobiology **6:**289-301.

114. **Maubert, B., L. J. Guilbert, and P. Deloron.** 1997. Cytoadherence of Plasmodium falciparum to intercellular adhesion molecule 1 and chondroitin-4-sulfate expressed by the syncytiotrophoblast in the human placenta. Infection and immunity **65:**1251-1257.

115. **Mayhew, T. M., L. Brotherton, E. Holliday, G. Orme, and P. G. Bush.** 2003. Fibrin-type fibrinoid in placentae from pregnancies associated with maternal smoking: association with villous trophoblast and impact on intervillous porosity. Placenta **24:**501-509.

116. **McGregor, J. L., B. Catimel, S. Parmentier, P. Clezardin, M. Dechavanne, and L. L. Leung.** 1989. Rapid purification and partial characterization of human platelet glycoprotein IIIb. Interaction with thrombospondin and its role in platelet aggregation. The Journal of biological chemistry **264:**501-506.

117. **Menendez, C., J. Ordi, M. R. Ismail, P. J. Ventura, J. J. Aponte, E. Kahigwa, F. Font, and P. L. Alonso.** 2000. The impact of placental malaria on gestational age and birth weight. J Infect Dis **181:**1740-1745.

118. **Miller, R. K., O. Genbacev, M. A. Turner, J. D. Aplin, I. Caniggia, and B. Huppertz.** 2005. Human placental explants in culture: approaches and assessments. Placenta **26:**439-448.

119. **Mitoma, J., T. Miyazaki, M. Sutton-Smith, M. Suzuki, H. Saito, J. C. Yeh, T. Kawano, O. Hindsgaul, P. H. Seeberger, M. Panico, S. M. Haslam, H. R. Morris, R. D. Cummings, A. Dell, and M. Fukuda.** 2009. The N-glycolyl form of mouse sialyl Lewis X is recognized by selectins but not by HECA-452 and FH6 antibodies that were raised against human cells. Glycoconj J **26:**511-523.

120. **Mitsuoka, C., N. Kawakami-Kimura, M. Kasugai-Sawada, N. Hiraiwa, K. Toda, H. Ishida, M. Kiso, A. Hasegawa, and R. Kannagi.** 1997. Sulfated sialyl Lewis X, the putative L-selectin ligand, detected on endothelial cells of high endothelial venules by a distinct set of anti-sialyl Lewis X antibodies. Biochem Biophys Res Commun **230:**546-551.

121. **Montgomery, J., F. A. Mphande, M. Berriman, A. Pain, S. J. Rogerson, T. E. Taylor, M. E. Molyneux, and A. Craig.** 2007. Differential var gene expression in the organs of patients dying of falciparum malaria. Molecular microbiology.

122. **Moore, J. M., S. Chaisavaneeyakorn, D. J. Perkins, C. Othoro, J. Otieno, B. L. Nahlen, Y. P. Shi, and V. Udhayakumar.** 2004. Hemozoin differentially regulates proinflammatory cytokine production in human immunodeficiency virus-seropositive and -seronegative women with placental malaria. Infection and immunity **72:**7022-7029.

123. **Moss, L., A. Prakobphol, T. Wiedmann, S. Fisher, and C. Damsky.** 1994. Glycosylation of human trophoblast integrins is stage and cell-type specific. Glycobiology **4:**567-575.

124. **Mouquet, H., S. Berrih-Aknin, J. Bismuth, P. Joly, D. Gilbert, and F. Tron.** 2008. Expression of pemphigus-autoantigen desmoglein 1 in human thymus. Tissue Antigens **71:**464-470.

125. **Muehlenbachs, A., T. K. Mutabingwa, S. Edmonds, M. Fried, and P. E. Duffy.** 2006. Hypertension and maternal-fetal conflict during placental malaria. PLoS Med **3:**e446.

126. **Muehlenbachs, A., T. K. Mutabingwa, M. Fried, and P. E. Duffy.** 2007. An unusual presentation of placental malaria: a single persisting nidus of sequestered parasites. Human pathology **38:**520-523.

127. **Muhlenhoff, M., M. Eckhardt, A. Bethe, M. Frosch, and R. Gerardy-Schahn.** 1996. Autocatalytic polysialylation of polysialyltransferase-1. The EMBO journal **15:**6943-6950.

128. **Muller, D., Z. Djebbara-Hannas, P. Jourdain, L. Vutskits, P. Durbec, G. Rougon, and J. Z. Kiss.** 2000. Brain-derived neurotrophic factor restores long-term potentiation in polysialic acid-neural cell adhesion molecule-deficient hippocampus. Proc Natl Acad Sci USA **97:**4315-4320.

129. **Murakami, S., T. Seki, U. Rutishauser, and Y. Arai.** 2000. Enzymatic removal of polysialic acid from neural cell adhesion molecule perturbs the migration route of luteinizing hormone-releasing hormone neurons in the developing chick forebrain. J Comp Neurol **420:**171-181.

130. **Muthusamy, A., R. Achur, M. Valiyaveettil, J. Botti, D. Taylor, R. Leke, and D. Gowda.** 2007. Chondroitin Sulfate Proteoglycan but Not Hyaluronic Acid Is the Receptor for the Adherence of Plasmodium falciparum-Infected Erythrocytes

in Human Placenta and Infected Red Blood Cell Adherence Up-Regulates the Receptor Expression. Am J Pathol.

131. **Muthusamy, A., R. N. Achur, V. P. Bhavanandan, G. G. Fouda, D. W. Taylor, and D. C. Gowda.** 2004. Plasmodium falciparum-infected erythrocytes adhere both in the intervillous space and on the villous surface of human placenta by binding to the low-sulfated chondroitin sulfate proteoglycan receptor. Am J Pathol **164:**2013-2025.

132. **Muthusamy, A., R. N. Achur, M. Valiyaveettil, J. J. Botti, D. W. Taylor, R. F. Leke, and D. C. Gowda.** 2007. Chondroitin Sulfate Proteoglycan but Not Hyaluronic Acid Is the Receptor for the Adherence of Plasmodium falciparum-Infected Erythrocytes in Human Placenta and Infected Red Blood Cell Adherence Up-Regulates the Receptor Expression. Am J Pathol.

133. **Muthusamy, A., R. N. Achur, M. Valiyaveettil, J. J. Botti, D. W. Taylor, R. F. Leke, and D. C. Gowda.** 2007. Chondroitin sulfate proteoglycan but not hyaluronic acid is the receptor for the adherence of Plasmodium falciparum-infected erythrocytes in human placenta, and infected red blood cell adherence up-regulates the receptor expression. Am J Pathol **170:**1989-2000.

134. **Nader, H. B.** 1991. Characterization of a heparan sulfate and a peculiar chondroitin 4-sulfate proteoglycan from platelets. Inhibition of the aggregation process by platelet chondroitin sulfate proteoglycan. The Journal of biological chemistry **266:**10518-10523.

135. **Norwitz, E. R., D. J. Schust, and S. J. Fisher.** 2001. Implantation and the survival of early pregnancy. The New England journal of medicine **345:**1400-1408.

136. **Ohtsubo, K., and J. D. Marth.** 2006. Glycosylation in cellular mechanisms of health and disease. Cell **126:**855-867.

137. **Okayama, M., K. Oguri, Y. Fujiwara, H. Nakanishi, H. Yonekura, T. Kondo, and N. Ui.** 1986. Purification and characterization of human platelet proteoglycan. Biochem J **233:**73-81.

138. **Oliveira, M. F., B. L. Timm, E. A. Machado, K. Miranda, M. Attias, J. R. Silva, M. Dansa-Petretski, M. A. de Oliveira, W. de Souza, N. M. Pinhal, J. J. Sousa, N. V. Vugman, and P. L. Oliveira.** 2002. On the pro-oxidant effects of haemozoin. FEBS Lett **512:**139-144.

139. **Ono, K., H. Tomasiewicz, T. Magnuson, and U. Rutishauser.** 1994. N-CAM mutation inhibits tangential neuronal migration and is phenocopied by enzymatic removal of polysialic acid. Neuron **13:**595-609.

140. **Ordi, J., M. R. Ismail, P. J. Ventura, E. Kahigwa, R. Hirt, A. Cardesa, P. L. Alonso, and C. Menendez.** 1998. Massive chronic intervillositis of the placenta associated with malaria infection. The American journal of surgical pathology **22:**1006-1011.

141. **Ordi, J., C. Menendez, M. R. Ismail, P. J. Ventura, A. Palacin, E. Kahigwa, B. Ferrer, A. Cardesa, and P. L. Alonso.** 2001. Placental malaria is associated with cell-mediated inflammatory responses with selective absence of natural killer cells. The Journal of infectious diseases **183:**1100-1107.

142. **Petridis, A. K., A. El-Maarouf, and U. Rutishauser.** 2004. Polysialic acid regulates cell contact-dependent neuronal differentiation of progenitor cells from the subventricular zone. Dev Dyn **230:**675-684.

143. **Pilobello, K. T., L. Krishnamoorthy, D. Slawek, and L. K. Mahal.** 2005. Development of a lectin microarray for the rapid analysis of protein glycopatterns. Chembiochem **6:**985-989.

144. **Pilobello, K. T., D. E. Slawek, and L. K. Mahal.** 2007. A ratiometric lectin microarray approach to analysis of the dynamic mammalian glycome. Proc Natl Acad Sci U S A **104:**11534-11539.

145. **Poole, C. A., T. T. Glant, and J. R. Schofield.** 1991. Chondrons from articular cartilage. (IV). Immunolocalization of proteoglycan epitopes in isolated canine tibial chondrons. J Histochem Cytochem **39:**1175-1187.

146. **Pouvelle, B., P. A. Buffet, C. Lepolard, A. Scherf, and J. Gysin.** 2000. Cytoadhesion of Plasmodium falciparum ring-stage-infected erythrocytes. Nature medicine **6:**1264-1268.

147. **Pouvelle, B., V. Matarazzo, C. Jurzynski, J. Nemeth, M. Ramharter, G. Rougon, and J. Gysin.** 2007. Neural cell adhesion molecule, a new cytoadhesion receptor for Plasmodium falciparum-infected erythrocytes capable of aggregation. Infection and immunity **75:**3516-3522.

148. **Prakobphol, A., O. Genbacev, M. Gormley, M. Kapidzic, and S. J. Fisher.** 2006. A role for the L-selectin adhesion system in mediating cytotrophoblast emigration from the placenta. Developmental biology **298:**107-117.

149. **Proll, J., A. Blaschitz, M. Hartmann, J. Thalhamer, and G. Dohr.** 1996. Human first-trimester placenta intra-arterial trophoblast cells express the neural cell adhesion molecule. Early Pregnancy **2:**271-275.

150. **Ramachandran, P., P. Boontheung, Y. Xie, M. Sondej, D. T. Wong, and J. A. Loo.** 2006. Identification of N-linked glycoproteins in human saliva by glycoprotein capture and mass spectrometry. J Proteome Res **5:**1493-1503.

151. **Rasti, N., F. Namusoke, A. Chene, Q. Chen, T. Staalsoe, M. Klinkert, F. Mirembe, F. Kironde, and M. Wahlgren.** 2006. Nonimmune immunoglobulin binding and multiple adhesion characterize Plasmodium falciparum-infected erythrocytes of placental origin. Proc Natl Acad Sci U S A **103:**13795-13800.

152. **Rasti, N., F. Namusoke, A. Chene, Q. Chen, T. Staalsoe, M. Q. Klinkert, F. Mirembe, F. Kironde, and M. Wahlgren.** 2006. Nonimmune immunoglobulin binding and multiple adhesion characterize Plasmodium falciparum-infected erythrocytes of placental origin. Proceedings of the National Academy of Sciences of the United States of America **103:**13795-13800.

153. **Red-Horse, K., P. M. Drake, M. D. Gunn, and S. J. Fisher.** 2001. Chemokine ligand and receptor expression in the pregnant uterus: reciprocal patterns in complementary cell subsets suggest functional roles. Am J Pathol **159:**2199-2213.

154. **Red-Horse, K., Y. Zhou, O. Genbacev, A. Prakobphol, R. Foulk, M. McMaster, and S. Fisher.** 2004. Trophoblast differentiation during embryo implantation and formation of the maternal-fetal interface. J Clin Invest **114:**744-754.

155. **Red-Horse, K., Y. Zhou, O. Genbacev, A. Prakobphol, R. Foulk, M. McMaster, and S. J. Fisher.** 2004. Trophoblast differentiation during embryo implantation and formation of the maternal-fetal interface. The Journal of clinical investigation **114:**744-754.

156. **Reeder, J. C., A. F. Cowman, K. M. Davern, J. G. Beeson, J. K. Thompson, S. J. Rogerson, and G. V. Brown.** 1999. The adhesion of Plasmodium falciparum-infected erythrocytes to chondroitin sulfate A is mediated by P. falciparum erythrocyte membrane protein 1. Proceedings of the National Academy of Sciences of the United States of America **96:**5198-5202.

157. **Reister, F., H. G. Frank, J. C. Kingdom, W. Heyl, P. Kaufmann, W. Rath, and B. Huppertz.** 2001. Macrophage-induced apoptosis limits endovascular trophoblast invasion in the uterine wall of preeclamptic women. Lab Invest **81:**1143-1152.

158. **Rey-Gallardo, A., C. Delgado-Martin, R. Gerardy-Schahn, J. L. Rodriguez-Fernandez, and M. A. Vega.** Polysialic acid is required for neuropilin-2a/b-mediated control of CCL21-driven chemotaxis of mature dendritic cells and for their migration in vivo. Glycobiology **21:**655-662.

159. **Rey-Gallardo, A., C. Escribano, C. Delgado-Martin, J. L. Rodriguez-Fernandez, R. Gerardy-Schahn, U. Rutishauser, A. L. Corbi, and M. A. Vega.** Polysialylated neuropilin-2 enhances human dendritic cell migration through the basic C-terminal region of CCL21. Glycobiology **20:**1139-1146.

160. **Richards, R. C., J. M. Beardmore, P. J. Brown, C. M. Molloy, and P. M. Johnson.** 1983. Epidermal growth factor receptors on isolated human placental syncytiotrophoblast plasma membrane. Placenta **4:**133-138.

161. **Ricke, C. H., T. Staalsoe, K. Koram, B. D. Akanmori, E. M. Riley, T. G. Theander, and L. Hviid.** 2000. Plasma antibodies from malaria-exposed pregnant women recognize variant surface antigens on Plasmodium falciparum-infected erythrocytes in a parity-dependent manner and block parasite adhesion to chondroitin sulfate A. J Immunol **165:**3309-3316.

162. **Rogerson, S. J., S. C. Chaiyaroj, K. Ng, J. C. Reeder, and G. V. Brown.** 1995. Chondroitin sulfate A is a cell surface receptor for Plasmodium falciparum-infected erythrocytes. The Journal of experimental medicine **182:**15-20.

163. **Rogerson, S. J., L. Hviid, P. E. Duffy, R. F. Leke, and D. W. Taylor.** 2007. Malaria in pregnancy: pathogenesis and immunity. The Lancet infectious diseases **7:**105-117.

164. **Rogerson, S. J., V. Mwapasa, and S. R. Meshnick.** 2007. Malaria in pregnancy: linking immunity and pathogenesis to prevention. Am J Trop Med Hyg **77:**14-22.

165. **Rogerson, S. J., E. Pollina, A. Getachew, E. Tadesse, V. M. Lema, and M. E. Molyneux.** 2003. Placental monocyte infiltrates in response to Plasmodium falciparum malaria infection and their association with adverse pregnancy outcomes. Am J Trop Med Hyg **68:**115-119.

166. **Romagosa, C., C. Menendez, M. R. Ismail, L. Quinto, B. Ferrer, P. L. Alonso, and J. Ordi.** 2004. Polarisation microscopy increases the sensitivity of hemozoin and Plasmodium detection in the histological assessment of placental malaria. Acta Trop **90:**277-284.

167. **Roth, J., C. Zuber, P. Wagner, D. J. Taatjes, C. Weisgerber, P. U. Heitz, C. Goridis, and D. Bitter-Suermann.** 1988. Reexpression of poly(sialic acid) units of the neural cell adhesion molecule in Wilms tumor. Proc Natl Acad Sci USA **85:**2999-3003.

168. **Rowe, J. A., J. M. Moulds, C. I. Newbold, and L. H. Miller.** 1997. P. falciparum rosetting mediated by a parasite-variant erythrocyte membrane protein and complement-receptor 1. Nature **388:**292-295.

169. **Rutishauser, U.** 2008. Polysialic acid in the plasticity of the developing and adult vertebrate nervous system. Nat Rev Neurosci **9:**26-35.

170. **Salanti, A., M. Dahlback, L. Turner, M. A. Nielsen, L. Barfod, P. Magistrado, A. T. Jensen, T. Lavstsen, M. F. Ofori, K. Marsh, L. Hviid, and T. G. Theander.** 2004. Evidence for the involvement of VAR2CSA in pregnancy-associated malaria. J Exp Med **200:**1197-1203.

171. **Salanti, A., T. Staalsoe, T. Lavstsen, A. T. Jensen, M. P. Sowa, D. E. Arnot, L. Hviid, and T. G. Theander.** 2003. Selective upregulation of a single distinctly structured var gene in chondroitin sulphate A-adhering Plasmodium falciparum involved in pregnancy-associated malaria. Molecular microbiology **49:**179-191.

172. **Sartelet, H., O. Garraud, C. Rogier, I. Milko-Sartelet, Y. Kaboret, G. Michel, C. Roussilhon, M. Huerre, and D. Gaillard.** 2000. Hyperexpression of ICAM-1 and CD36 in placentas infected with Plasmodium falciparum: a possible role of these molecules in sequestration of infected red blood cells in placentas. Histopathology **36:**62-68.

173. **Schieck, E., J. M. Pfahler, C. P. Sanchez, and M. Lanzer.** 2007. Nuclear run-on analysis of var gene expression in Plasmodium falciparum. Molecular and biochemical parasitology **153:**207-212.

174. **Schofield, L.** 2007. Intravascular infiltrates and organ-specific inflammation in malaria pathogenesis. Immunol Cell Biol **85:**130-137.

175. **Schofield, L., and I. Mueller.** 2006. Clinical immunity to malaria. Current molecular medicine **6:**205-221.

176. **Scholander, C., C. J. Treutiger, K. Hultenby, and M. Wahlgren.** 1996. Novel fibrillar structure confers adhesive property to malaria-infected erythrocytes. Nature medicine **2:**204-208.

177. **Schwarzer, E., M. Alessio, D. Ulliers, and P. Arese.** 1998. Phagocytosis of the malarial pigment, hemozoin, impairs expression of major histocompatibility complex class II antigen, CD54, and CD11c in human monocytes. Infection and immunity **66:**1601-1606.

178. **Schwarzer, E., and P. Arese.** 1996. Phagocytosis of malarial pigment hemozoin inhibits NADPH-oxidase activity in human monocyte-derived macrophages. Biochim Biophys Acta **1316:**169-175.

179. **Seki, T., T. Namba, H. Mochizuki, and M. Onodera.** 2007. Clustering, migration, and neurite formation of neural precursor cells in the adult rat hippocampus. J Comp Neurol **502:**275-290.

180. **Sherman, I.** 1998. A Brief History of Malaria and Discovery of the Parasite's Life Cycle. *In* I. Sherman (ed.), Malaria: parasite biology, pathogenesis, and protection, First ed. American Society for Microbiology, Washington, DC.

181. **Shih, I.-M., and R. J. Kurman.** 2002. Molecular Basis of Gestational Trophoblastic Diseases. Current Molecular Medicine **2:**1-12.

182. **Shimaoka, M., T. Xiao, J. H. Liu, Y. Yang, Y. Dong, C. D. Jun, A. McCormack, R. Zhang, A. Joachimiak, J. Takagi, J. H. Wang, and T. A. Springer.** 2003. Structures of the alpha L I domain and its complex with ICAM-1 reveal a shape-shifting pathway for integrin regulation. Cell **112:**99-111.

183. **Shulman, C. E., T. Marshall, E. K. Dorman, J. N. Bulmer, F. Cutts, N. Peshu, and K. Marsh.** 2001. Malaria in pregnancy: adverse effects on haemoglobin levels and birthweight in primigravidae and multigravidae. Trop Med Int Health **6:**770-778.

184. **Simister, N. E., and C. M. Story.** 1997. Human placental Fc receptors and the transmission of antibodies from mother to fetus. J Reprod Immunol **37:**1-23.

185. **Skerrow, C. J., and A. G. Matoltsy.** 1974. Chemical characterization of isolated epidermal desmosomes. J Cell Biol **63:**524-530.

186. **Smetsers, T. F., E. M. van de Westerlo, G. B. ten Dam, I. M. Overes, J. Schalkwijk, G. N. van Muijen, and T. H. van Kuppevelt.** 2004. Human single-chain antibodies reactive with native chondroitin sulfate detect chondroitin sulfate alterations in melanoma and psoriasis. The Journal of investigative dermatology **122:**707-716.

187. **Smith, C. H., D. M. Nelson, B. F. King, T. M. Donohue, S. Ruzycki, and L. K. Kelley.** 1977. Characterization of a microvillous membrane preparation from human placental syncytiotrophoblast: a morphologic, biochemical, and physiologic, study. American journal of obstetrics and gynecology **128:**190-196.

188. **Smith, D. F., X. Song, and R. D. Cummings.** 2010. Use of glycan microarrays to explore specificity of glycan-binding proteins. Methods Enzymol **480:**417-444.

189. **Smith, J. D., A. G. Craig, N. Kriek, D. Hudson-Taylor, S. Kyes, T. Fagan, R. Pinches, D. I. Baruch, C. I. Newbold, and L. H. Miller.** 2000. Identification of a Plasmodium falciparum intercellular adhesion molecule-1 binding domain: a parasite adhesion trait implicated in cerebral malaria. Proceedings of the National Academy of Sciences of the United States of America **97:**1766-1771.

190. **Sugahara, K., and T. Mikami.** 2007. Chondroitin/dermatan sulfate in the central nervous system. Current opinion in structural biology **17:**536-545.

191. **Sugiyama, T., L. E. Cuevas, W. Bailey, R. Makunde, K. Kawamura, M. Kobayashi, H. Masuda, and M. Hommel.** 2001. Expression of intercellular adhesion molecule 1 (ICAM-1) in Plasmodium falciparum-infected placenta. Placenta **22:**573-579.

192. **Sullivan, A. D., T. Nyirenda, T. Cullinan, T. Taylor, A. Lau, and S. R. Meshnick.** 2000. Placental haemozoin and malaria in pregnancy. Placenta **21:**417-421.

193. **Suzuki, M., J. Nakayama, A. Suzuki, K. Angata, S. Chen, K. Sakai, K. Hagihara, Y. Yamaguchi, and M. Fukuda.** 2005. Polysialic acid facilitates tumor invasion by glioma cells. Glycobiology **15:**887-894.

194. **Talle, M. A., P. E. Rao, E. Westberg, N. Allegar, M. Makowski, R. S. Mittler, and G. Goldstein.** 1983. Patterns of antigenic expression on human monocytes as defined by monoclonal antibodies. Cell Immunol **78:**83-99.

195. **Tanaka, F., Y. Otake, T. Nakagawa, Y. Kawano, R. Miyahara, M. Li, K. Yanagihara, J. Nakayama, I. Fujimoto, K. Ikenaka, and H. Wada.** 2000. Expression of polysialic acid and STX, a human polysialyltransferase, is

correlated with tumor progression in non-small cell lung cancer. Cancer Res **60:**3072-3080.

196. **Turner, G. D., H. Morrison, M. Jones, T. M. Davis, S. Looareesuwan, I. D. Buley, K. C. Gatter, C. I. Newbold, S. Pukritayakamee, B. Nagachinta, and et al.** 1994. An immunohistochemical study of the pathology of fatal malaria. Evidence for widespread endothelial activation and a potential role for intercellular adhesion molecule-1 in cerebral sequestration. Am J Pathol **145:**1057-1069.

197. **Ueda, S. M., T. L. Mao, F. P. Kuhajda, C. Vasoontara, R. L. Giuntoli, R. E. Bristow, R. J. Kurman, and M. Shih Ie.** 2009. Trophoblastic neoplasms express fatty acid synthase, which may be a therapeutic target via its inhibitor C93. Am J Pathol **175:**2618-2624.

198. **Viebig, N., B. Gamain, C. Scheidig, C. Lepolard, J. Przyborski, M. Lanzer, J. Gysin, and A. Scherf.** 2005. A single member of the Plasmodium falciparum var multigene family determines cytoadhesion to the placental receptor chondroitin sulphate A. EMBO Rep **6:**775-781.

199. **Viebig, N. K., B. Gamain, C. Scheidig, C. Lepolard, J. Przyborski, M. Lanzer, J. Gysin, and A. Scherf.** 2005. A single member of the Plasmodium falciparum var multigene family determines cytoadhesion to the placental receptor chondroitin sulphate A. EMBO reports **6:**775-781.

200. **Vutskits, L., Z. Djebbara-Hannas, H. Zhang, J. P. Paccaud, P. Durbec, G. Rougon, D. Muller, and J. Z. Kiss.** 2001. PSA-NCAM modulates BDNF-dependent survival and differentiation of cortical neurons. Eur J Neurosci **13:**1391-1402.

201. **Vutskits, L., E. Gascon, and J. Z. Kiss.** 2003. Removal of PSA from NCAM affects the survival of magnocellular vasopressin- and oxytocin-producing

neurons in organotypic cultures of the paraventricular nucleus. Eur J Neurosci **17:**2119-2126.

202. **Vutskits, L., E. Gascon, E. Zgraggen, and J. Kiss.** 2006. The polysialylated neural cell adhesion molecule promotes neurogenesis in vitro. Neurochem Res **31:**215-225.

203. **Wahl, J. K., 3rd.** 2002. Generation of monoclonal antibodies specific for desmoglein family members. Hybrid Hybridomics **21:**37-44.

204. **Walter, P. R., Y. Garin, and P. Blot.** 1982. Placental pathologic changes in malaria. A histologic and ultrastructural study. Am J Pathol **109:**330-342.

205. **Wang, X., S. Fu, R. S. Freedman, J. Liu, and J. J. Kavanagh.** 2006. Immunobiology of gestational trophoblastic diseases. Int J Gynecol Cancer **16:**1500-1515.

206. **Ward, J. V., and M. A. Packham.** 1979. Characterization of the sulfated glycosaminoglycan on the surface and in the storage granules of rabbit platelets. Biochim Biophys Acta **583:**196-207.

207. **Waschke, J.** 2008. The desmosome and pemphigus. Histochem Cell Biol **130:**21-54.

208. **Wassmer, S. C., C. Lepolard, B. Traore, B. Pouvelle, J. Gysin, and G. E. Grau.** 2004. Platelets reorient Plasmodium falciparum-infected erythrocyte cytoadhesion to activated endothelial cells. The Journal of infectious diseases **189:**180-189.

209. **Watkinson, M., and D. I. Rushton.** 1983. Plasmodial pigmentation of placenta and outcome of pregnancy in West African mothers. Br Med J (Clin Res Ed) **287:**251-254.

210. **Weigel, P. H., V. C. Hascall, and M. Tammi.** 1997. Hyaluronan synthases. The Journal of biological chemistry **272:**13997-14000.

211. **Williams, D., V. Hodgetts, and J. Gupta.** 2010. Recurrent hydatidiform moles. Eur J Obstet Gynecol Reprod Biol **150:**3-7.

212. **Winn, V. D., R. Haimov-Kochman, A. C. Paquet, Y. J. Yang, M. S. Madhusudhan, M. Gormley, K. T. Feng, D. A. Bernlohr, S. McDonagh, L. Pereira, A. Sali, and S. J. Fisher.** 2007. Gene expression profiling of the human maternal-fetal interface reveals dramatic changes between midgestation and term. Endocrinology **148:**1059-1079.

213. **Yabe, U., C. Sato, T. Matsuda, and K. Kitajima.** 2003. Polysialic acid in human milk. CD36 is a new member of mammalian polysialic acid-containing glycoprotein. J Biol Chem **278:**13875-13880.

214. **Yagel, S., R. S. Parhar, J. J. Jeffrey, and P. K. Lala.** 1988. Normal nonmetastatic human trophoblast cells share in vitro invasive properties of malignant cells. J Cell Physiol **136:**455-462.

215. **Yamada, M., R. Steketee, C. Abramowsky, M. Kida, J. Wirima, D. Heymann, J. Rabbege, J. Breman, and M. Aikawa.** 1989. Plasmodium falciparum associated placental pathology: a light and electron microscopic and immunohistologic study. The American journal of tropical medicine and hygiene **41:**161-168.

216. **Yazdani, S. S., P. Mukherjee, V. S. Chauhan, and C. E. Chitnis.** 2006. Immune responses to asexual blood-stages of malaria parasites. Current molecular medicine **6:**187-203.

217. **Yui, J., M. Garcia-Lloret, T. G. Wegmann, and L. J. Guilbert.** 1994. Cytotoxicity of tumour necrosis factor-alpha and gamma-interferon against primary human placental trophoblasts. Placenta **15:**819-835.

218. **Zhang, H., L. Vutskits, V. Calaora, P. Durbec, and J. Z. Kiss.** 2004. A role for the polysialic acid-neural cell adhesion molecule in PDGF-induced chemotaxis of oligodendrocyte precursor cells. J Cell Sci **117:**93-103.

219. **Zhou, Y., K. Bianco, L. Huang, J. Nien, M. McMaster, R. Romero, and S. Fisher.** 2007. Comparative analysis of maternal-fetal interface in preeclampsia and preterm labor. Cell Tissue Res.

220. **Zhou, Y., K. Bianco, L. Huang, J. K. Nien, M. McMaster, R. Romero, and S. J. Fisher.** 2007. Comparative analysis of maternal-fetal interface in preeclampsia and preterm labor. Cell Tissue Res.

221. **Zhou, Y., S. J. Fisher, M. Janatpour, O. Genbacev, E. Dejana, M. Wheelock, and C. H. Damsky.** 1997. Human cytotrophoblasts adopt a vascular phenotype as they differentiate. A strategy for successful endovascular invasion? J Clin Invest **99:**2139-2151.

222. **Zhou, Y., O. Genbacev, C. Damsky, and S. Fisher.** 1998. Oxygen regulates human cytotrophoblast differentiation and invasion: implications for endovascular invasion in normal pregnancy and in pre-eclampsia. J Reprod Immunol **39:**197-213.

223. **Zupancic, M. L., M. Frieman, D. Smith, R. A. Alvarez, R. D. Cummings, and B. P. Cormack.** 2008. Glycan microarray analysis of Candida glabrata adhesin ligand specificity. Molecular microbiology **68:**547-559.

Publishing Agreement

It is the policy of the University to encourage the distribution of all theses, dissertations, and manuscripts. Copies of all UCSF theses, dissertations, and manuscripts will be routed to the library via the Graduate Division. The library will make all theses, dissertations, and manuscripts accessible to the public and will preserve these to the best of their abilities, in perpetuity.

Please sign the following statement:

I hereby grant permission to the Graduate Division of the University of California, San Francisco to release copies of my thesis, dissertation, or manuscript to the Campus Library to provide access and preservation, in whole or in part, in perpetuity.

Bethany S. Hannah
Author Signature

7/28/2011
Date